DISCLAIMER

This report was prepared as an account of work sponsored by an agency of the United States Government. Neither the United States Government nor any agency thereof, nor any of their employees, makes any warranty, express or implied, or assumes any legal liability or responsibility for the accuracy, completeness, or usefulness of any information, apparatus, product, or process disclosed, or represents that its use would not infringe privately owned rights. Reference herein to any specific commercial product, process, or service by trade name, trademark, manufacturer, or otherwise does not necessarily constitute or imply its endorsement, recommendation, or favoring by the United States Government or any agency thereof. The views and opinions of authors expressed herein do not necessarily state or reflect those of the United States Government or any agency thereof. Reference herein to any social initiative (including but not limited to Diversity, Equity, and Inclusion (DEI); Community Benefits Plans (CBP); Justice 40; etc.) is made by the Author independent of any current requirement by the United States Government and does not constitute or imply endorsement, recommendation, or support by the United States Government or any agency thereof.

Final Report for ARPA-E LOCOMOTIVES Advanced Locomotive Technology and Rail Infrastructure Optimization System (ALTRIOS) Project

Jason Lustbader,[1] Matthew Bruchon,[1] Chad Baker,[1] Nick Reinicke,[1] Yi Min Zhang,[1] Kandler Smith,[1] Alicia Birky,[1] Grant Payne,[1] Tyler Dick,[2] Geordie Roscoe,[2] Steven Shi,[2] Steven Fritz,[3] Garrett Anderson,[3] Prativa Hartnett,[3] Joel Allardyce,[3] Mike Swaney,[4] Joshua Soles,[4] Allen Doyel,[4] Corey Pasta,[4] Matthew Duncan,[4] and Nathan Williams[4]

1 National Renewable Energy Laboratory
2 University of Illinois at Urbana Champaign
3 Southwest Research Institute
4 BNSF Railway Company

NREL is a national laboratory of the U.S. Department of Energy
Office of Energy Efficiency & Renewable Energy
Operated under Contract No. DE-AC36-08GO28308

This report is available at no cost from NREL at www.nrel.gov/publications.

Technical Report
NREL/TP-5400-96872
November 2025

Final Report for ARPA-E LOCOMOTIVES Advanced Locomotive Technology and Rail Infrastructure Optimization System (ALTRIOS) Project

Jason Lustbader,[1] Matthew Bruchon,[1] Chad Baker,[1] Nick Reinicke,[1] Yi Min Zhang,[1] Kandler Smith,[1] Alicia Birky,[1] Grant Payne,[1] Tyler Dick,[2] Geordie Roscoe,[2] Steven Shi,[2] Steven Fritz,[3] Garrett Anderson,[3] Prativa Hartnett,[3] Joel Allardyce,[3] Mike Swaney,[4] Joshua Soles,[4] Allen Doyel,[4] Corey Pasta,[4] Matthew Duncan,[4] and Nathan Williams[4]

1 National Renewable Energy Laboratory
2 University of Illinois at Urbana Champaign
3 Southwest Research Institute
4 BNSF Railway Company

Suggested Citation
Lustbader, Jason, et. al. 2025. *Final Report for ARPA-E LOCOMOTIVES Advanced Locomotive Technology and Rail Infrastructure Optimization System (ALTRIOS) Project*. Golden, CO: National Renewable Energy Laboratory. NREL/TP-5400-96872. https://www.nrel.gov/docs/fy26osti/96872.pdf.

NREL is a national laboratory of the U.S. Department of Energy
Office of Energy Efficiency & Renewable Energy
Operated under Contract No. DE-AC36-08GO28308

This report is available at no cost from NREL at www.nrel.gov/publications.

Technical Report
NREL/TP-5400-96872
November 2025

15013 Denver West Parkway
Golden, CO 80401
303-275-3000 • www.nrel.gov

NOTICE

This work was authored in part by NREL for the U.S. Department of Energy (DOE), operated under Contract No. DE-AC36-08GO28308. Funding provided by U.S. Department of Energy Advanced Research Projects Agency–Energy. The views expressed herein do not necessarily represent the views of the DOE or the U.S. Government.

This report is available at no cost from NREL at www.nrel.gov/publications.

U.S. Department of Energy (DOE) reports produced after 1991 and a growing number of pre-1991 documents are available free via www.OSTI.gov.

Cover Photo from iStock 583994704

NREL prints on paper that contains recycled content.

M3.4 Final Report and Draft Final Scientific/Technical Closeout Report

Advanced Locomotive Technology and Rail Infrastructure Optimization System (ALTRIOS)

Award Number: 20/CJ000/07/06, LOCOMOTIVES

Award:	20/CJ000/07/06
Lead Recipient:	National Renewable Energy Laboratory
Project Title:	Advanced Locomotive Technology and Rail Infrastructure Optimization System (ALTRIOS)
Program Director:	Dr. Robert Ledoux
Principal Investigator:	Jason A. Lustbader
Contract Administrator:	Rachelle Ihly
Date of Report:	June 30, 2023
Reporting Period:	[January 1, 2022–June 30, 2023]

National Renewable Energy Laboratory (NREL): Jason Lustbader (PI), Chad Baker, Nicholas Reinicke, Matthew Bruchon, Yimin Zhang, Kandler Smith, Alicia Birky, and Grant Payne.
University of Illinois Urbana-Champaign: Tyler Dick (Co-PI), Geordie Roscoe, and Steven Shi.
Southwest Research Institute: Steven Fritz, Garrett Anderson, Prativa Hartnett, and Joel Allardyce.
BNSF Railway: Mike Swaney, Joshua Soles, Allen Doyel, Corey Pasta, Matthew Duncan, and Nathan Williams.

Public Executive Summary

The Advanced Locomotive Technology and Rail Infrastructure Optimization System (ALTRIOS) is a unique, fully integrated, open-source software tool used to evaluate strategies for cost-effectively deploying advanced locomotive technologies and associated infrastructure. ALTRIOS simulates freight-demand-driven train scheduling, mainline meet-pass planning, locomotive dynamics, train dynamics, energy conversion efficiencies, and energy storage dynamics of line-haul train operations. Because new locomotives represent a significant long-term capital investment and new technologies must be thoroughly demonstrated before deployment, this tool provides guidance on the risk/reward trade-offs and operation integration of different technology rollout strategies. An open, integrated simulation tool is valuable for identifying future research needs and making decisions on technology development, routes, and train selection.

The U.S. freight rail system consumes roughly 3.4 billion gallons (12.9 billion liters) of diesel annually. Combustion of the diesel produces criteria pollutants (e.g., hydrocarbons, carbon monoxide, nitrogen oxides, and particulate matter) and emissions (including carbon dioxide, methane, and nitrous oxides). All six Class I North American railroads have signed up for Science Based Targets initiative carbon reduction goals, with commitments to reduce greenhouse gas (GHG) emissions on the order of 30%–40% by 2030. The path to reaching these goals remains uncertain. Challenges include significant capital costs for locomotives, supporting appurtenances such as energy tenders and refueling infrastructure, high instantaneous power requirements for locomotives, large energy demand, the need for that energy in remote locations, and interoperability of locomotives throughout North America. The industry has a large installed base of diesel-electric locomotives (approximately 22,000) and the need for high reliability. Many potential advanced technologies—such as hydrogen, biofuels, and batteries—are being developed and promoted as potential solutions, but the question remains about how each pathway can be used to minimize cost and environmental impacts. This is compounded by the potential for decreased operational efficiency.

ALTRIOS provides a framework to simulate the trade-offs and rollout deployment strategies of these potential technologies. For a given rail corridor, freight transportation demand, and alternative technology locomotive deployment strategy, ALTRIOS develops a logistically feasible train plan, simulates 21 days of baseline train operations over the corridor, and calculates the corresponding yearlong costs, energy consumption, and emissions. Then, according to the year-by-year locomotive deployment strategy and user-specified traffic growth, the process of developing a feasible train plan is repeated, simulating train operations and calculating outputs for each subsequent year in the specified time horizon. At the end of the time horizon, annual and cumulative results are reported. The user can then adjust various tunable parameters and repeat the entire model process to quantify changes in the annual and cumulative outputs.

The system architecture of ALTRIOS consists of a set of modules that are coordinated by the simulation manager. The major components include a train planner, meet-pass planner, train performance calculator (TPC), powertrain model, refueling infrastructure model (integrated with several other modules), economic model, GHG life cycle analysis model, topology

and topography, and rollout strategy. Users can interact with ALTRIOS through either Python scripts or a web-based ALTRIOS Lite interface.

ALTRIOS is coded with a mix of Python and Rust. Python serves as the outer interface to allow flexibility, and Rust was used to accelerate the core computational aspects. The code has been built as a pip-installable package with hierarchical, object-oriented locomotive component classes, unit tests, and extensive use of Python Enhancement Proposal-257-compliant doc strings. All Rust variables are typed with units of measure, such that any invalid operations (e.g., adding a power in watts to a length in meters) will fail during compilation, and only valid operations (e.g., adding a power to a power) will be allowed. This ensures consistency in units and helps make models physically accurate.

ALTRIOS was calibrated and validated using data from a Zero- and Near-Zero-Emission Freight Facility (ZANZEFF) project funded by the California Air Resources Board that was supplemented with additional event recorder data. The data included a 2.4-MWh Wabtec battery-electric locomotive (BEL) and two Wabtec Tier 4 ET44C4 diesel locomotives. The route was approximately 375 miles one way, and the consist made 17 round trips during the 3-month monitoring period, with a total of 12,750 miles traveled. Over the trips suitable for use, the conventional locomotives had a time-averaged trip error of 4.2%. The team chose not to reverse-engineer the BEL controls, but despite this, the model shows good trendwise agreement with the BEL test data. The train data have substantially more uncertainty due to a variety of unknown environmental and train configuration factors. The TPC had a time-averaged error of 17.7%. Given the uncertainties in locomotive and train performance and operational data, this agreement was determined to be acceptable and possibly within the uncertainty of the data. Additionally, the calibration and validation framework can be used to improve calibration as more data become available and models improve.

ALTRIOS was then applied to a 30-year rollout case study targeting high penetration of BELs by 2050 for two BNSF Railway routes: loaded taconite ore trains from Hibbing, Minnesota, to Superior, Wisconsin, and mixed-freight trains from Superior to Minneapolis, Minnesota. For a hybrid locomotive consist with a 2.4-MWh BEL, the percentage reduction in diesel fuel during the final year of each rollout study relative to the initial year was 55% for the Taconite route and about 23% for the mixed-freight route. These rollouts targeted a BEL fraction of about two-thirds in 2050, and included a business rule that each consist must have at least one diesel-electric locomotive to help ensure sufficient energy and power on each route even if battery storage capacity were exhausted. For both routes, results indicate that an optimal battery size exists for energy recovery on each specific route, which is a function of the terrain, track profile, train weight, and other factors. Additional analysis is needed to quantify the optimal battery size considering economic assumptions.

For additional information on ALTRIOS and where to access it, see www.nrel.gov/transportation/altrios.

The public GitHub can be found at github.com/NREL/altrios.
The ALTRIOS Python package can be installed via PyPI: pypi.org/project/altrios.

Acknowledgments

The authors would like to thank the Advanced Research Projects Agency – Energy (ARPA-E) for financially supporting the research through the LOCOMOTIVES program and Dr. Robert Ledoux for his vision and support. We would also like to thank the ARPA-E team for their support and guidance: Dr. Apoorv Agarwal, Dr. Mirjana Marden, Alexis Amos, and Catherine Good. We would also like to thank BNSF Railway for their cost-share financial support, guidance, and deep understanding of the rail industry's needs. Additionally, we would like to thank Jinghu Hu for his contributions to the core ALTRIOS code. We would like to thank Chris Hennessy at Southwest Research Institute for his support. Thank you to Michael Cleveland (formerly at BNSF Railway, now with Progress Rail) for his help with developing and kicking off this project.

Table of Contents

List of Tables

List of Figures

Accomplishments and Objectives

The National Renewable Energy Laboratory (NREL), University of Illinois Urbana-Champaign, Southwest Research Institute, and BNSF Railway successfully developed the Advanced Locomotive Technology and Rail Infrastructure Optimization System (ALTRIOS). ALTRIOS is a unique, fully integrated, open-source software tool used to evaluate strategies for cost-effectively deploying advanced locomotive technologies and associated infrastructure. ALTRIOS simulates energy conversion and storage dynamics, locomotive and train dynamics, meet-pass planning (detailed train timetabling), and freight-demand-driven train scheduling in a Pareto optimization. Because new locomotives represent a significant long-term capital investment, and new technologies must be thoroughly demonstrated before deployment, this tool provides guidance on the risk/reward trade-offs of different technology rollout strategies. An open, integrated simulation tool is essential for identifying future research needs and making decisions on technology development, routes, and train selection.

Key Milestones and Deliverables

Tasks and milestones defined at the beginning of the project are described in Table 1, including actual performance against the stated milestones. All project tasks have been completed and objectives successfully met. Due to contracting delays and the impacts of the COVID-19 pandemic, the project period of performance was extended to June 30, 2023.

Table 1. Key Milestones and Deliverables

Tasks	Milestones and Deliverables
Task 0: Management plan M0.1 Management plan delivered M0.2 Signed intellectual property agreements	*This task will define the management plan for the team.* M0.1: The team will provide the management plan that will include team leaders for specific tasks, team meeting frequency, etc. **Actual performance:** (Fiscal Year [FY] 2022 Q2) The project management plan, M0.1, was delivered to the Advanced Research Projects Agency – Energy (ARPA-E) on March 8, 2022. The plan was reviewed and approved by the program director, successfully completing the milestone. M0.2: Intellectual property agreement(s) signed with priority concept team(s). **Actual performance:** (FY22 Q3) After overcoming contracting delays caused by the COVID-19 pandemic and challenges with controlled unclassified information, the full ALTRIOS team was able to begin work collaboratively starting in May 2022, completing the milestone.

Tasks	Milestones and Deliverables
Task 1: Data collection and test scenario definition M1.1 Data collected M1.2 Test scenarios defined	*This task will gather and/or synthetically generate necessary data (train, route, and event recorder data over a range of scenarios) to validate the performance of ALTRIOS. This task will also define the test scenarios for ALTRIOS validation.* M1.1 Data collected: Generate 3 weeks of 1-Hz route time-series data over a validation test route. Collect shorter-duration supplemental data for a range of scenarios required for ALTRIOS development and validation. Associated train and route data will also be collected. Define full data requirements. Document is submitted for Program Director approval. **Actual performance:** (FY22 Q4) The data collection milestone report, M1.1, was delivered to ARPA-E on July 3, 2022. The report provides a summary of data collected, which met the needs for ALTRIOS development and validation. This included data from the Zero- and Near-Zero-Emission Freight Facility (ZANZEFF) program for two Wabtec Tier 4 ET44C4 diesel locomotives and one battery-electric locomotive (BEL). These data were collected between Barstow and Stockton, California, over 3 months and include 17 round trips, 12,750 miles traveled, and more than 900 hours of operational data. M1.2 Test scenarios defined: The scenarios for validation are identified and represent a wide range of operating conditions, including extreme scenarios. Document is submitted for Program Director approval. **Actual performance:** (FY22 Q4) A report documenting the completion of milestone M1.2 test scenarios defined was delivered to ARPA-E on July 12, 2022. The report provides a calibration and validation plan over operational test scenarios. The calibration and validation process uses 17 round trips from the BNSF ZANZEFF data described in detail in Milestone M1.1, coving a wide range of locomotive operating condition scenarios.
Task 2: System/platform architecture M2.1 Simulation framework defined M2.2 Performance metrics	*This task will develop the overall rail corridor and train performance simulation framework for ALTRIOS that coordinates simulation modules. It will also establish a data bus structure with variable naming conventions and establish simulation time.* M2.1 Simulation framework defined: A simulation framework template comprising a PyPI-compliant structure of Python packages for the ALTRIOS model modules, which includes formally defined variable naming conventions and other coding standards, is submitted for Program Director approval. This includes platform workflow, customer interaction points, and data flow. This should detail how the

Tasks	Milestones and Deliverables
	ALTRIOS model components interact and pass information, as well as how a central management system keeps track of various algorithm progress and results. A GitHub repository with enforced peer review is established for the team to facilitate efficient co-editing. Define base system, including details on existing practices. Provide details of new approach, including details on modification to existing practices and additional data requirements. Provide mathematical formulation(s) for new approach. Document is submitted for Program Director approval. **Actual performance:** (FY22 Q2) A simulation framework definition document was completed and submitted to ARPA-E. This document provides the ALTRIOS framework definition and includes an introduction, system architecture, and programming standards. M2.2 Performance metrics: Identify performance metrics targeted. These may include computational performance (i.e., hardware specifications, computing cost targets, solution time, solution quality, operational performance metrics). The full rollout model is expected to include many time-dependent parameters, including but not limited to projected energy system performance and cost, freight rail fleet turnover, manufacturing scale/capacity, infrastructure build-out, diesel, and other fuel costs. Document is submitted for Program Director approval. **Actual performance:** (FY22 Q3) ALTRIOS performance metrics were defined, completing this milestone. The overall performance objective of ALTRIOS was to determine a train consist plan and rail traffic, as well as meet the single-train accuracy targets from Milestone M1.2, while achieving reasonable simulation time. This was defined as 12.5 minutes for a full ALTRIOS scenario for 500 single-way train trips over a 700-km rail corridor for a 21-day period on a modern laptop. The key output performance metrics for ALTRIOS are levelized cost per megonne-kilometer (LCOTKM), emissions, and any technology-caused delay time.

Tasks	Milestones and Deliverables
Task 3: Framework development and validation M3.1 Go/No-Go alpha framework M3.2 Beta framework M3.3 Full rollout model M3.4 Final report	*This task will develop and validate the alpha and beta version on the simulation framework.* M3.1 Go/No-Go alpha framework: The initial simulation framework that coordinates simulation modules, establishes a data bus structure, and maintains simulation time. Alpha placeholders for each module are connected to this simulation framework. Data flow through the model is confirmed, and an incremental code testing method is established. Input/output table is documented. Performance metric defined in M2.2 assessment validated through test scenarios defined in M1.2. **Actual performance:** (FY22 Q3) The ALTRIOS team completed the alpha framework, meeting Milestone M3.1, and a "Go" determination was received to begin work on the beta version. The alpha framework coordinated simulation modules, established a data bus structure, and maintained simulation time. This framework consisted of a simulation manager; train consist planner; meet-pass planner; train performance calculator (TPC); a consist powertrain model for conventional diesel-electric, hybrid, and battery variants; and various validation utilities (plotting tools and checks for energy conservation). Data flow through the model was confirmed, and incremental code testing methods were established. The ALTRIOS alpha framework speed and computational targets were exceeded. Preliminary calibration and validation was on track to meet requirements. M3.2 Beta framework: Beta-level submodules have been created for each component and integrated into the framework. This includes models for the physical train energy, rail network, infrastructure, operations, energy system technology, and output metric calculators (including target level of emissions), and LCOTKM. Rollout strategy is documented, as well as input/output user interface per funding opportunity announcement request. Performance metric defined in M2.2 assessment validated through test scenarios defined in M1.2. **Actual performance:** (FY22 Q4) ALTRIOS team completed the beta framework in FY22 Q4, meeting Milestone M3.2. The beta framework provided improved integration and updated submodules. The core functionality of the beta framework was the train corridor simulator. The train corridor simulator consists of the train consist planner, meet-pass planner, TPC, powertrain model, and simulation manager. Each of these components was significantly improved and more fully integrated.

Tasks	Milestones and Deliverables
	M3.3 Full rollout model: Full rollout model validation. Data from the ZANZEFF project are used to conduct train model energy estimation validation over a varying set of conditions and characterize the model accuracy. Illustrative examples of full rollout model scenarios are documented. Document is submitted for Program Director approval. **Actual performance:** (FY23 Q2) The team completed the full rollout model, which pulls together the envisioned functionality of ALTRIOS. The team successfully used ALTRIOS to simulate a range of operating conditions, estimating energy use, and compared this to ZANZEFF data to achieve improved validation of ALTRIOS. ALTRIOS was then used to conduct an improved proof-of-concept rollout analysis, including electric vehicle supply equipment, to illustrate how it can be used to evaluate scenarios for advanced technology deployment. M3.4 Final report: Documentation on all full rollout models, including validation of all metrics. A realistic physical model that can accommodate a wide range of energy system technologies is built, and system performance and energy consumption on a route-by-route basis is validated. **Actual performance:** (FY23 Q3) This document serves as the final report for the ALTRIOS LOCOMOTIVES project. This report includes documentation on the full rollout model. The realistic physical models and supporting framework are described. These models can accommodate a wide range of energy source technologies and provide performance and energy consumption on a route-by-route basis. Validation of these route-by-route energy predictions are provided.
Task 4: Technology to market M4.1 Workshop and stakeholder engagement M4.2 Release open-source code	*This task will provide stakeholder engagement, technology demonstrations (who will receive results and what must be proven to further engage with stakeholders), differentiation of available market products/existing practices, techno-economic analysis, and intellectual property strategy or open-source release plan. Software release plan should include platform (i.e., GitHub), access, curation, and management (post-ARPA-E funding).* M4.1 Workshop and stakeholder engagement: A public stakeholder half-day virtual workshop is held to gather inputs from the broader community and ensure the final product will benefit future technology development and decision-making.

Tasks	Milestones and Deliverables
	The document on stakeholder engagement (value proposition, barriers, and criteria for adoption), model structure, functionality, tech demonstration of planned capabilities, and intellectual property strategy for open-source is submitted for Program Director approval. **Actual performance:** (FY22 Q4) The ALTRIOS team successfully completed M4.1, organizing a LOCOMOTIVES session at the 2022 Railroad Environmental Conference on November 2, 2022, at the University of Illinois Urbana-Champaign campus in Champaign, Illinois. The team worked with the ARPA-E director to plan the session. The session included a recorded introduction by the ARPA-E LOCOMOTIVES program director, presentations from all four LOCOMOTIVES project teams, and a panel discussion on the needs, challenges, and opportunities of modeling to support rail advancements, featuring railroad, locomotive manufacturer, and agency stakeholders. M4.2 Release open-source code: The open-source software code is prepared and publicly released on GitHub. Documentation of the code is provided. A "getting started" tutorial will guide new users through setting up and running a simulation. A set of example assumptions that reflect the most current public information is provided with example results. **Actual performance:** (FY23 Q3) ALTRIOS was released on June 23, 2023, as an open-source software tool using the BSD 3-Clause license open-source license agreement on GitHub: www.nrel.gov/transportation/altrios.html. This includes documentation, a "getting started" guide, and a set of example assumptions. This successfully meets Milestone M4.2. ALTRIOS Lite, a web-based version of ALTRIOS, was also released and can be found at the same website.

Background

The U.S. freight rail system consumes roughly 3.4 billion gallons (12.9 billion liters) of diesel fuel annually. Combustion of this diesel produces criteria pollutants (hydrocarbons, carbon monoxide, nitrogen oxides, and particulate matter) and emissions (including carbon dioxide [CO_2], methane [CH_4], and nitrous oxides). All six Class I North American railroads have signed up for Science Based Targets initiative goals, with commitments to reduce greenhouse gas (GHG) emissions on the order of 30%–40% by 2030. The path to reach these goals remains uncertain. Challenges include significant capital costs for locomotives, supporting appurtenances such as energy tenders and refueling infrastructure, high instantaneous power

requirements for locomotives, large energy demand, the need for that energy in remote locations, and interoperability of locomotives throughout North America. The industry has a large installed base of diesel-electric locomotives (approximately 22,000) and a need for high reliability. Many potential advanced technologies—such as hydrogen, biofuels, and batteries—are being developed and promoted as potential solutions, but the question remains about how each pathway can be used to minimize cost and environmental impacts, compounded by the potential for decreased operational efficiency.

ALTRIOS Overview

ALTRIOS is a unique, fully integrated, open-source software tool used to evaluate strategies for cost-effectively deploying advanced locomotive technologies and associated infrastructure. ALTRIOS simulates freight-demand-driven train scheduling, mainline meet-pass planning, locomotive dynamics, train dynamics, energy conversion efficiencies, and energy storage dynamics of line-haul train operations. Because new locomotives represent a significant long-term capital investment, and new technologies must be thoroughly demonstrated before deployment, this tool provides guidance on the risk/reward trade-offs and operational integration of different technology rollout strategies. An open, integrated simulation tool is invaluable for identifying future research needs and making decisions on technology development, routes, and train selection.

For a given rail corridor, freight transportation demand, and alternative technology locomotive deployment strategy, ALTRIOS will develop a logistically feasible train plan, simulate 21 days of baseline train operations over the corridor, and calculate the corresponding yearlong energy consumption, costs, and emissions, including CO_2, CH_4, and nitrous oxides. Then, according to the year-by-year locomotive deployment strategy and user-specified traffic growth, the process of developing a feasible train plan is repeated, simulating train operations and calculating outputs for each subsequent year in the specified time horizon. At the end of the time horizon, annual and cumulative results are reported. The user, or an automated optimization routine, can then adjust various tunable parameters and repeat the entire model process to quantify changes in the annual and cumulative outputs. The schematic shown in Figure 1. describes the process flow of the software with tunable parameter and simulation-time-variant assumptions feeding modules that carry out the calculations. The “Simulation Manager: Rail Corridor and Train Performance Simulator” module manages communication between the various other modules at appropriate time intervals. External models can be used to model emissions, electric grid costs, and hydrogen costs with respect to renewable fraction and demand growth. The outputs of emissions, time, LCOTKM, and optional user-defined objectives can also be provided to a multi-objective optimization algorithm.

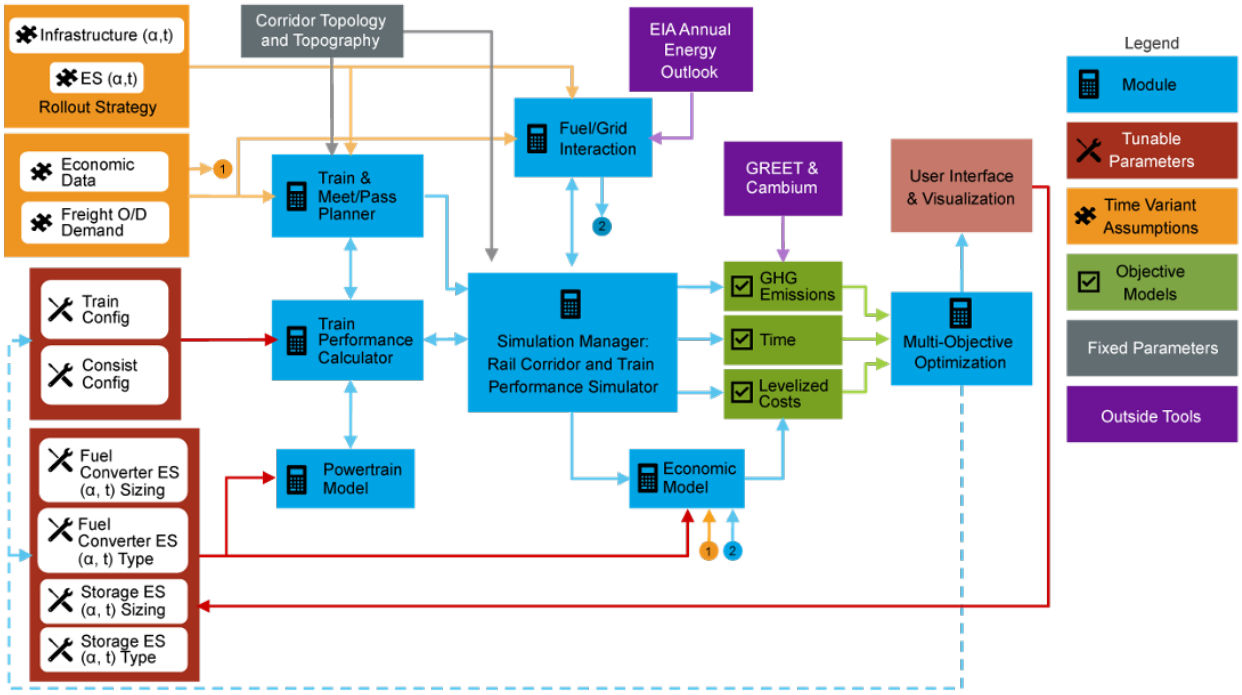

Figure 1. ALTRIOS schematic, high-level data flow, major models, and output simulation modes

Simulation Modes

To allow flexibility and meet the needs of various simulation scopes, ALTRIOS is designed to support five simulation modes: locomotive/consist, single train, network, technology rollout, and calibration.

The locomotive/consist simulation is the simplest simulation mode. This mode uses a subset of the "train model" to simulate a single locomotive or consist based on a required power trace. It is intended to verify locomotive performance and operation prior to full-scale simulations. The inputs for this mode are locomotive type (conventional, hybrid, fuel cell, or BEL) and the power trace, specified in watts. Component parameters such as state-of-charge (SOC)-dependent and charge/discharge-rate-dependent battery efficiency, alternator efficiency, engine efficiency, and auxiliary loads have been calibrated to current production locomotives and components but can be modified as desired. This mode outputs a time series of powertrain performance data. It also includes aggregate data such as total fuel or energy usage.

The single-train simulation mode is used to simulate one train along a specified route. This simulation mode is intended to help understand train performance in a single configuration on a specific route. The additional inputs for this mode are the network; locomotive type and count; railcar type, count, and load; and an optional speed trace for a given territory. If a speed trace is not specified, the maximum speed limit is followed as closely as physically possible. The output of this mode includes aggregate and time-series data, including powertrain performance and train dynamics.

The network simulation mode allows a user to schedule, configure, and simulate a fleet of locomotives and cars based on origin/destination freight demands for a rail network. Figure 2.

shows the data flow for the network simulation. Note that a subset of this diagram is needed for the single-train simulation described above. The network simulation can be used to understand how a fixed locomotive pool can be used to move a fixed freight demand within a network. It can help answer questions like how BEL charging time, infrastructure location, and refueling infrastructure sizing will impact the required locomotive pool size. This mode requires inputs of locomotive fleet size and type, locomotive servicing intervals, rail network definition, infrastructure location and type, and freight demands. The outputs for this mode will include aggregate and time-series data for each train that can be processed using the life cycle analysis calculator described later in this document.

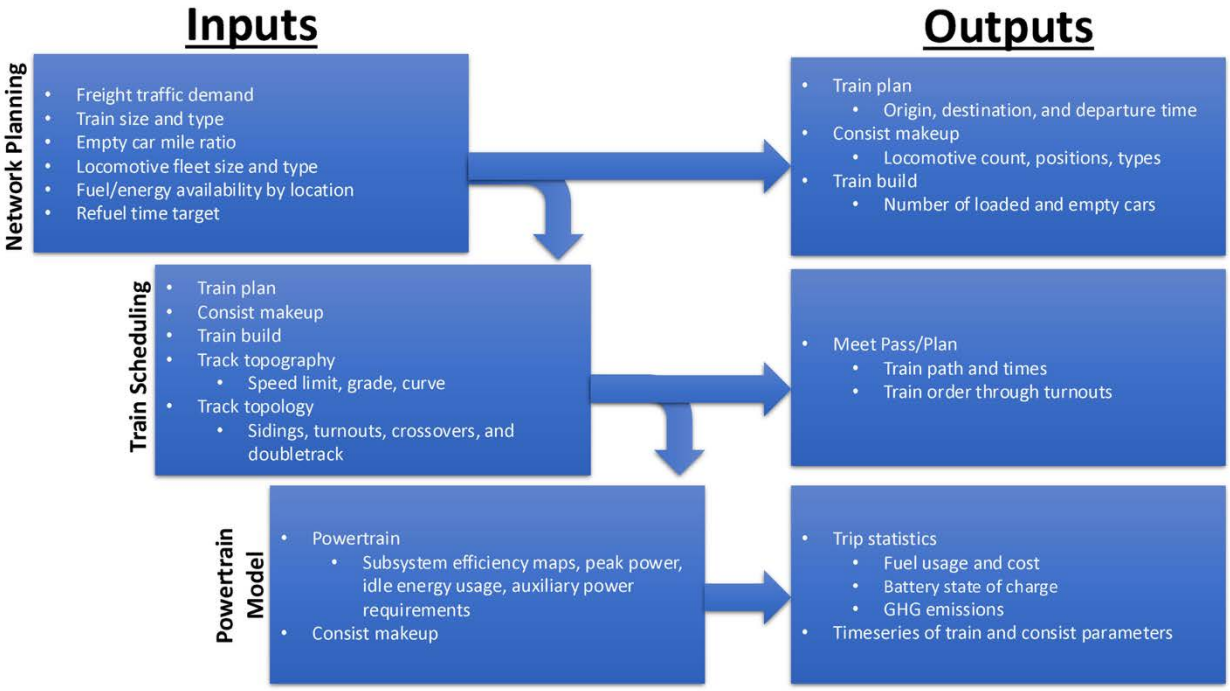

Figure 2. Overview of ALTRIOS network simulation conceptual data flow

The rollout simulation mode is used to understand multidecadal technology rollout strategies. This includes the changing technology characteristics (e.g., $/kWh of battery), economic environment (e.g., fuel costs), and adoption rates and infrastructure needed for various technologies to achieve desired outcomes, such as emissions reductions. For example, it can simulate how many new BELs are purchased, delivered, and deployed per year over a user-defined timeline. The inputs for this simulation mode are similar to the network simulation; however, the parameters can change for each year simulated. These include locomotive fleet composition, energy cost, energy, emissions, and freight demand. Time-related parameters such as fleet turnover rate also need to be defined. The outputs for this simulation are grouped by year and include cost, emissions, energy usage by type and location, and detailed train performance. These data can then be used by the life cycle analysis calculator to calculate the marginal carbon abatement cost in U.S. dollars per metric ton of CO_2 equivalent.

The calibration simulation mode was developed to calibrate railcar, locomotive, and component models against actual test data. These simulations use a single train or locomotive simulation to fit the model to test data. The exact inputs will vary based upon what is being calibrated.

System Architecture and Modules

The train corridor simulation, illustrated in Figure 3., is the foundation of ALTRIOS simulations and consists of the train planner, meet-pass planner, TPC, and powertrain model. It is coordinated by the simulation manager.

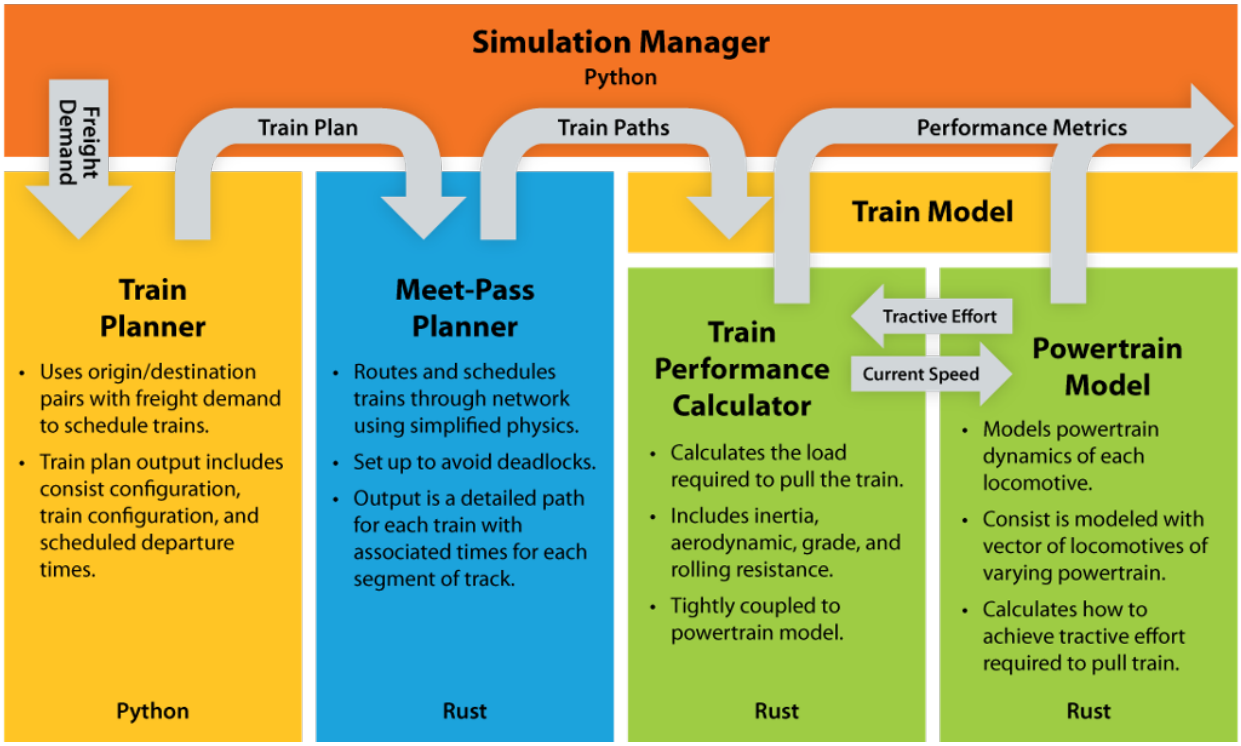

Figure 3. Train corridor simulator

Simulation Manager

The simulation manager performs various functions to coordinate the activities of individual ALTRIOS modules and track the overall performance of the rail network under study. The simulation manager first runs the train planner, which uses railway freight transportation demand by train type between origin and destination or entry/exit points along the corridor to develop a train plan, generating the traffic demand over the rail network. The train plan is then passed by the simulation manager to the meet-pass planner, which generates target train path time/distance profiles for the full set of trains, assuring a conflict-free schedule. The train paths are then used by the simulation manager to queue a set of train simulations for the coupled TPC and powertrain models. The TPC does car- and locomotive-wise calculations of train-resistive forces. The TPC and powertrain model then iteratively pass information in each time step to simulate the train performance. The powertrain model provides an energy flow model of each locomotive and the locomotive consist using interpolation-based models of powertrain components including the engine, generator, battery, power electronics, and motor with

tunable energy-optimal control features. Once the train performance and energy use are simulated, the simulation manager collects these results and prepares them for the GHG emissions and LCOTKM calculators.

Train Planner

The primary function of the train planner is to transform user-specified railway freight transportation demand by train type between origin and destination (entry/exit) points along the corridor into a train plan. The train plan specifies the number and type of trains to operate between each origin and destination pair during the simulated mainline operations. For each train, the train plan further specifies the number of empty and loaded railcars in the train consist, the number of each type of locomotive assigned to that train, and the scheduled departure time of the train from its origin terminal on the simulated corridor or network.
The train planner requires user input (Table 2.) specifying freight traffic demand on the study corridors, including origin, destination, type of traffic, and quantity in number of railcars or intermodal units (trailers or containers). The freight traffic input is divided into three categories: intermodal, bulk unit train commodities, and general carload manifest train shipments. The user must also specify an initial assignment of locomotives to the various train origin points in the network. The required locomotive information includes an estimate of the maximum number of tons or railcars the locomotive is capable of hauling, type of locomotive (fuel/energy source), and estimated refuel/charge time before it is capable of redeployment. The types of locomotives specified by the user may include a combination of advanced energy source locomotives and current diesel-electric locomotives to reflect the state of alternative locomotive technology deployment in the scenario being investigated.

Table 2. High-Level Inputs for the Train Planner

Input	Description
Manifest empty return ratio	Ratio of railcars in manifest train service that are returned to origin location empty.
Locomotive pool	A list of locomotives that are available to pull trains, including the type and power rating of each locomotive.
Locomotive types	Defines the specifications for each locomotive type, including servicing (refueling) time and capacity. Each type can have a different servicing time to capture different behaviors.
Simulation days	The number of days to simulate. The default is 21 days so that the middle week can be used as an average/steady-state snapshot for the network.
Freight demand	Annual freight rail transportation demand between each origin/destination pair for each of three train types specified: intermodal trains by annual number of containers shipped, unit trains by number of loaded bulk commodity railcars, and/or manifest trains by number of loaded single-carload freight railcars.

Other user input required by the train planner includes a target manifest train empty railcar return ratio (R), which is defined as the ratio of empty to loaded railcars traveling in manifest

trains between all demand pairs. The *R* value can either be defined for each demand pair separately, or set as a constant value for the entire simulated network.

A summary of the high-level inputs for this module is shown in Table 2.. These inputs are what the user will most likely interact with when performing a network simulation. Additional inputs can be configured for each locomotive, rail vehicle, and network, but the default values for these items will be satisfactory for most users.

An overview of functions included in the train planner is shown in Figure 4. The train planner uses four major component processes and several intermediate steps to transform the freight demand and network topology provided by the user into a final train plan that serves as input to other modules. Each of the four component processes are described in the following sections.

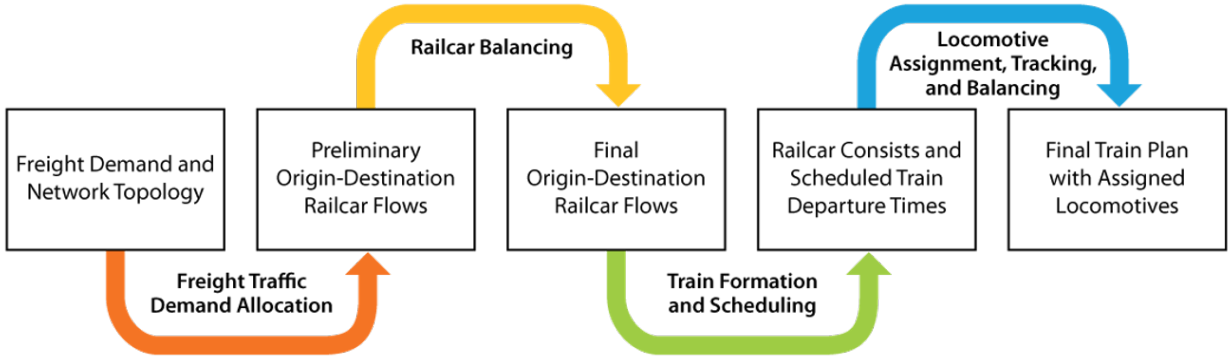

Figure 4. Overview of the train planner

Freight Traffic Demand Allocation

Using the freight demand and network topology input data specified by the user, the train planner code initiates an automatic train planning and scheduling process that, for each train operating between a given origin-destination pair, outputs its theoretical planned time of departure at origin, number of loaded and empty cars in the train consist, and locomotive assignment. To accurately simulate a network traffic pattern based on the pattern of loaded freight traffic demand specified by the user, empty railcar return trips back to their origin must be generated and added to the origin-destination traffic demand matrix. The number of empty cars generated for the loaded traffic demand moving between each origin-destination pair is calculated and merged into the overall preliminary origin-destination railcar flows output from this intermediate step. The number of empty cars generated by each train type is different and calculated as follows:

- For bulk commodity unit trains, each loaded train from origin *i* to destination *j* is assumed to generate a corresponding empty unit train moving from node *j* to node *i*.
- For intermodal trains, the railcars are assumed to shuttle between a given pair of nodes. For a given pair of nodes (*i*, *j*), the direction with the largest container demand will not have any empty railcars, while the direction with the lower container demand is supplied with additional empty railcars to balance-match the total demand for loaded railcars in the opposite direction.

- For single-carload manifest train shipments, empty carloads in both directions are generated according to the manifest empty return ratio *R* specified by the user. Based on the number of loaded manifest cars to be transported from node *i* to node *j* (Lij) and node *j* to node *i* (Lji) specified by the user, the train planner calculates a corresponding number of empty manifest cars to transport from node *i* to node *j* (Eij) and node *j* to node *i* (*Eji*), such that the desired empty return ratio for each *i-j* link can be achieved, and the total number of railcars in the network is conserved:

$$Rij = (Eij + Eji)/(Lij + Lji) \quad (1)$$

The example output of a planned train is shown in Figure 5.

```
34 D to B 17.0 Train Type: Intermodal
number of  loaded cars: 44.0 number of  empty cars: 55.0
Engine_Number    4005
```

Figure 5. Example output of the train planner

Railcar Balancing

For manifest traffic, most origin and destination pairs will have different loaded railcar demands in each direction. When these directional demands are substantially different, it is difficult to satisfy the empty railcar return ratio on an origin and destination train pair basis while also conserving the number of railcars in the system. Differences in train sizes can cause an excess of empty railcars at one node, while unsatisfied demand for empty railcars to load continually builds at another node. To alleviate this situation, the train planner conducts a railcar balancing process step to create additional empty railcar movements.

The railcar balancing algorithm uses a method similar to a bubble sort that finds the first node with a surplus of empty railcars, and then, during the first iteration, sends a number of empty cars to the first node with a deficit of empty railcars. After each iteration, the number of cars dispatched and received is updated, a new first surplus node is identified, and another iteration is initiated until all nodes have a balanced number of dispatched cars and received cars. This algorithm will repeat the process of searching for unbalanced railcars across all nodes and plan for additional empty car shipments after each iteration. When possible, these empty railcar movements are added to trains that are already in the train plan. In rare cases, if the number of empty railcars to reposition exceeds the length constraints of planned trains, additional trains of empty railcars are inserted into the train plan. Once complete, this intermediate step generates a final set of origin-destination railcar flows.

Train Formation and Scheduling

After the railcar rebalancing algorithm ends, the final number of railcars for all origin-destination pairs and all train types is calculated and summarized. The total number of loaded and empty railcars for each origin-destination pair and for each train type is assigned to specific trains through the train formation and scheduling process. The number of trains of each type between each origin-destination pair is calculated and rounded by dividing the final railcar flows by the desired train length.

Once the total number of trains of all types departing from a given node each day is determined, the individual train departure times are scheduled. To help create an even flow of train departures that minimizes congestion and demand on origin terminal servicing facilities, the train departures at a given node are evenly distributed during a 24-hour period. For example, if a given node departs six manifest trains, four intermodal trains, and two unit trains per day for a total of 12 outbound trains, the trains will be scheduled to depart at 2-hour intervals. The output of this train formation and scheduling process is a set of train departure times and corresponding train consists with numbers of loaded and empty railcars.

As an alternative to this train planning process, a user can also simulate a specific set of trains with known individual characteristics (e.g., total tons, length, and number of loaded and empty railcars). These trains must be defined in an input file with the same format and data fields as the output of the train planner so that this user-specific information can be used by other ALTRIOS modules.

Locomotive Assignment, Tracking, and Balancing

The final train planner component process is to assign locomotives to each planned train departing each origin node. Each node is assigned an initial reservoir of locomotives with corresponding power and identification information. The pool of locomotives can contain locomotives of different types, including conventional diesel-electric locomotives. A key constraint is that locomotives can only be assigned to pools at terminals that also have the corresponding fueling and/or energy supply infrastructure required to service that locomotive type. After each train departure is planned, the reservoir of locomotives is updated with the departing locomotives removed from the origin reservoir, and added to the en route locomotives that are processed with respective travel time. The locomotives arriving at destination nodes are put into the back of the servicing queue that refuels or charges the locomotives depending on the type of power and SOC. The estimated ready time consists of two parts, travel time and servicing time. The detailed ready-time formula is as follows:

$$T_{Ready} = T_{Travel} + T_{Service} = \frac{D_{Travel}}{v_{average}} + \max\left(T_{handling}, T_{queuing} + \frac{V_{empty}}{r_{refuel}}\right) \quad (2)$$

Where r_{refuel} represents the refuel rate in percentage per time unit or volume per time unit, depending on the propulsion energy; $T_{queuing}$ represents time spent waiting in the refueling queue; $T_{handling}$ represents a separate minimum amount of time needed for handling locomotive turnaround; and V_{empty} stands for required refueling volume or SOC that needs to be serviced.

As each train is planned, the origin pool runs a precheck to identify the locomotive(s) to assign to the train based on factors such as train size/weight, power requirements, and available locomotive charge and fuel refill status. The higher-level logic is to assign locomotives in a first-in, first-out order, with locomotives arriving at the servicing facility earliest being the next to be assigned to planned outbound trains, shown in Figure 6..

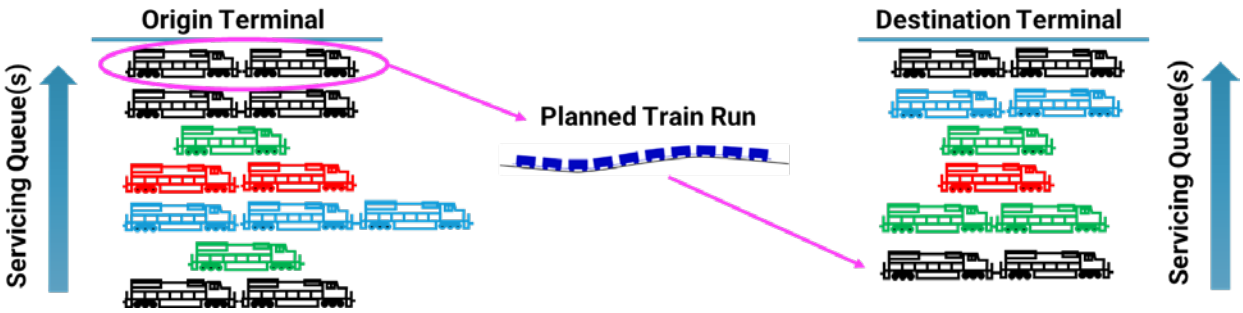

Figure 6. Demonstration of the locomotive pool order arrangement

A screenshot of the locomotive pool updating process for a hypothetical test scenario is shown in Figure 7. For a hypothetical test case, the train planner can develop a final train and consist plan output of 1,320 locomotive dispatches (and 1,320 refueling or recharging sessions) and 440 total train consists, operating over 21 days, in 15 seconds.

Pool B	Engine_Number	Type	Capacity_Cars	Capacity_Tonnage	Refill_Time
0	2009.0	BEL	100.0	25000.0	0.0
1	2011.0	BEL	100.0	25000.0	0.0
2	2012.0	Type1	60.0	30000.0	0.0
3	2013.0	Hydrogen_Cell	80.0	20000.0	0.0
4	2014.0	Type1	60.0	30000.0	0.0
5	2015.0	Hydrogen_Cell	80.0	20000.0	0.0
6	2016.0	Type2	100.0	25000.0	0.0
7	2017.0	Hydrogen_Cell	80.0	20000.0	0.0
8	2018.0	Diesel_Medium	120.0	30000.0	0.0
9	2019.0	Diesel_Small	90.0	20000.0	0.0
10	4000.0	Diesel_Medium	120.0	30000.0	0.0
11	4001.0	Type2	100.0	25000.0	0.0
12	1000.0	BEL	100.0	25000.0	0.0
13	3002.0	Diesel_Small	90.0	20000.0	0.0
14	4004.0	Diesel_Small	90.0	20000.0	0.0
15	4005.0	Type2	100.0	25000.0	0.0

Figure 7. Example intermediate locomotive pool at a node

The output of the train planner is a final train plan consisting of a set of scheduled trains and locomotive assignments. Each scheduled train includes a departure time, consist of specific locomotives, and a set of empty and/or loaded railcars. This information is subsequently used by the meet-pass planner. The train planner output also includes the location and timing of planned locomotive fueling and charging events for later use by the economic model.

Meet-Pass Planner

The meet-pass planner takes the network topology file and the output of the train planner as input, and develops a complete, conflict-free, time-distance path for each train to take through the track network. The path specifies the exact tracks the train will follow from origin to destination, and estimates of times and speeds along the route to serve as performance targets for the later train performance simulation. The meet-pass plan and corresponding set of train paths are typically constructed to minimize train delay (waiting) time and can be formulated as an optimization problem. However, the train volume, geographic, and temporal scope of operations that most users wish to simulate will likely exceed the capability of a mixed-integer

program to generate an optimal train dispatch and meet-pass plan. Thus, a heuristic solution is required, and the project team developed and implemented an appropriate dispatching algorithm to arrange meets and passes between opposing conflicting trains and determine the individual train paths. The meet-pass planner has two major components:

- The train pre-simulator uses the TPC (described in the next section) to generate a compactly represented network of estimated travel times for each potential path from origin to destination for each train. The estimated times are subsequently used by the dispatching algorithm to track the order trains pass control points along the network, identify conflicts, and reroute trains to resolve them. The pre-simulation also estimates overall train energy consumption to help ensure that the locomotive assignment for each train is satisfactory and estimate the remaining fuel/energy on board each locomotive when the train arrives at its destination.
- The deadlock-free dispatching algorithm resolves all conflicts between train paths that arise based on their scheduled departure times in the final train plan created by the train planner. Without such an algorithm, the simulation manager could unrealistically depart trains from terminals and advance them along the corridor in such a manner that opposing trains are permanently halted by irreconcilable train conflicts with no feasible path forward. This is a particular challenge for managing train traffic flow on the single-track corridors that compose approximately 70% of high-density mainline corridors within the U.S. rail network. The novel dispatching algorithm implemented within ALTRIOS works with any combination of trains and track layout configuration. The algorithm uses the estimated times from the pre-simulator to identify train path conflicts and then arrange meets between opposing trains to ensure that all trains have a free path all the way to their destination at all intermediate meet-pass plan solution time steps. For more details on the algorithm, see [1], [2].

The final output of the meet-pass planner is a set of train paths. Each train path is an exact sequence of train departure, meet, and pass events for execution, on an individual train-by-train basis, by the main simulation manager using the TPC and corresponding locomotive powertrain models.

Figure 8. is a time-distance “stringline” diagram of the train meet-pass plan output for a portion of a simulation scenario examining a single-track mainline corridor with 18 trains/day. This meet-pass result (set of train paths) shows that the dispatching algorithm consistently resolves conflicts between opposing trains by “meeting” trains at passing sidings in a manner that generally optimizes train trajectories to minimize total overall train delay. In the example stringline diagram, trains traveling in opposing directions pass each other where their train paths (diagonal lines) cross. The horizontal portions of these train path lines indicate where the train is waiting for another train to pass.

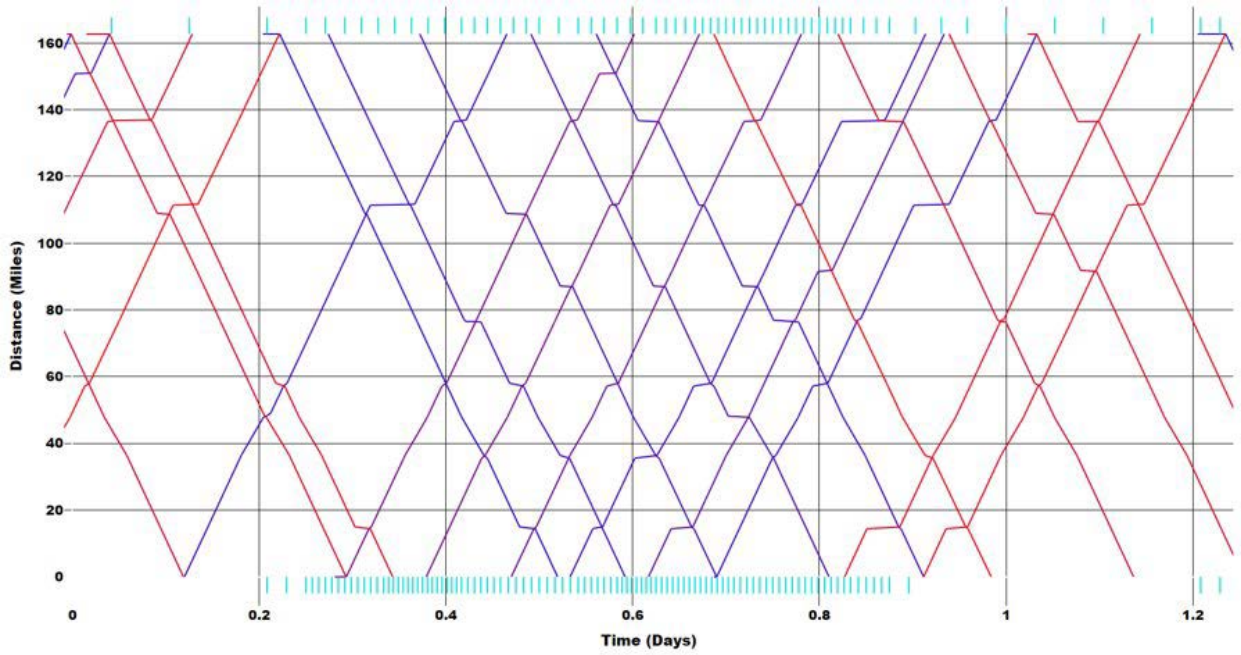

Figure 8. Portion of the meet-pass planner stringline for a single-track mainline corridor

Train Performance Calculator

The TPC calculates all train-resistive forces (bearing, rolling, aerodynamic, grade, and curve) given only current location, current speed, track location topological information (e.g., grade, curvature along the path the train currently occupies), and train consist information from the train consist planner. The TPC is tightly coupled to the powertrain model, which captures locomotive dynamics. The two modules execute concurrently and have been highly optimized so that simulations complete rapidly.

Train Consist and Resistance Model

Within the TPC, each train is represented by a distinct train consist model that includes total length, weight, axle count, braking force, a rotational inertia factor, and several train resistance factors—specifically a constant resistance value (composed of bearing resistance and rolling resistance), an aerodynamic resistance factor C_dA, and a truck type factor that relates to the curve resistance table in the Association of American Railroads (AAR) Train Energy Model [3]. These parameters are computed by appropriately combining the characteristics of each individual railcar in the train.

To minimize the required computing time, the TPC uses only these summary train consist parameters. For example, the total train weight is assumed to be distributed evenly (in a "mass strap") along the entire length of the train. If minimizing computation time for the TPC becomes less important in the future or more accurate computations become necessary, the TPC could be expanded to simulate each railcar as a discrete object with rigid connections between each. This would allow the computation of quasi-static in-train forces at each coupler connection in the train. This information could then also be used to improve the train driving strategy at the cost of further complexity and computing time.

The TPC operates using Euler numerical integration and a configurable discrete time step [4], enabling a trade-off between simulation accuracy and computation time. For each discrete time step, the net resistance D_N is calculated as follows:

$$D_N = D_R + D_A + D_G + D_C \tag{3}$$

where D_R is the current rolling resistance, D_A is the current aerodynamic resistance, D_G is the current grade resistance, and D_C is the current curve resistance. Several of these resistance terms have more detailed expressions, starting with rolling resistance:

$$D_R = a_n n + a_Q mg \tag{4}$$

where a_n is the average bearing resistance per axle, n is the number of axles, a_Q is the average rolling resistance per weight, and $g = 9.81\ \mathrm{m/s^2}$ (gravitational acceleration). Note that this value is assumed to be constant within the train consist model.

Aerodynamic resistance is calculated using Equation (5):

$$D_A = \frac{1}{2}\rho C_D A v^2 \tag{5}$$

where ρ is the density of air, $C_D A$ is the drag coefficient multiplied by the drag area of the entire train, and v is the current velocity of the train. ρ is currently a constant value, but will become dependent on elevation in a future version of the TPC. The constant term $C_D A$ includes both cross-sectional drag and skin friction. There are no terms directly proportional to velocity in Equations (4) or (5) because these terms are typically negligible for freight trains.

Grade resistance is calculated with the following equation:

$$D_G = mg\frac{h_f - h_b}{L} \tag{6}$$

where h_f is the front-of-train elevation, h_b is the back-of-train elevation, and L is the train length. The fractional term is the current average gradient over the train length. Thus, it is implicitly assumed that train mass is evenly distributed along the length of the train ("mass strap" assumption).

Curve resistance is based on interpolating over the table of curve resistances in the AAR Train Energy Model according to the specified railcar truck (bogie) types in the train consist model [3]. Curve resistance is calculated using a strap method similar to that used for vertical gradient, in which truck type coefficients are averaged over the train length and multiplied by curvature along the route to obtain cumulative curve resistance.

Simulation of Train Motion and Dynamics

To efficiently ensure that the train is never required to exceed its braking capabilities, a backward pass along the train path is first performed. All instances of speed limit decreases (in the forward time direction) are sequentially marked and simulated backward using the maximum braking force plus the net resistance (as calculated above) as the force applied to the train. The acceleration of the train is thus computed as follows:

$$a = \frac{F_{Bmax} + D_N}{m_{adj}} \tag{7}$$

where a is the train acceleration, F_{Bmax} is the maximum braking force, and m_{adj} is the train mass adjusted for the rotational inertia of the wheels and axles assuming rolling without slipping. m_{adj} is typically about 3% larger than m and is derived from the rotational inertia factor in the train consist model.

Assuming this acceleration value (and thus the associated forces) is constant for each time step, Euler integration is performed to determine the new position and velocity as follows:

$$v = v_0 + at_s \tag{8}$$

$$x = x_0 + t_s\left(v_0 + \frac{at_s}{2}\right) \tag{9}$$

where t_s is the discrete time step, v_0 is the previous velocity, v is the current velocity, x_0 is the previous position, and x is the current position.

The result of this back-calculation process is an ordered list of speed targets that, when viewed in the forward direction, can be used in the following equation to calculate the target force for the locomotive consist F_{LT}:

$$F_{LT} = D_N + m_{adj}\frac{v_t - v}{t_s} \tag{10}$$

where v_t is the target velocity (result of back-calculated braking curves) and v is the current velocity. This target locomotive force will often exceed the capabilities of the consist because the value for t_s is on the order of 1 second. Thus, the actual locomotive consist output power and force will be limited later in the TPC. Also note that the placement of the v_t values is such that so long as the train applies maximum braking if it is going faster than the v_t value, its speed will drop below the v_t value before the actual speed limit goes into effect.

To determine the actual force output by the locomotive consist, the maximum available tractive force of the locomotive consist F_{max} is first calculated as follows:

$$F_{max} = \min\left(F_{\mu}, \frac{P_{max}}{\min(v_t, v_{max})}\right) \tag{11}$$

where F_{μ} is the tractive force at the adhesion limit, P_{max} is the current maximum power that the consist can produce, and v_{max} is the speed that the train would reach after the consist outputs maximum power for one time step. v_{max} is calculated according to the following equation:

$$v_{max} = 0.5 * \left(v - \frac{D_N t_s}{m_{adj}} + \sqrt{\left(v - \frac{D_N t}{m_{adj}}\right)^2 + \frac{4P_{max}t_s}{m_{adj}}}\right) \tag{12}$$

After the maximum available tractive force is calculated, the actual locomotive consist force F_L is calculated as follows:

$$F_L = \min(F_{max}, max(-F_{Bmax}, F_{LT})) \tag{13}$$

Lastly, the train acceleration is calculated as:

$$a = \frac{F_L - D_N}{m_{adj}} \tag{14}$$

and Euler numerical integration is used according to Equations (8) and (9) to update the position and velocity of the train. In addition to this, the total power output by the locomotive consist P_L is calculated as:

$$P_L = F_L v \tag{15}$$

and sent to the powertrain model along with the current time $t = t_0 + t_s$ and the current velocity v.

After simulating a train along the entire path specified by the meet-pass planner, the total dwell, running time, and energy consumption for each type of locomotive in the consist are computed as key outputs. This process is repeated in parallel for all trains in the train plan to generate the complete output. Lastly, this module has an option to log its detailed internal state at each time step to help with debugging and validation, and to produce graphics for train performance by time and location.

Train Braking and Speed Control

The TPC also includes a train brake model that simulates idealized, instantaneous full-service braking, and this idealization has minimal impact on energy consumption accuracy due to the fact that the majority of braking effort in both real-world train operation and the model is handled by dynamic braking of the locomotive consist.

Train control is currently handled by the following algorithm using the equations introduced in the previous section:

1. Transform all speed limits into a single speed path of maximum authorized speeds referenced to the position of the front of the train. This differs from the network speed limit representation because this new representation extends each speed restriction by the train length. This refinement ensures that a train cannot begin accelerating to a higher speed until the final car in the train has passed the end of a speed restriction.
2. Sequentially find all speed limit reductions starting at the destination and simulate a full-service brake application backward until intersecting with the speed limit path. Additional adjustments have been added to account for the delay and ramp-up time in the improved braking model. This calculation is used to control train deceleration during the forward simulation.
3. As the train is simulated traveling forward, calculate the desired acceleration by dividing the change in speed required to reach the target speed (minimum of speed limit and limit defined by backward braking calculations) by a single time step. To make this desired acceleration feasible, enforce an upper limit of the maximum power and force that the powertrain can currently output and enforce a lower limit of the maximum braking force.

In addition to the above control algorithm, stop targets (zero speed limits) are sequentially removed from the speed path based on the need to meet and/or stop for opposing trains as prescribed in the meet-pass planner dispatching results. This has the effect of ensuring that the

simulated train never exceeds the limits of the planned path provided by the meet-pass planner.

Powertrain Model

The powertrain model was written to allow for the definition of a range of powertrain types, including conventional diesel-electric locomotives, with various fuels, hybrid, and battery-electric powertrain options. The model uses a component-based power flow approach. This approach simplifies the calibration process and enables flexibility when creating different powertrain architectures. The powertrain module consists of several submodules and corresponding component classes with the following structure:

- Locomotive submodule, comprising:
    - Class for conventional locomotive, comprising:
        - Fuel converter: Converts fuel into energy (e.g., engine, fuel cell).
        - Generator: Converts mechanical energy from the fuel converter into electrical energy that can be used in the reversible energy storage (RES) or electric drivetrain.
        - Electric drivetrain (i.e., power electronics and motors).
    - Class for hybrid locomotive, comprising:
        - Fuel converter.
        - Generator.
        - RES: Includes batteries, ultracapacitors, and similar technologies. The model will allow for stopped and/or in-motion catenary charging capability.
        - Electric drivetrain.
    - Class for BEL, comprising:
        - RES.
        - Electric drivetrain.
- Consist submodule, comprising:
    - Class for modeling locomotive consist as vector of locomotives.
    - Methods for aggregating various results and parameters across vector of locomotives.
- Fuel converter submodule with class for fuel converter, comprising:
    - Function for getting current maximum possible shaft power at current time step based on maximum power rating, ramp-up rate, and actual power output at previous time step.
    - Function for getting efficiency and fueling rate as a function of required output power based on a 1D interpolation of a table containing a vector of possible powers and a corresponding efficiency vector.

- Generator submodule with class for generator, comprising:
    - Function for getting maximum possible electrical output power and maximum possible ramp-up rate at the current time step based on efficiency, maximum power rating, and maximum possible engine shaft output power.
    - Function for getting efficiency and required mechanical power input as a function of required output power based on a 1D interpolation of a table containing a vector of possible powers and a corresponding efficiency vector.
- RES submodule with class for generator, comprising:
    - Function for getting current maximum possible electrical output power at current time step based on current RES state of charge, maximum power rating, and ramp-in and ramp-out minimum and maximum SOC buffers.
    - Function for getting efficiency as a function of required output power, SOC, and temperature based on a 3D interpolation of a table containing vectors of C-rate, SOC, temperature, and corresponding efficiencies for chemical ↔ electrical energy conversions.
- Electric drivetrain submodule with class for electric drivetrain, comprising:
    - Function for getting maximum possible mechanical output power at the current time step based on device efficiency, maximum power rating, and maximum possible generator + RES output power.
    - Function for getting efficiency and required electrical power input as a function of required output power based on a 1D interpolation of a table containing a vector of possible powers, and a corresponding 1D efficiency vector.

These components and possible irreversible and reversible mechanical, electrical, and chemical energy flows are shown in Figure 9.

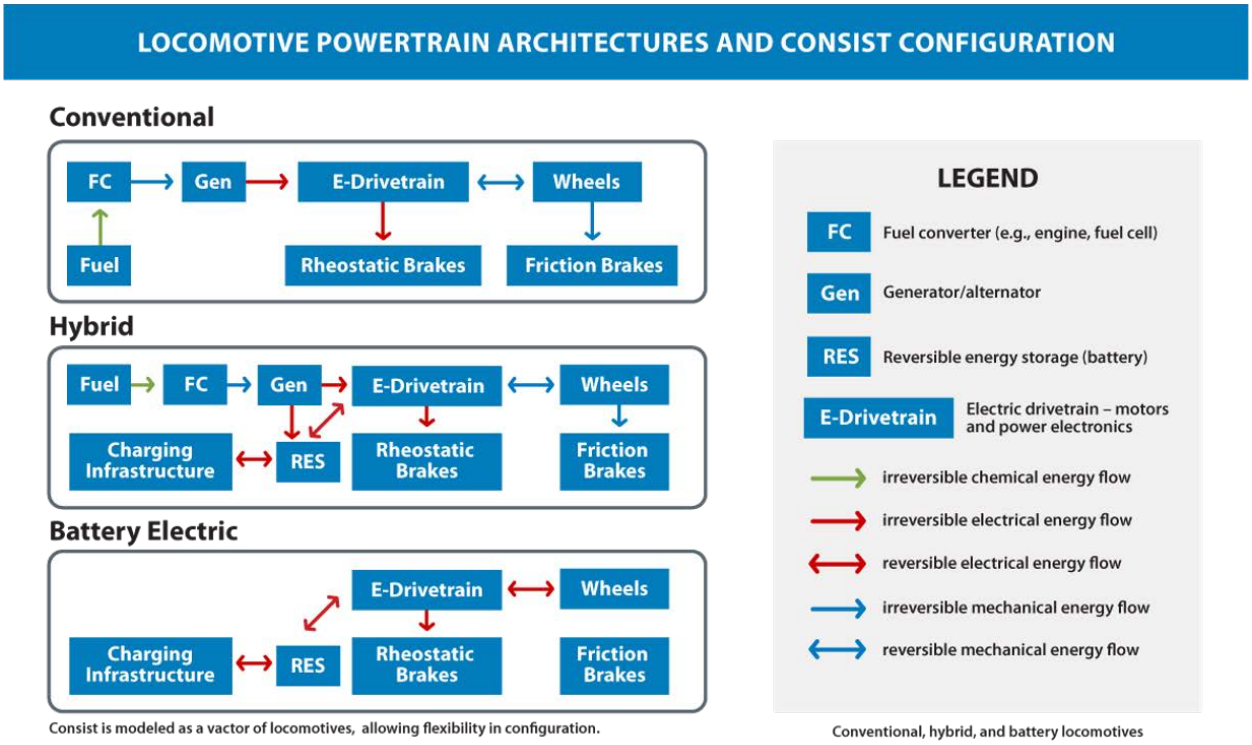

Figure 9. Diagram of possible power flow paths for conventional, hybrid, and battery-electric locomotives.

Note: Green arrows indicate chemical energy flows, red arrows indicate electrical energy flows, and blue arrows indicate mechanical energy flows. Lines with beginning and ending arrows indicate reversible (with efficiency limitations) power flows. Lines with only ending arrows indicate irreversible power flows.

Fuel Converter

Fuel converters are modeled as a submodule of the locomotive. A fuel converter is any device that converts fuel energy to another form of energy (e.g., mechanical, electrical). For example, a fuel converter can be an engine, fuel cell, generator, energy storage system (battery), or electric drivetrain (power electronics and motor). Fuel converters and generators are both currently modeled with 1D efficiency versus output power maps. The electric drivetrain is also currently modeled this way, but this is possible to expand to include train speed as a second dimension.

An example of a 1D efficiency map is shown in Figure 10. This is the map used for the default diesel engine used by the model. This map was derived from test data from a Wabtec ET44C4 locomotive, which meets Tier 4 emissions requirements designed to significantly decrease emissions from non-road diesel engines. A 1D map is sufficient to represent this engine because it operates on a notch schedule, which is a set of discrete engine speed and load combinations. Note that this default engine efficiency map may not be representative of other diesel locomotive engine models and U.S. Environmental Protection Agency tiers, and the user should use engine efficiency values applicable to their particular case study.

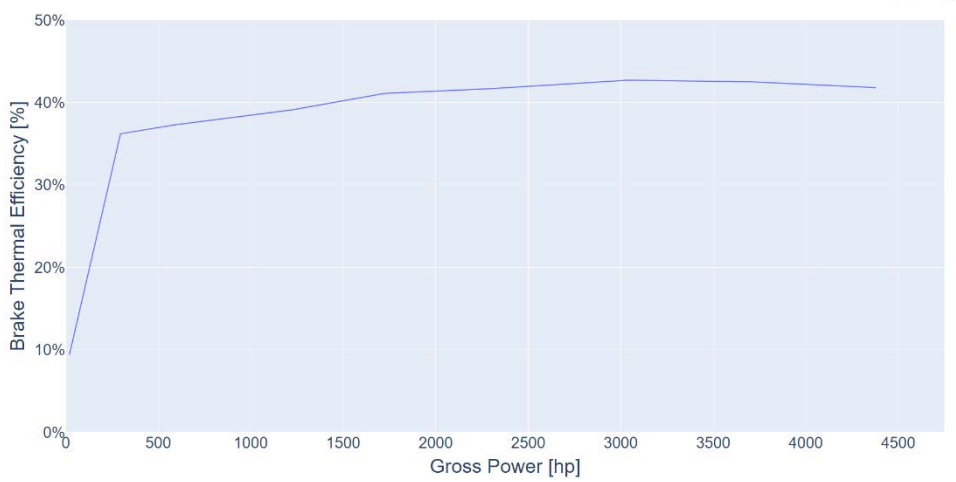

Figure 10. One-dimensional efficiency map for a default diesel engine used by the model

Energy Systems Model

The energy storage system, or RES in ALTRIOS nomenclature, is modeled as a user-specified 3D charge/discharge efficiency map as a function of C-rate, SOC, and temperature, as shown in Figure 11. The model for the battery currently assumes constant component temperature but will include a thermal model in a future update.

$$\eta_{chg\ or\ dischg} = 1 - \frac{losses}{P_{applied,chg\ or\ dischg}} = f(SOC, T, C-rate)$$

Efficiency @ 25°C	SOC 0	0.1	0.2	0.3	0.4	0.5	0.6	0.7	0.8	0.9	1
C-Rate -5	0.760719	0.819685	0.861126	0.878992	0.886132	0.892098	0.898813	0.903575	0.901256	0.910206	0.919701
-3	0.896858	0.893136	0.917434	0.927739	0.932119	0.93563	0.938134	0.93651	0.941019	0.946355	0.95208
-1	0.953838	0.964734	0.972619	0.976009	0.977453	0.978613	0.979539	0.978933	0.980413	0.982158	0.984043
-0.5	0.976652	0.982182	0.986317	0.988009	0.988731	0.98931	0.989772	0.989455	0.990204	0.991081	0.992023
-0.1	0.995393	0.996477	0.997264	0.997602	0.997746	0.997862	0.997955	0.997891	0.998041	0.998216	0.998405
0.1	0.9957	0.996894	0.997386	0.997647	0.997785	0.997884	0.997973	0.998031	0.998189	0.998104	0.998358
0.5	0.980396	0.98354	0.985541	0.986009	0.986723	0.987235	0.987695	0.987844	0.99081	0.9914	0.991681
1	0.99914	0.986787	0.972326	0.975418	0.976917	0.977988	0.97895	0.97926	0.981272	0.983496	0.983078
2	0.910458	0.92857	0.941255	0.948188	0.951513	0.953874	0.955985	0.956662	0.961041	0.963685	0.961933
3	0.850496	0.883691	0.905898	0.917717	0.923303	0.927243	0.930748	0.931867	0.939063	0.943372	0.945396
5	0.862623	0.761323	0.816481	0.843364	0.855587	0.864026	0.871414	0.873752	0.888534	0.897189	0.901206

Efficiency @ 30°C	SOC 0	0.1	0.2	0.3	0.4	0.5	0.6	0.7	0.8	0.9	1
C-Rate -5	0.834097	0.865745	0.888862	0.901761	0.906979	0.91092	0.91391	0.912025	0.918509	0.925533	0.932697
-3	0.901686	0.920139	0.933728	0.941348	0.944437	0.946773	0.948548	0.947429	0.951278	0.955453	0.959719
-1	0.967459	0.973507	0.977985	0.980502	0.981524	0.982298	0.982885	0.982515	0.98379	0.985175	0.986591
-0.5	0.983741	0.98676	0.988996	0.990254	0.990764	0.991151	0.991445	0.991259	0.991897	0.992589	0.993296
-0.1	0.996749	0.997352	0.997799	0.998051	0.998153	0.99823	0.998289	0.998252	0.998379	0.998518	0.998659
0.1	0.997052	0.997652	0.997898	0.998067	0.998183	0.998247	0.998316	0.998344	0.998484	0.998583	0.99863
0.5	0.984908	0.987267	0.989051	0.990182	0.990781	0.991108	0.991465	0.991608	0.992325	0.992835	0.993074
1	0.908854	0.973855	0.977603	0.979964	0.981211	0.98189	0.982629	0.982926	0.984407	0.985458	0.985952
2	0.933344	0.944696	0.953027	0.958199	0.96091	0.962378	0.963972	0.964611	0.967786	0.970027	0.971073
3	0.892143	0.911791	0.925833	0.934401	0.938849	0.941245	0.943838	0.944874	0.949999	0.953595	0.955267
5	0.783115	0.830076	0.861023	0.879006	0.888101	0.892934	0.898117	0.900173	0.910233	0.917182	0.920382

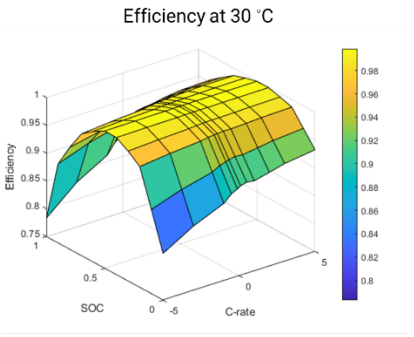

Figure 11. Energy storage one-way efficiency maps

The ALTRIOS team developed an energy system model formulation that will capture performance, lifetime, cost, and emissions, as well as technical readiness of various secondary battery, flow battery, fuel cell, engine, and capacitor technologies. However, this framework has not yet been incorporated into the ALTRIOS framework and will be included in a future update. To accomplish this, the overall energy system model consists of (1) a database of surveyed technologies, (2) component models, and (3) inputs for technology rollout scenarios. Taken from our proposal, Table 3 provides a high-level example map of technologies. For brevity, it lumps multiple quantitative metrics into color-coded relative rankings. Based on rankings and anticipated technology improvements over 40 years, this information can help guide technology rollout scenarios.

Table 3. Energy Storage Technology Review Example

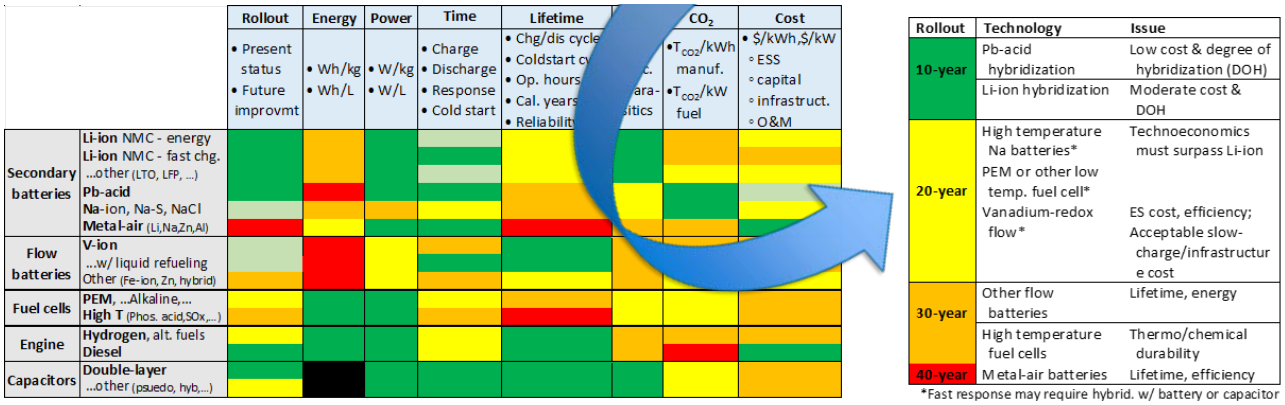

Rollout	Technology	Issue
10-year	Pb-acid hybridization	Low cost & degree of hybridization (DOH)
	Li-ion hybridization	Moderate cost & DOH
20-year	High temperature Na batteries*	Technoeconomics must surpass Li-ion
	PEM or other low temp. fuel cell*	
	Vanadium-redox flow*	ES cost, efficiency; Acceptable slow-charge/infrastructure cost
30-year	Other flow batteries	Lifetime, energy
	High temperature fuel cells	Thermo/chemical durability
40-year	Metal-air batteries	Lifetime, efficiency

*Fast response may require hybrid. w/ battery or capacitor

Table 4. provides a detailed list of energy system attributes that are collected to parameterize the models. These include:

- **Readiness:** Technology readiness level, safety ranking, and environmental ranking with text fields for comments on each.
- **Performance:** Energy and power density at the component and systems levels; maximum continuous power rates and response time; and efficiency and parasitic power draws.
- **Lifetime:** Cycle life, operating life, calendar life (capturing different fade mechanisms of batteries vs. fuel cells vs. engines), and in-service reliability (impacting cost as an energy system that is only 50% reliable will require twice the capital investment compared to a 100% reliable energy system).
- **Cost:** Broken out by energy system cost, other capital and infrastructure costs, operating and maintenance costs, and end-of-life costs.
- **Fuel and GHG emissions:** Fuel type, fuel cost, and anticipated emissions during the manufacturing of the energy system.
- **References:** Capture the source of the information.
- **Learning rates:** Relative to the year of the source/publication, annual improvement rate parameters provide a means to forecast year-by-year improvements for select energy system attributes (technology readiness level, all performance metrics, all lifetime metrics, and reductions in all costs).

The energy system database is presently stored in Excel; however other options are being discussed for the future, such as CSV files or an SQL database.

Table 4. Detailed List of Energy System Attributes To Be Cataloged in a Database, Serving as Inputs to ALTRIOS

	ES Attributes	Units
Readiness	TRL (1-9)	1-9
	TRL annual improvement rate	%
	*Technology advantages	text
	*Technology disavantages & issues	text
	Safety ranking (1-5)	1-5
	*Safety issues	text
	Environmental ranking (1-5)	1-5
	*Environmental issues	text
Performance	Energy - Gravimetric	Wh/kg
	Energy - Volumetric	Wh/L
	Power - Gravimetric	W/kg
	BOP packing effic. - Weight	%
	BOP packing effic. - Volume	%
	Max continuous rate - discharge	hours
	Max continuous rate - charge	hours
	Ramp time to full power	seconds
	Coldstart time	minutes
	Efficiency - Stack/cell/engine	% f(T; pwr)
	Parasitics - Pumps	kW/kWh f(pwr)
	Parasitics - Thermal management	kW/kWh f(T; pwr)
	Parasitics - Self discharge	kW/kWh
	Performance annual improv. rate	%

	ES Attributes	Units
Lifetime	Cycle life	#
	Cold-start cycle life	#
	Operating hours	hours
	Calendar life	years
	In-service reliability	%
	Life annual improvement rate	%
Cost	System-level per unit energy	$/kWh
	System-level per unit power	$/kW
	Capital deployed	$/kWh
	Infrastructure deployed	$/kWh
	O&M	$/kWh/year
	$/kWh, end of life	$/kWh
	Cost annual improvement rate	%
T	Operating temperature	Celsius
Fuel & GHG	Fuel type	electric; H2; biofuel; nat. gas; diesel
	Fuel cost	$/kWh
	GHG emitted during manufacturing	T_{CO2}/kWh
Ref.	Source	DOI or link
	Year	year
	Author	text

Energy system models must strike a good balance between simplicity and realism. Electrical/thermal performance models will simulate energy balance, power flows, efficiency, and temperature rise with sufficient transient detail to capture impact to charge response, discharge ramping, and cold-start cycle-life limitations (important for high-temperature technologies like Na-S and NaCl batteries and molten carbonate and solid-oxide fuel cells).

The energy system model framework involves:

- **Inputs:** Size (kW and kWh), device on/off, operating time, calendar age, and power demand.
- **Outputs:** Power flows (fuel in, shaft power out, and heat and parasitic losses), costs (energy system device, fuel, and operations and maintenance), GHG emissions, energy system mass, volume, and overall state of health.
- **Internal states:** SOC (or fuel level), state-of-health values (cycles, cold-start cycles, operating hours, and calendar years), and temperature.

Refueling Infrastructure

Refueling infrastructure can be defined at origin and destination nodes along the railroad network. Figure 12. illustrates an example data frame defining a scenario's refueling infrastructure for a simple two-node, all-BEL case, but the input format is structured to allow flexibility in defining multiple fuel types and combinations of fuel types at each refueling yard. The string specified in the "Node" field should match a unique node identifier string assigned to a node number specified in a separate network locations definition file, and the string specified in "Locomotive_Type" should match a compatible locomotive definition provided to the train planner module.

Node	Charger_Type	Locomotive_Type	Fuel_Type	Refuel_Rate_J_Per_Hr	Cost_Per_Port	Port_Count
Barstow	Megawatt	BEL	Electricity	3.60E+09	$1,000,000	2
Stockton	350 kW DCFC	BEL	Electricity	1.26E+09	$350,000	6

Figure 12. Example rail yard refueling input data frame, where "Node" matches a named network location and "Locomotive_Type" matches a named locomotive definition provided to the train planner

For each fuel type, one or more refueling ports can be assigned to each origin or destination node. For each fuel type and node, ports of the same fuel type are handled as a single first-in, first-out refueling queue, with each port operating in parallel. For example, if a node has two BEL empty chargers and then five BELs arrive in sequence, the first two BELs to arrive will recharge simultaneously while the other three wait. Separately from these refueling queues, a minimum required servicing time can be defined for each fuel type as part of the locomotive definition provided to the train planner module. For example, even if a diesel locomotive needs only a few minutes to be refueled, it may take 90 minutes to conduct other necessary servicing steps, conduct inspections, couple/uncouple locomotives, and move them between the terminal arrival/departure tracks and the locomotive servicing facility.

Refueling queues are tracked in two steps. First, as the train planner determines a consist dispatch plan, it estimates conservative versions of consists' arrival times and each locomotive's net energy consumption along a route, and queueing and refueling are tracked accordingly. Each locomotive is made available for its next consist assignment once its energy level reaches maximum capacity. Next, after the train model walks each consist along its timed path (incorporating meet-pass delays), each locomotive's exact arrival time and energy consumption are used in a similar queueing model. In this second step, consist assignments are predetermined, so locomotives stop refueling when they either reach maximum energy capacity or when their consist must leave, whichever comes first.

For locomotives with an energy storage device, SOC is tracked from trip to trip. A data frame of spatiotemporally specified charge sessions is output by the train model and later used in the metrics calculators.

Economic Model

The calculation steps for economic and environmental metrics were implemented within the economics module. Given a set of simulation results from the simulation manager and a set of input assumptions (costs, emissions factors, and locomotive lifespans), the economics module computes the key output metrics. In addition to returning those key outputs pertaining to total costs and emissions, it also returns a set of intermediate metrics that must be computed to determine those total costs and emissions.

Modeled Cost Components

ALTRIOS models capital and variable costs. Capital investment costs are modeled on a per-item basis (where per-unit costs can be specified separately for each component and year). For locomotives and refueling infrastructure, capital unit costs are modeled as a lump sum investment paid when each locomotive enters the fleet. Per-locomotive capital costs are

intended to be inclusive of the cost of upgrading, converting, and/or purchasing new-technology locomotives. Separate fuel or battery tenders are not explicitly modeled but can be added to each locomotive specification's defined cost and operational parameters (e.g., usable energy capacity). Refueling infrastructure investment costs are modeled per refueling or recharging port, and they are intended to include costs of purchase, construction, and/or installation of infrastructure associated with refueling, energy supply, and charging stations (including factors such as tanks, transformers, and grid connections, depending on configuration).

Unit variable costs can be specified by the user separately for each fuel type and locomotive type. Fuel price projections (diesel, natural gas, hydrogen, electricity, and biofuel) will be handled as external inputs, which may be provided as location-specific and time-indexed costs of dispensed energy for the locomotive. Locomotive variable costs (which can be specified by the user by locomotive type and year) are intended as a "catchall" to represent any remaining non-fuel operations and maintenance costs.

Default Cost Assumptions

A default set of cost assumptions was developed for the public release of ALTRIOS. These assumptions are uncertain and may also vary widely across rail networks, but default values are intended to construct a plausible "starting point" representation of present-day and forecasted economic and financial inputs from publicly available sources. All assumed values can be fully customized by users of ALTRIOS.

Technology costs are highly speculative for the very high-power battery chargers that BELs may require to operate with no changes to train dispatch plans. We scale up NREL cost estimates for present-day charging technologies to the default energy storage device's power level, borrowing from a trend seen in that study and elsewhere that costs (while highly uncertain) scale in a very roughly linear manner with charger power [5]. Regarding future changes in charging costs, a 2019 study showed that economies of learning (which tend to reduce costs over time) may be offset by increased costs related to land use and permitting [6]. As a default, we assume new charger acquisition and installation costs are static over time and allow the user to test alternative user-defined assumptions.

BEL acquisition costs are not publicly available at present, and thus are highly uncertain. Our default assumptions for diesel locomotives are derived from a peer-reviewed study by Zenith et al. [7]. To account for the cost premium of a BEL, we adapt "all-in" battery pack cost estimates per kilowatt-hour from the 2022 NREL Annual Technology Baseline [8]. These estimates are available as forecasts through the year 2050. These assumptions do not map perfectly to BELs because they represent the costs of stationary battery storage. However, it is not clear in what direction these estimates may alter results; some stationary storage costs such as permitting and land development may not apply to mobile storage devices, but other costs such as any ruggedization and shock-proofing of mobile storage are not included in these estimates.

ALTRIOS adds a default retail price equivalent multiplier of 1.15 to all locomotive and recharging infrastructure costs, representing an assumed markup of 15% that rail companies

pay above the costs of production. Another key financial parameter is discount rate, which affects the trade-off between short-term costs of new technology investments and cost savings (e.g., reduced fuel expenditures), which may only add up in the long term. Following Federal Railroad Administration guidance for cost-benefit analyses, ALTRIOS assumes a default 7% real discount rate (i.e., nominal discount rate minus inflation) [9].

For default fuel and electricity price forecasts (dollars per gallon of diesel and per kilowatt-hour of electricity), ALTRIOS uses the U.S. Energy Information Administration's 2023 Annual Energy Outlook [10]. These estimates are available through 2050 at the national level and can be replaced by user-defined values for each network node at which charging occurs in each simulation year.

Computational Steps

For each fixed and variable cost component, unit costs (default or user-specified) are multiplied by the corresponding quantities specified in the rollout plan or calculated as an output from the train planner module and the train model. This yields a system-scale cost; system-scale variable costs will then be annualized (e.g., variable costs based on a 21-day simulation would be converted to full calendar year costs).

After completing all years of simulation, the economics mode combines fixed costs—represented as a set of investments and retirements spread out over the planning horizon—and annualized variable costs into a table of cash flows occurring in each simulation year. These future cash flows will then be discounted using a default or user-specified real discount rate.

Output Metrics

LCOTKM

One key metric computed by the module is the levelized cost per megatonne-kilometer of freight delivered (LCOTKM). LCOTKM is equivalent to the revenue per megatonne-kilometer that would be necessary to recover all costs that are considered by the module. For a simulation including years t from 1 to n, where each year results in fixed acquisition costs A_t and variable costs V_t, and F_t megatonne-kilometers of freight are delivered, LCOTKM is defined as:

$$LCOTKM = \frac{sum\ of\ lifetime\ \cos t\ s}{sum\ of\ lifetime\ freight\ delivered} = \sum_{t=1}^{n} \frac{\frac{A_t + V_t}{(1+r)^t}}{\frac{F_t}{(1+r)^t}}$$

Costs and freight deliveries are each treated as discounted flows over time using a real discount rate r. By default, $r = 0.07$ and the simulation is run for $n = 20$ years. Following the Federal Railroad Administration's cost-benefit analysis guidance for rail projects, we simulate investments and operations for n years but include each acquired asset's residual value in year $n + 1$ as a discounted revenue stream [9].

The simulation used for testing includes 21 simulation days. The simulation manager outputs include a variable recording how many days were simulated; the metric calculator extends variable costs (and emissions) to a full calendar year so they can be included in life cycle metric calculations.

Net Present Value

Total net present value (represented as NPV in Equation

$$\text{NPV} = \text{sum of lifetime cash flows} = \sum_{t=1}^{n} \text{F}_t \times \text{R-A}_t\text{-V}_t \quad (16)$$

equals the sum of net present values for all discounted cash flows over the planning time horizon. Using similar notation as for LCOTKM, where a simulation includes years from 1 to n and where each year results in fixed acquisition costs A_t, variable costs V_t, and freight deliveries F_t each earning fixed revenue R per megatonne-kilometer, net present value is defined as:

$$NPV = sum\ of\ lifetime\ cash\ flows = \sum_{t=1}^{n} F_t \times R - A_t - V_t \quad (16)$$

As with LCOTKM, we include residual asset value in year $n + 1$ as a discounted revenue stream. If revenue is included in the model and the net present value is negative, the simulated freight rail service will not recover costs; if it is positive, it will earn profit.

Intermediate Output Metrics

Along the way to computing these two key economic metrics and the life cycle emissions metric (described above), the economics module computes a set of intermediate metrics. These metrics are also returned as output by the economics module. Intermediate output metrics include:

- Itemized cash flow components for each simulation year, currently including fleetwide sums of energy use (diesel, electricity, and total energy), locomotive and charging infrastructure acquisition, and end-of-simulation residual value.
- Energy use for each simulation year (megajoules and gallons of diesel, megajoules and megawatt-hours of electricity).
- Itemized emissions for each simulation year (diesel, electricity, and total).
- Fleet acquisition and makeup for each simulation year (count of newly acquired and total locomotives of each type, percentage of consist members across the fleet that are BELs, and percentage of total locomotives that are BELs).
- Gross ton-miles of freight delivered for each simulation year.

These output metrics enable deeper analysis of rollout strategies and resulting outcomes.

Output Format

The economics module returns all key and intermediate metrics as a single table and as a CSV file. These outputs enable further analysis by the end user or creation of user-defined metrics (e.g., total acquisition costs per unit of GHG emissions). Each row of that CSV file includes metric name, metric unit of measurement, simulation year, and metric value for that simulation year.

Greenhouse Gas Life Cycle Analysis Input Data

Life Cycle Emissions of Fuels

An input format was defined for fuel-based life cycle emissions. This format provides flexibility to define life cycle emission values by fuel type, region, and time of day (for electricity, in particular). Life cycle carbon intensities (CIs) of diesel fuel (incumbent) and selected alternative fuels, including soybean biodiesel, electricity, and hydrogen, were compiled or estimated for rail applications. To develop default values, the most relevant data were collected from open sources such as life cycle emissions inventory databases, models (e.g., Greenhouse Gases, Regulated Emissions, and Energy Use in Technologies [GREET] model), and literature, with a primary focus on fuels used in California. The CI data cover the entire life cycle of the fuel, from feedstock production to fuel production and fuel combustion, as well as associated transportation of materials. Details on data and data sources are elaborated below.

Carbon Intensity Estimates

Fuels evaluated include petroleum-based ultra-low-sulfur diesel (ULSD), soybean biodiesel, hydrogen, and electricity. All emissions are reported in CO_2e, calculated using global warming potentials (GWPs) of CO_2, CH_4, and nitrous oxide (N_2O) of 1, 25, and 298 g CO_2e per gram of emissions, respectively, for a 100-year time horizon, per the California GREET (CA-GREET 3.0) model. Note that the GWPs in the latest CA-GREET [11] were based on the default GWPs in the 2016 version of the GREET model, which are different than those in the current GREET model (2022 version). Future updates may be required to ensure consistencies in GWPs. The CI values of liquid fuels (ULSD and soybean biodiesel), gaseous hydrogen, and electricity are reported in terms of a functional unit of 1 MJ (low heating value).

ULSD

The U.S. Environmental Protection Agency regulates locomotive diesel fuel through its diesel fuel standards [12], enacted in 2006, which state that new and existing locomotive engines must be operated with ULSD. Therefore, ULSD is used as the petroleum baseline in this analysis. The life cycle CI of the California ULSD pathway was derived from CA-GREET 3.0 [11]. GHG emissions associated with the key life cycle stages including crude oil recovery, refining, fuel transportation, and fuel combustion are shown in Table 5, and total CI is estimated at **100.5 g CO_2e MJ^{-1}** based on CA-GREET 3.0 [11].

Table 5. CI of ULSD as Reported by CA-GREET 3.0 [11]

Process Stage	CI [11] (g CO_2e MJ^{-1})
Crude recovery and transport	11.8
Crude oil refining	13.6
ULSD transport	0.2
Fuel combustion	74.9

The life cycle CI of ULSD was further refined on a Petroleum Administration for Defense District (PADD) level by using the results of Cooney et al. [13]. The results are representative of ULSD

production and consumption in the year 2014 and is the most complete dataset available at the PADD resolution. The well-to-wheel analysis includes GHG emissions of the crude extraction, crude transport, refining, ULSD transport, and combustion stages in the five different PADDs. The results were calculated using CO_2, CH_4, and N_2O GWPs of 1, 36, and 298 g CO_2e, respectively. As shown in Table 6, GHG emissions of ULSD range from **90.1 to 96.2 g CO_2e MJ^{-1}**, with the highest value corresponding to PADD 5 (Western United States, Hawaii, and Alaska). The PADD 5 CI is 4% lower than the value reported in CA-GREET [11].

Table 6. CI of ULSD as Reported by Cooney et al. [13]

PADD	CI [13] (g CO_2e MJ^{-1})
PADD 1	90.1
PADD 2	92.8
PADD 3	90.8
PADD 4	90.8
PADD 5	96.2

Biodiesel

The CI estimated in CA-GREET 3.0 [11] includes the cultivation of soybean, oil extraction, conversion to biodiesel, transportation of the fuel, and fuel combustion, as well as land use change. This pathway generates a glycerin coproduct, and energy allocation is used to determine the emissions attributed to the biodiesel product. As reported by CA-GREET 3.0 [11], 95.1% of the total energy output is attributed to biodiesel [11]. Land use change emissions were also included in the total CI of this pathway (29.1 g CO_2e MJ^{-1}). The life cycle CI of soybean biodiesel is **56.3 g CO_2e MJ^{-1}**. Land use change is found to be the most significant source of emissions. The breakdown of emissions by activity is shown in Table 7

Table 7. CI of Soybean Biodiesel, as Reported in CA-GREET 3.0 [11]

Process Stage	CI [11] (g CO_2e MJ^{-1})
Soybean cultivation	10.4
Land use change	29.1
Soy oil extraction	4.7
Biodiesel production	9.8
Transportation	1.5
Fuel combustion	0.8

The CI of soybean biodiesel was updated using the results reported by Xu et al. [14]. The soybean biodiesel emissions are representative of 2018 and were calculated using soybean yield and fertilizer data from the U.S. Department of Agriculture [14]. In addition, the emissions emitted by the biodiesel conversion process were estimated using data from 27 biodiesel production plants in the United State [14]. Xu et al. [14] also used three different models to estimate land use change emissions, giving a range of CI values of **30.2–50 g CO_2e MJ^{-1}**.

In addition to soybean biodiesel, the CI of biodiesel derived from canola, carinata, corn oil, tallow, and used cooking oil were also retrieved from Xu et al. [14]. For canola- and carinata-derived biodiesel, the well-to-wheel emissions include emissions from feedstock production, oilseeds crushing, conversion, transportation, and combustion. Land use change emissions for canola were also included by leveraging two different land use change models [14]. Similarly, the well-to-wheel emissions of tallow and used cooking oil include the same life cycle stages, with the difference that these feedstocks require a rendering step instead of a crushing process. In terms of corn oil, there is no preprocessing step required, and feedstock production emissions include those from the electricity required to separate corn oil from distiller's grains and solubles, as well as transportation to the biodiesel plant. The total CIs of the different biodiesel pathways presented in Table 8 were calculated using GWPs of 1, 25, and 298 for CO_2, CH_4, and N_2O, respectively.

Table 8. CI of Soybean Biodiesel Pathways as Reported in Xu et al. [14]

Feedstock	CI [14] (g CO_2e MJ^{-1})
Soybean	30.2–50
Canola	45–51.2
Carinata	26.1
Corn oil	13.7
Tallow	19.1
Used cooking oil	18.6

Hydrogen

The CI of compressed gaseous hydrogen production was retrieved from CA-GREET 3.0 [11]. This pathway outputs compressed gaseous hydrogen through the steam methane reforming of North American natural gas. The system boundary includes the natural gas recovery process, hydrogen production, and transportation processes, as well as compression and precooling stages (the latter takes place in hydrogen refueling stations [11]). As reported by CA-GREET 3.0 [11], the total CI is **117.7 g CO_2e MJ^{-1}**, with the hydrogen production stage contributing the most to the overall emissions. A detailed breakdown of the emissions contribution of each subprocesses is provided in Table 9

Table 9. CI of Gaseous Compressed Hydrogen, as Reported by CA-GREET 3.0 [11]

Process Stage	CI (g CO_2e MJ^{-1})
Natural gas recovery	6.1
Natural gas processing	3.3
Natural gas transportation	5.5
Hydrogen production	20.5
Hydrogen production (non-combustion)	64.1
Hydrogen transportation	7.2
Hydrogen compression and precooling	11.0

To understand the variation in CI of hydrogen across regions, we estimated regional hydrogen CIs by using regional natural gas and hydrogen production CIs. The regional CIs of natural gas extraction and processing were estimated by aggregating basin-level data reported by Littlefield et al. [15] into three different regions. The natural gas dataset includes CIs for 27 different natural gas basins across the United States [15], which were aggregated into West, Central, and East regions based on their location. The regional CI for the three natural gas regions are illustrated in Figure 13. A conversion efficiency of 3,719 grams of natural gas per kilogram of hydrogen [16] was then used to estimate the feedstock emissions per energy content of hydrogen (e.g., megajoules).

Next, regional CIs of the hydrogen production process were estimated by processing hydrogen production plant data for 33 plants across the United States from the Hydrogen Production Tool [17]. The dataset includes annual hydrogen production output, CO_2, CH_4, and N_2O emissions for the year 2016. The plants were aggregated into the three different regions, and average CIs were calculated. Emissions from the transportation and compression and precooling stages were assumed to be constant across regions, and values from CA-GREET [11] were used. A complete breakdown of the hydrogen CIs for the three different regions is provided in Table 10.

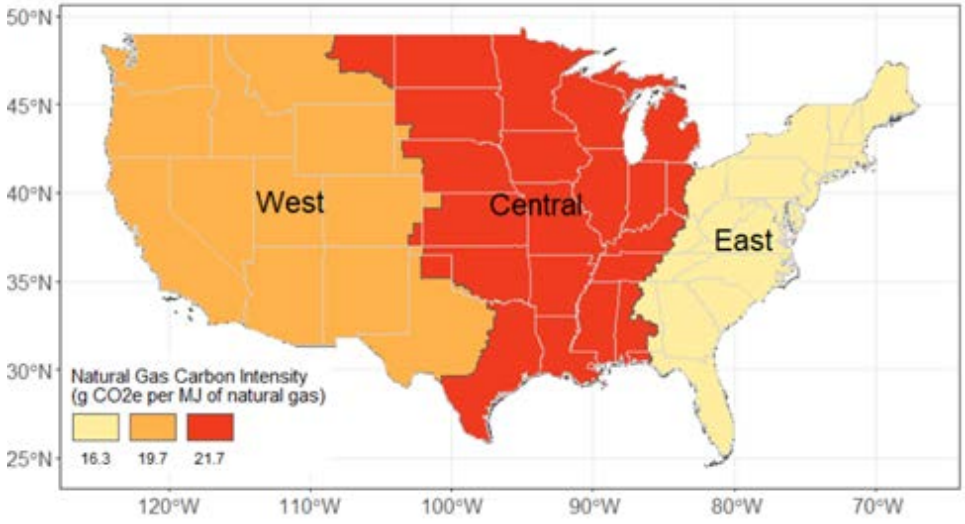

Figure 13. Regional CIs of natural gas extraction and processing

Table 10. Calculated Regional CIs of Gaseous Hydrogen Production From Steam Methane Reforming

Region	Average Regional Emissions (g CO_2e per MJ H_2)				
	Feedstock (Natural Gas)	Production	Transportation	Compression and Precooling	Total
Central	27.1	79.1	7.2	11.0	124.4
East	20.9	58.8	7.2	11.0	98.0
West	25.3	76.2	7.2	11.0	119.7

Electricity

The CI values for battery charging were retrieved from CA-GREET 3.0 [11]. These are CI values reported for each hour of the day, aggregated over the four quarters of the year. The reported values represent the average emissions rates at a given hour based on California's 2020 grid mix. As such, these are the annual average CI values when using the California grid for battery charging. Further details are provided in the CA-GREET 3.0 documentation [11]. The hourly average CIs are tabulated in Table 11

Table 11. CI of Electric Charging in California 2020 Calculated From Data Reported by CA-GREET 3.0 [11]

Hour of the Day	CI (g CO_2e MJ^{-1})
12:00 a.m.	81.5
1:00 a.m.	80.7
2:00 a.m.	80.2
3:00 a.m.	80.5
4:00 a.m.	80.7
5:00 a.m.	83.9
6:00 a.m.	98.3
7:00 a.m.	91.2
8:00 a.m.	62.3
9:00 a.m.	48.9
10:00 a.m.	42.5
11:00 a.m.	55.5
12:00 p.m.	52.3
1:00 p.m.	61.6
2:00 p.m.	70.7
3:00 p.m.	77.9
4:00 p.m.	79.4
5:00 p.m.	98.9
6:00 p.m.	124.5
7:00 p.m.	134.6
8:00 p.m.	125.4
9:00 p.m.	105.8
10:00 p.m.	89.2
11:00 p.m.	83.0

In addition to hourly electric charging CIs, average 2020 grid electricity CIs were calculated at a state resolution. The life cycle emissions of electricity generation, including upstream, operational (non-combustion and combustion), and downstream emissions, were calculated by combining upstream, non-combustion operational, and downstream CIs from Nicholson and Heath [18] with state-level operational CIs from the U.S. Environmental Protection Agency's 2020 Emissions and Generation Resource Integrated Database (eGRID) [19]. These datasets include CIs for coal, natural gas, oil, nuclear, hydropower, biomass, wind, solar, and geothermal

generation. Upstream and downstream emissions for the different generation technologies were assumed to be constant across states, while emissions from combustion were estimated using the state-level generation mix included in the 2020 eGRID [20]. The CIs retrieved from Nicholson and Heath [18] are provided in Table 12, while the total CIs for average grid electricity are illustrated in Figure 14.

Table 12. CIs of Electricity Generation Technologies, as Reported by Nicholson and Heath [18]

Generation Technology	CI (g CO_2e kWh^{-1})		
	Upstream	Ongoing Non-Combustion	One-Time Downstream
Coal	5	10	5
Oil	0	0	0
Gas	0.8	71	0.02
Nuclear	2	12	0.7
Hydro	6.2	1.9	0.004
Biomass	0	0	0
Wind	12	0.74	0.43
Solar	28	10	5
Geothermal	15	6.9	0.12
Other unknown/purchased fuel	5	0.74	0.12
Other fossil	0.8	10	0.02

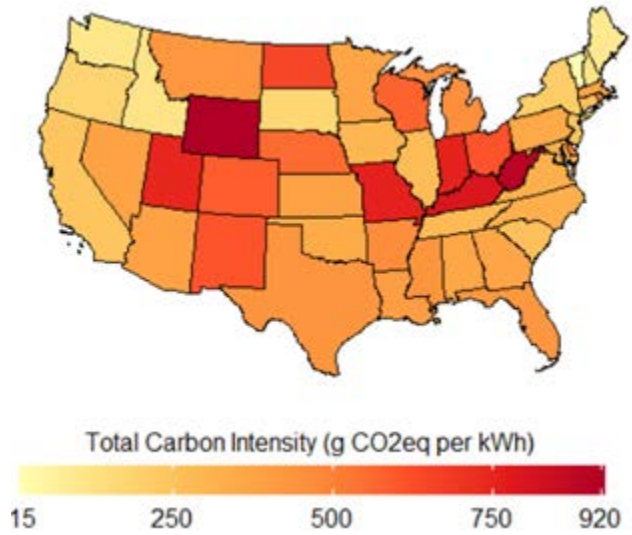

Figure 14. State-level CIs for average grid electricity in 2020

For future-year CIs, ALTRIOS includes in its default assumption set the long-run marginal emissions rate estimates provided by the 2022 version of Cambium [21]. Cambium is an NREL-developed model, and its long-run marginal emissions rates are intended to capture the total pre-combustion and combustion effects of new electricity demand, taking into account not only induced changes in electricity generator dispatch, but also induced changes in electricity

generation capacity expansion over time. These estimates are included in the ALTRIOS release at the Cambium generation and emission assessment region level (Figure 15.), but other levels of aggregation can be imported into ALTRIOS, provided the imported grid region names correspond to grid regions linked to a network node number specified in the network locations definition file.

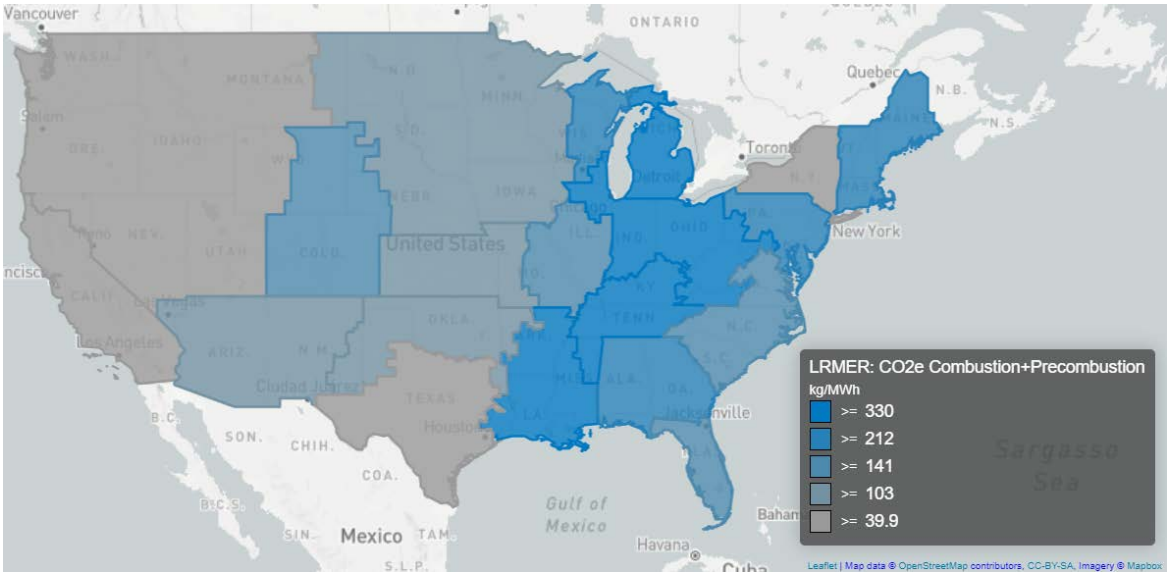

Figure 15. Cambium long-run marginal emissions rates by generation and emission assessment region for 2030

Topology and Topography

The physical layout of the rail network is required to accurately model train performance and schedule trains. A utility within ALTRIOS enables all users to create representative network models. The key items needed to define these networks are grade, curvature, speed restrictions, and track layout. There are two different options to create these networks based upon the data available to the user:

1. Use railroad-proprietary XML network files that conform to AAR S-9503.V2.0.
2. Compile publicly available data sources to create a realistic network.

Option 1 is the easier of the two methods to generate a network. This approach will work well for routes that have positive train control (PTC) implemented. The main drawback to this approach is that the user must be part of a railroad or supported by a railroad to have access to these data. The route being studied must also have PTC implemented over its entirety.

Option 2 uses publicly available data sources to model the network. This approach will require more work, but it enables all users to have access to a representative network. The utility to create networks using this approach is implemented in QGIS. QGIS is an open-source geographic information system (GIS) editor. This editor simplifies the process of joining multiple geospatial data sources to create a single network. A specific example of a relatively short network is included in the ALTRIOS install package so that new users can run the program with the sample network, then adapt as needed for their particular case study.

The network for the BNSF Taconite case study was developed from open data sources. This was done for two reasons. First, the team wanted to release this network publicly with the release of the framework. Second, there are no PTC data for the Taconite route.

The process for developing the network involves several steps. The first step is gathering track layout, elevation data, and timetables from the railroad subdivision. The second step is trimming the network. The third is filtering the elevation data. The fourth is draping the track layout onto the filtered elevation data. The next step is cleaning up errors in the data, and the final step is converting this information from a shapefile to the ALTRIOS network format.

The track data were downloaded from Geofabrik with the complete OpenStreetMap data for this region [22]. The OpenStreetMap data include rail data from the OpenRailway project [23], [24]. These data are generated by individuals within the rail community and are publicly available. The data include details like sidings and yards that are not present within publicly available data from the Federal Railroad Administration. The data available from the Federal Railroad Administration only include mainline tracks. This level of detail is not sufficient for the modeling details with the meet-pass planner.

The digital elevation model (DEM) was downloaded from the U.S. Geological Survey [25]. These data had a resolution of 1/3 arc seconds. It is available for the entire United States if needed for building networks in other locations.

Employee timetables for this project were supplied by BNSF, but it is possible to find older timetables on the internet. It should be noted, however, that historic timetables are not necessarily reflective of current rail operations. The timetables will have information on speed restrictions by subdivision. Elevation data for each subdivision, from engineering track charts, can be used for validation of the network.

Once all of the data were gathered, the network was trimmed to the desired area using the event recorder data for this study. This involved finding all sections of the network that were within 10 meters of any event recorder data point. An example of this can be seen in Figure 16. The brown points represent each sample of data from the event recorder data. The red line represents the track that was extracted for the Taconite network. The south branch of the track ends where the event recorder data turn north because the event record data did not travel in that direction. This step was completed in one step for both routes in the network. It is also possible to trim the track manually if event recorder data are not available.

Figure 16. Example of event recorder data and trimmed network derived from event record data

The trimming of the network is an important step because it ensures the trains will take appropriate routes through the network. A network with extra segments may allow trains to travel through the network with unrealistic routes.

Preparation of the elevation data is an important step for the network development. The data for the Taconite case study were derived using a process that was validated using two steps. The first validation step used the ZANZEFF data between Stockton and Barstow, California. The event recorder average was compared against then PTC track files to verify its accuracy. The second validation step compared the elevation estimate that was derived from event recorder data to a filtered DEM. This step was completed using the routes from the Taconite case study. The elevation estimate derived from the event recorder data requires data from multiple trains. Each locomotive will have a GPS elevation measurement, but the accuracy of GPS elevation is not always precise. This is due to variability in how many satellites are available and their position in the sky, among other things. Once the event recorder dataset has been collected, the data are then averaged based upon the track layout.

The first step to derive elevation from event recorder data is to obtain the track layout. The lines that make up the track consist of many points, known as vertexes. These points are used to make buffers that represent a circular area around the point. The final radius selected for this process was 25 meters, but radii of up to 100 meters were evaluated. The buffers are then used to select points from the event recorder data. The data within each buffer are averaged to estimate the elevation at each point along the track. A depiction of these data is shown in Figure 17.

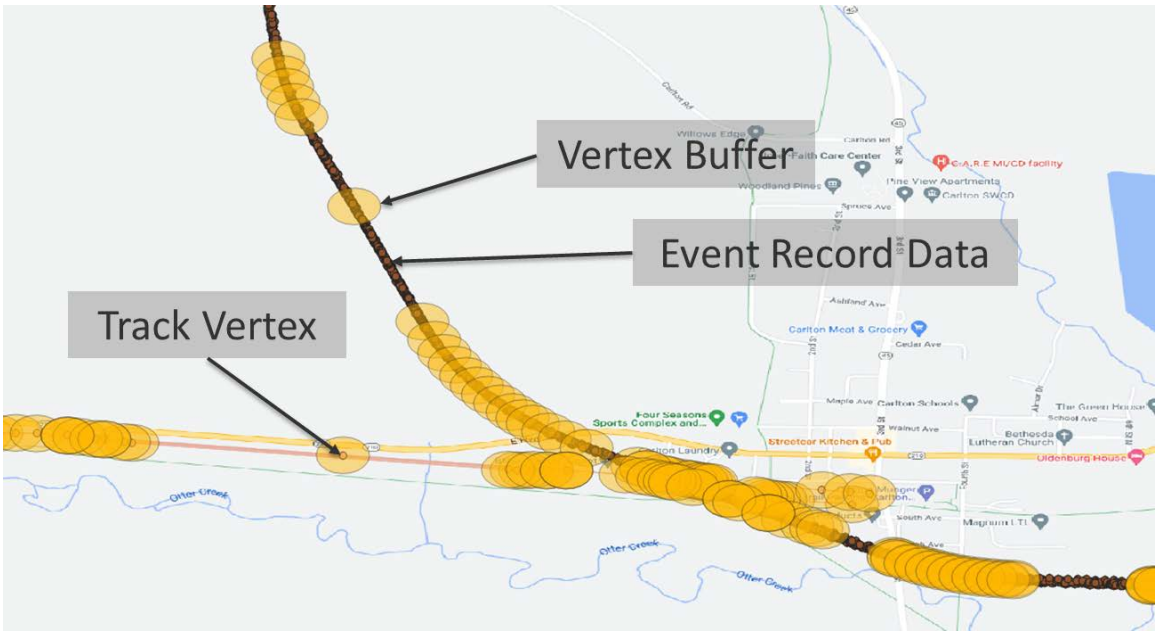

Figure 17. Map depicting how track vertexes were used to average elevation from event recorder data

The complete ZANZEFF dataset was used for the verification with PTC-derived elevation. This yielded an almost identical match to the PTC data (Figure 18). The red points were derived from the PTC data, while the blue points were derived from the event recorder data. This step of the process demonstrated that event recorder-derived elevation could yield a representative elevation for the rail network.

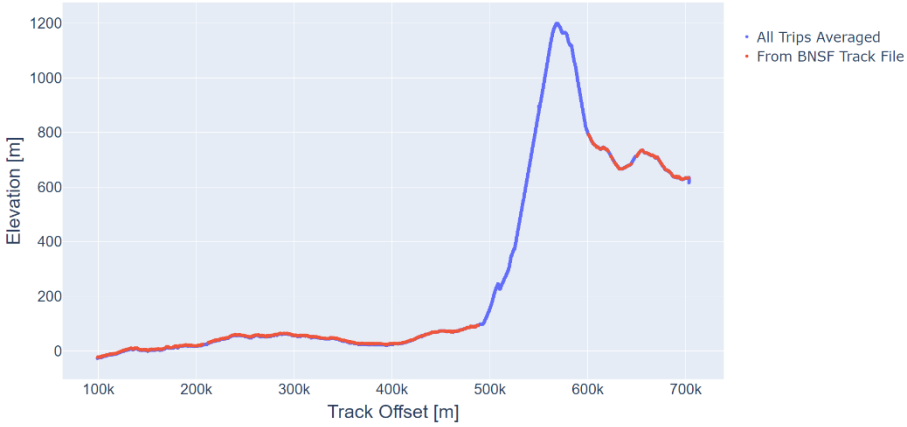

Figure 18. Comparison of elevation with BNSF PTC track data and GPS data from locomotive event recorders

The elevation for the Taconite case study was derived from a DEM obtained from the U.S. Geological Survey [25]. This DEM consists of raster data. Raster data use a digital image coupled with geographic information to represent geographic data over an area.

The first step of this process was to filter the DEM. This was done to remove noise from the elevation data. The filtering is also used to smooth the elevation to estimate where tracks are above grade, below grade, or crossing a bridge. The raw DEM will not properly capture this due to the spatial resolution of the points.

A comparison of the filtered and unfiltered data is shown in Figure 19, showing an area where the track crosses a creek bed. The drop in elevation is depicted by the black area. The train crosses this creek bed with a bridge. Filtering elevation allows for properly modeling this bridge.

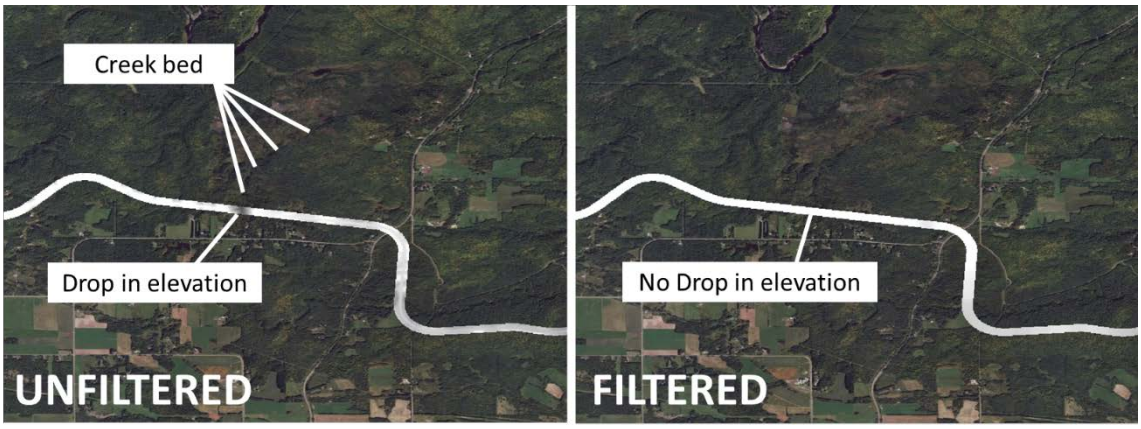

Figure 19. Comparison of filtered and unfiltered elevation along track

The first step in filtering the elevation is to trim the DEM to within 50 meters of the track. This is to remove the influence of data farther from the tracks. This could be important in areas where tracks are on a steep slope or near a cliff. The filtering algorithm used a circular area that could have a radius up to 1 km. An example of the trimmed DEM is shown in Figure 20. The DEM is represented by grayscale and is shown as the black area on this map rather than the white seen in Figure 19.

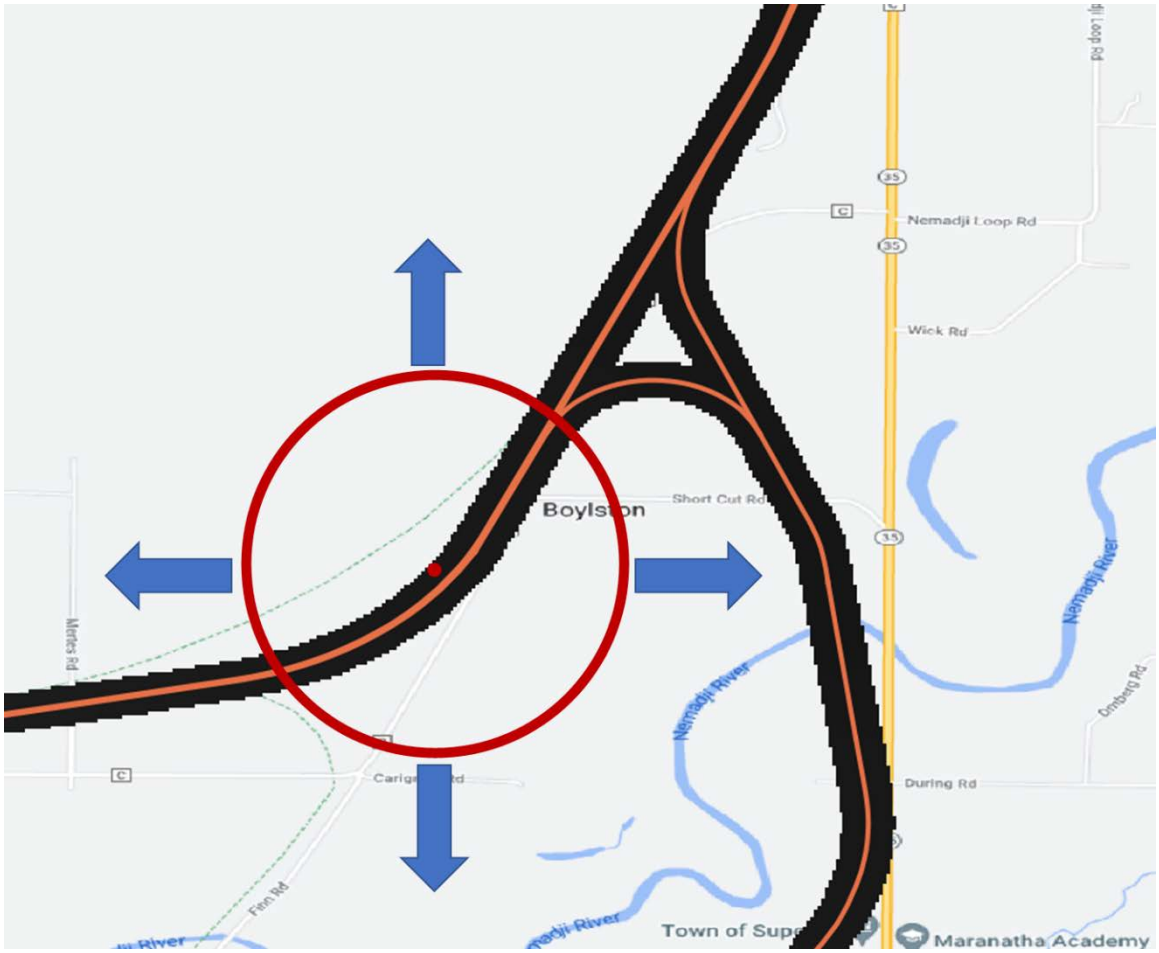

Figure 20. Map showing how the DEM was trimmed to within 50 meters of the track prior to performing the filtering operation

The filtering of the elevation data was conducted using a rank filter. A rank filter is similar to a median filter, except it is possible to choose the percentile from the distribution. The area used for this calculation was a circular area, as shown in Figure 20. The centroid of the circle is the point at which the filtered value is being calculated. The circle represents the area being considered. This is done for every pixel within the DEM.

A sweep of radius and rank was carried out to determine which combination of parameters yielded the closest fit to actual data. The radius was swept from 1 to 50 pixels in 5-pixel increments. The rank was swept from 1 to 90 in 5% increments. These results were then compared to data derived from the event recorder data. The SAGA GIS package was used for this operation [26]. Once completed, the track network can be processed and draped onto the DEM. The cleaning operations include extending lines where there are gaps and breaking track segments at track junctions. This is all done using a QGIS processing plug-in that was developed for this project [27].

The validation of this process was completed using data from four trains in each direction for both routes, Hibbing-Superior and Superior-Minneapolis. This yielded a total of 16 trains. Each train contained two or three locomotives. The evaluation at each track vertex was compared to

find the filter configurations that yielded the lowest error. The second step of the selection process involved generating a network with elevations from each filter configuration. Another network was generated from the event recorder data averages. Each network was then used to simulate a series of trains to estimate fuel usage.

The last step prior to the conversion of the network from a shapefile to the ALTRIOS network format was to clean up the data. The most common problems are incorrect subdivision names. These names are quite easy to edit in QGIS and are needed to apply speed restrictions. This is a manual process that is not easily automated.

The final step is conversion of the network to the ALTRIOS format. This is done using a Python script that is not yet incorporated into the QGIS processing plug-in. This script reads in two shapefiles that are generated by the QGIS plug-in mentioned earlier. The first is the line data from the track, and the second is a point layer that represents each track vertex. This script applies speed limits, links each section of track, and converts it to the YAML file format used by ALTRIOS.

Rollout Strategy

ALTRIOS supports two approaches to simulating multiyear rollout strategies: a prescribed rollout in terms of electrification percentage targets, or a fully user-defined rollout of user-defined locomotive and refueling infrastructure types. The former approach requires specifying the number of years to simulate and a target fleet electrification level (percentage of all locomotives that are battery electric by the final simulated year). Given those inputs, the rollout model determines each simulation year's fleet mix of battery-electric versus diesel locomotives, assuming linear year-over-year change in fleet electrification levels.

The rollout model interfaces with the train planner and simulation manager to prescribe, simulate, and compute lifetime metrics for a fleet replacement schedule, including both end-of-life replacement with equivalent locomotives (e.g., diesel-to-diesel) and replacement of diesel locomotives with BELs (at scheduled end of life or early as needed to meet the electrification target). As a simplifying assumption for proof of concept to determine scheduled end of life, the rollout model does not currently determine retirement as a function of gross miles traveled by each locomotive unit, but rather assumes a fixed percentage of the locomotive fleet must be retired each year. That fixed percentage of turnover may be exceeded (resulting in early retirements) if a rollout strategy transitions to alternative technologies rapidly enough.

For rollout strategies, a finite modeling time frame must be chosen, but output metrics should reflect impacts to rail operations beyond that time frame. Otherwise, it would not make sense to purchase any new locomotive or refueling infrastructure in the later portion of a rollout model (since the investment would not be used long enough to show value). To model the full value of purchased assets, ALTRIOS follows guidance from the Federal Railroad Administration for cost-benefit analyses and includes remaining asset value as a positive cash flow in the year

following the end of the model run (assuming constant yearly depreciation) [9]. This is financially equivalent to selling off remaining assets after the close of the modeling time frame. To conduct prescribed rollouts inclusive of BELs, the ALTRIOS rollout strategy includes refueling infrastructure. These infrastructure investments can be user-defined (as illustrated in Figure 12.) or, if no user-defined refueling infrastructure is provided, determined using a heuristic. In the latter case, the train planner determines charger port counts based on route network topology (number of freight corridors arriving at each destination node), locomotive fleet mix (percentage of locomotive fleet using each refueling infrastructure type), and a user-configurable scaling parameter.

The rollout model allows users to define a rollout schedule by analysis year and to include non-battery-electric alternative powertrains. It also allows user-defined assumptions for each technology input by year, such as powertrain component performance metrics (e.g., energy storage, fuel converter), economics (e.g., component costs), market conditions (freight demand by train type and origin/destination), and emissions (life cycle GHG values). For each scenario, the incumbent fleet of existing locomotives is designated by type (fuel and technology) and is treated as already purchased for cost computations.

The flexible format of rollout strategy definitions enables the user to analyze rollout strategies as exploratory "what-if" scenarios. Each of the defined analysis scenarios is simulated by the simulation manager, and the results are collected for later review, comparison, or visualization.

User Interface and Output Visuals

Python Interface

ALTRIOS uses several example scripts demonstrating numerous ways it can be used. These scripts show how to run ALTRIOS for common use cases with examples of loading models, editing model configuration parameters, running models, post-processing results, and visualizing results. Users can obtain these examples by following the instructions in the ALTRIOS README file (github.com/NREL/altrios/#how-to-run-altrios).

Web-Based User Interface: ALTRIOS Lite

ALTRIOS Lite is a lightweight web interface framework that meets NREL and federal accessibility requirements for websites [28], shown in Figure 21.. The web interface is a way to interact with a select set of features in ALTRIOS and visualize results without having to install any program. It is accessible to any user with an internet connection and is built in an expandable way to facilitate future capability additions. The web application comprises a front end, JavaScript-powered interface, and a back-end Python-powered web server. This decoupling allows users to utilize the application in two ways: by directly interacting with the graphical front end in a web browser or by programmatically querying the back end.

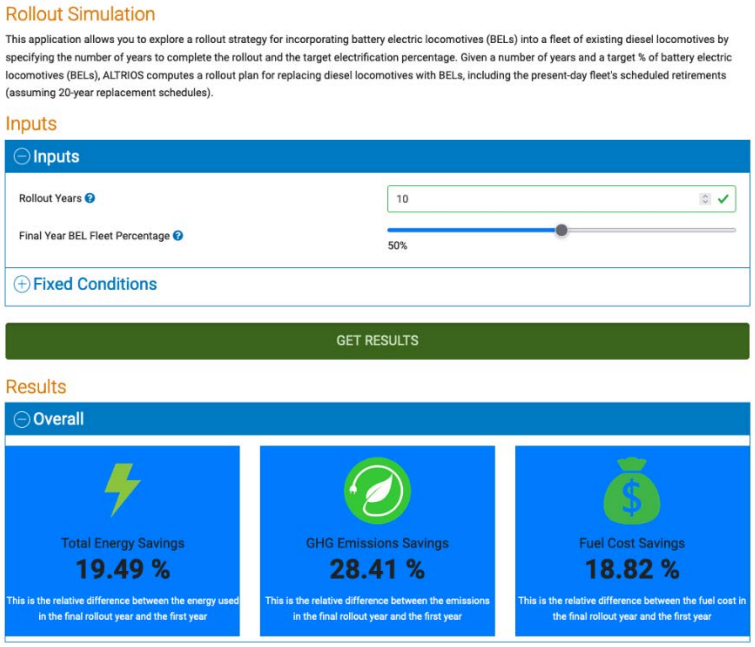

Figure 21. Screen capture of the prototype ALTRIOS Lite web interface. The interface is fast and responsive and will provide a rich interface for exploring select features of ALTRIOS without the need for installing any program.

Programming Standards

Coding Standards

Each train component throughout the hierarchy (from train or consist level all the way to base components, like fuel converters) has two classes: one class comprising static attributes (e.g., RES capacity [kWh], fuel converter peak power [kW], efficiency maps) and with methods for performing calculations at each time step, and another class comprising state variables that are modified at each time step. This enables rapid calculation of aggregate results (e.g., fuel consumption for an extended period of operation) while also allowing detailed tracking of how components behave over time by optionally storing the state classes in a state history vector at each time step, at a user-specified interval, or not at all.

The ALTRIOS code has been built as a pip-installable package (packaging.python.org/en/latest/tutorials/installing-packages/#use-pip-for-installing) with hierarchical, object-oriented, locomotive component classes; unit tests; and extensive use of PEP-257-compliant doc strings (peps.python.org/pep-0257).

All Rust variables are typed with units of measure (docs.rs/uom/latest/uom) such that any invalid operations (e.g., adding a power in watts to a length in meters) will fail during compilation, and only valid operations (e.g., adding a power to a power) will be allowed. This makes developing physically correct models in ALTRIOS slightly more tedious but provides the benefit of making it impossible to run simulations with invalid handling of units.

Data Description

Each component object in ALTRIOS tracks its own state data. Under normal operation, these data will be the state class instance at the current time step. Optionally, if the *save_interval*

variable is specified, a history variable will store the state at time steps at the *save_interval*. If *save_interval* is 2, for example, every other time step will be saved through the history of the simulation. This allows for fast, memory-efficient simulation when only aggregate-level variables are needed (e.g., when minimizing objectives using multi-objective optimization) and detailed output when second-by-second information is needed (e.g., when calibrating and validating the model against test data). Because each component stores its own state and optional history as public attributes, no extra effort is needed to collect the data at the end of the simulation. Additionally, the outermost component will propagate the *save_interval* hierarchically down to the innermost components.

Variable Naming Convention

Due to the object-oriented approach of ALTRIOS, variable naming implicitly handles component naming and hierarchy similarly to how components are hierarchically related in actual physical systems (e.g., fuel converter peak power inside of an instantiated *LocomotiveConsist* inside of an instantiated *TrainSimulation* is accessed as *train_sim.loco_con.fc.pwr_out_max_w*). Note that the units, which will always be standard SI units, are appended to the variable name with an underscore. All component-level variables are named according to the following scheme: <*type of quantity*>_<*out/in* in normal positive traction conditions>_<*conditional modifier*, if applicable>_<*unit abbreviation*>. A few more examples are as follows:

- *loco_con.fc.state.pwr_out_w*: Fuel converter (e.g., engine, fuel cell) output power at each time step.
- *loco_con.ess.state.pwr_out_w*: RES (e.g., battery) power output at each time step (negative for regenerative braking conditions).
- *loco_con.ess.pwr_out_max_w*: RES peak charge/discharge power.

Documentation

All user-facing Rust and Python code has been documented with idiomatic documentation strings, which are accessible via Python's Help function or directly via the "__doc__" attribute in Python and through Rust's native automatically generated HTML documentation with features for browsing and searching documentation. An example of Rust documentation is shown in Figure 22. This documentation can be generated and opened with "cargo doc –no-deps –open" in the "rust/" folder inside the Git repository.

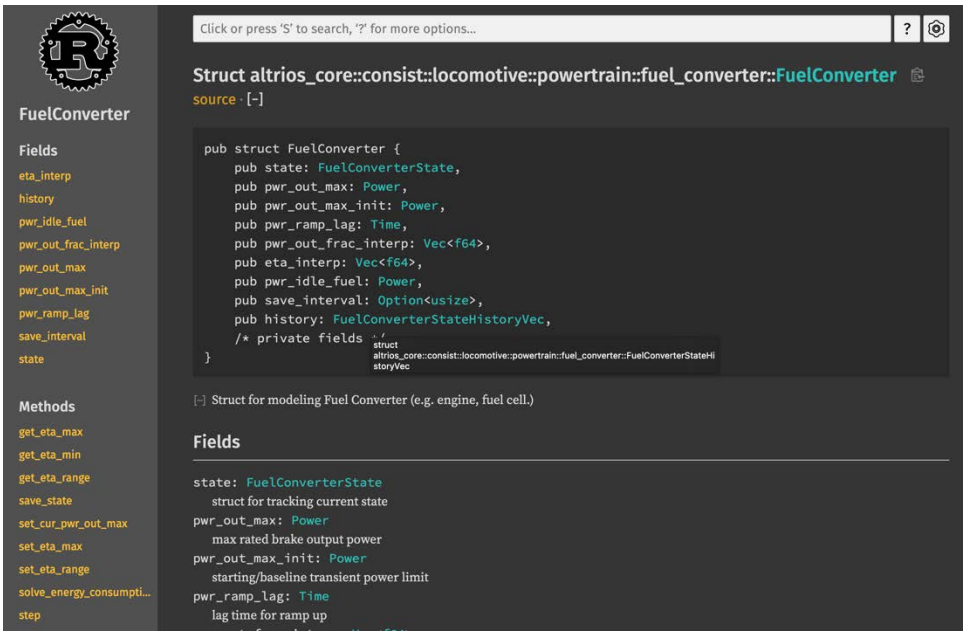

Figure 22. Example of auto-generated Rust HTML documentation for the fuel converter

Open-Source Release

ALTRIOS has been released with a BSD 3-Clause license at github.com/NREL/altrios and pypi.org/project/altrios. The GitHub repository has source code and build instructions, as well as the PyPI package, allowing for "pip install altrios" in any Python 3.8–3.10 environment.

Calibration and Validation

Data

The data used for the ALTRIOS model validation were obtained from the ZANZEFF program [4], in which BNSF was the key participant. Data included performance of a BEL that was demonstrated as part of this program. The BEL was used in a consist containing it and two Wabtec Tier 4 ET44C4 diesel locomotives.

Under the ZANZEFF project, the BEL consist was evaluated on a route between Barstow and Stockton, California, during the first quarter of 2021. The route is approximately 375 miles one way (Figure 23.). The consist made 17 round trips during the 3-month monitoring period, with a total of 12,750 miles traveled. The total duration of the data recorded is 900 hours.

Figure 23. Map of the route between Barstow and Stockton, California

The geography along the route made it well suited for validation of the ALTRIOS BEL and diesel-electric locomotive models. The elevation profile of the route can be seen in Figure 24. The mountains provided opportunities for high-power traction or regenerative braking for long durations. The long flat plain between Bakersfield and Stockton provided another extreme in geography. This portion of the data will exhibit lower power demand upon the locomotive consist. This ensures that the models will be validated across the entire operating space of the locomotives.

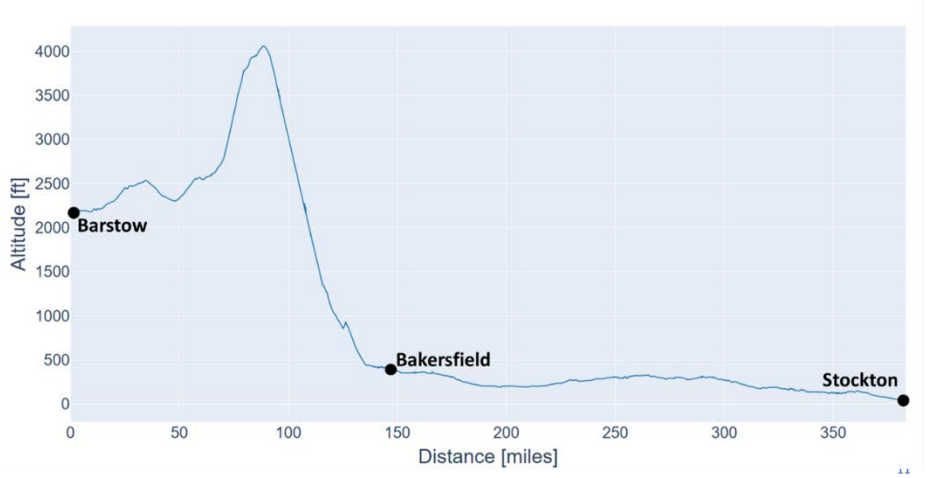

Figure 24. Elevation profile of the Stockton-Barstow route

Additional data were also joined, and time was aligned with the ZANZEFF dataset, including event recorder data and train consist data.

The event recorder data were recorded by each locomotive. They include signals such as train speed, tractive effort, GPS coordinates, and locomotive notch. The event recorder data are needed in addition to the ZANZEFF data to validate the full train model. The trains pulled in the

ZANZEFF program included additional wild-card locomotives that were not recorded in the ZANZEFF dataset.

The train consist data are needed to understand the makeup of the train and how it changed throughout the trip as cars were dropped off and additional cars added to the train at various stops along the route. The train consist data include parameters like miles traveled, start time, end time, trailing tons, numbers of railcars, number of locomotives, and locomotive state, which are all needed to properly model the train.

Conventional Diesel-Electric Locomotive Validation

The conventional diesel-electric locomotive model was calibrated by adjusting idle fuel rate and drivetrain efficiency. The engine efficiency map was not adjusted because it was based upon actual test data that were captured for AAR end-of-useful-life testing. A segment of the validation data that demonstrates the capability of the model is plotted in Figure 25. This example covers one of the segments that exhibited a better fit.

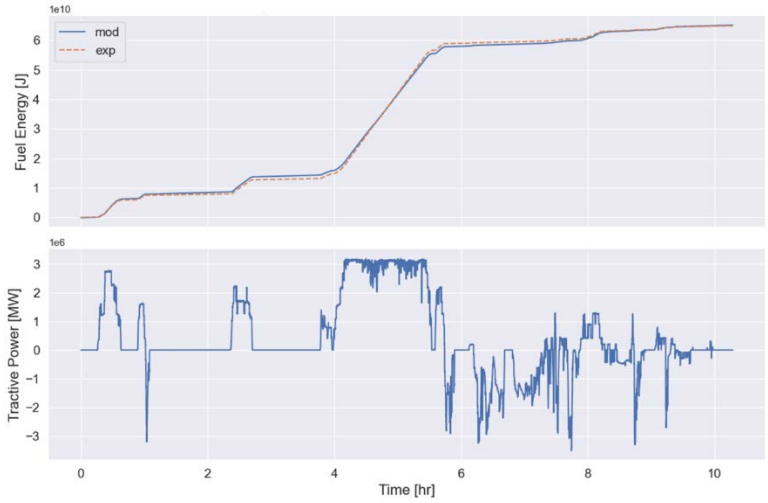

Figure 25. Plots comparing experimental and modeled fuel flow and tractive power that were used for calibration and validation of conventional locomotive

The scatter plot in Figure 26 compares the total fuel energy used for each trip segment. The error for the calibration produced a 5.9% time-weighted mean error when compared against the hold-out validation data. The calibrated data produced a 3.3% error in fuel energy across all trips. The error was 4.2% when averaged across both datasets.

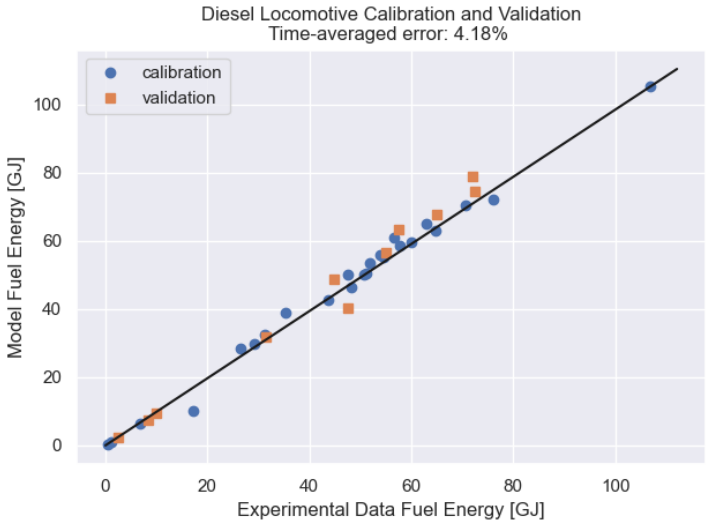

Figure 26. Scatter plot comparing experimental and modeled fuel energy usage for diesel locomotive calibration

BEL Validation

Because the BEL tested in the ZANZEFF data was a prototype with an air-cooled battery and an unoptimized control system, we decided to use the BEL data for validation of trendwise behavior. Comparisons of experimental and modeled SOC and tractive power are shown in Figure 27. Another important reason for not calibrating the BEL against ZANZEFF test data is to avoid reverse-engineering the BEL design, including the control system. Wabtec has significant intellectual property invested in this design, and it is critical to avoid exposing it. Several modern hybrid control algorithms were implemented from which the user can choose. These algorithms were based upon NREL's experience modeling on-highway hybrid cars and trucks. However, it is important to note the data in Figure 27. show that the BEL energy management algorithm captures many of the same behaviors as the algorithm contained in the prototype BEL.

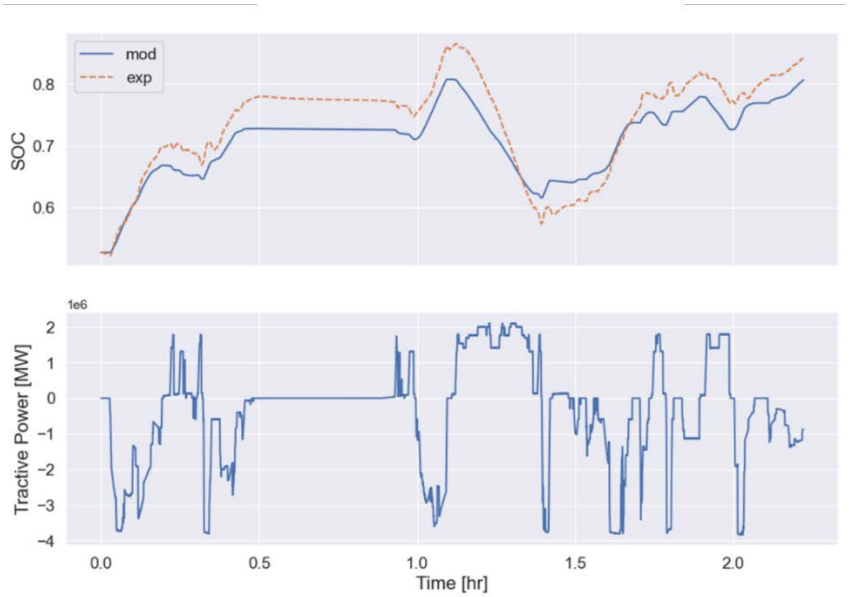

Figure 27. Plots comparing experimental and modeled SOC and tractive power used for validation of the BEL locomotive

TPC Validation

For the TPC, calibration and validation were performed by imposing speed traces from test data on the train and comparing the second-by-second cumulative tractive energy required to pull the train predicted by the model to the value calculated from the test data. Calibration parameters for this were C_dA (product of drag coefficient and frontal area) of unloaded cars, C_dA of loaded cars, rolling resistance ratio, and bearing resistance. In some of the trips, wild-card locomotives and other anomalous factors rendered the data unsuitable for calibration. Of the trips that were suitable for calibration, 70% were randomly chosen, while 30% were reserved for validation. Example time-series results are shown in Figure 28.

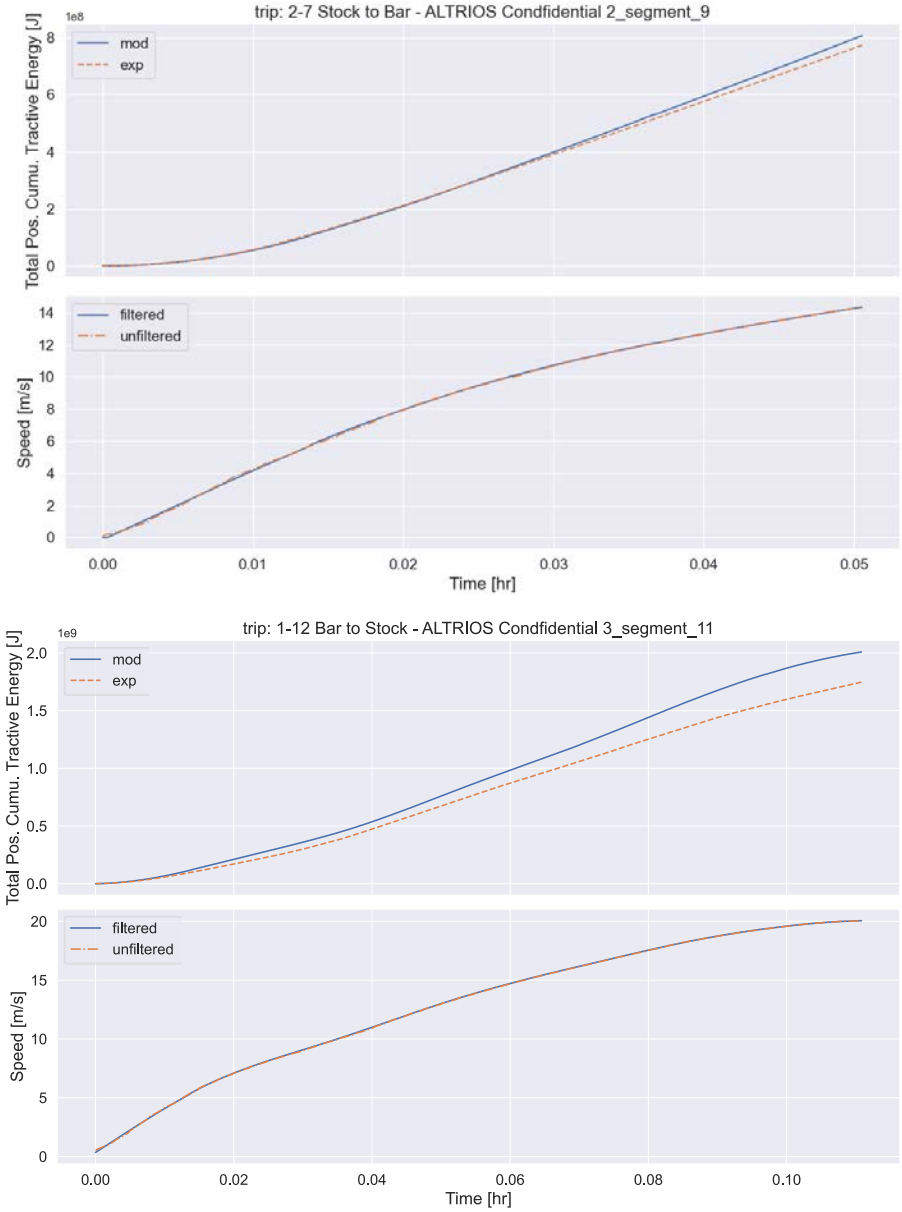

Figure 28. Example results of TPC calibration for two trips: onefrom the calibration set (upper panel) and one from the validation set (lower panel).

Note: The bottom axis in each plot shows the imposed speed trace from the ZANZEFF data, and the top plots shows the cumulative tractive energy required to pull the train.

The scatter plot in Figure 29. compares the total cumulative tractive energy used for each trip segment. The error for the calibration produced 16.66% time-averaged mean error when compared against the hold-out validation data. The calibrated data produced 21.29% error in tractive energy across all trips. The error was 17.69% when averaged across both datasets. Given the high level of measurement uncertainty, environmental impacts from unknown conditions (e.g., wind), and other real-world considerations, this shows acceptable agreement between the model and validation dataset.

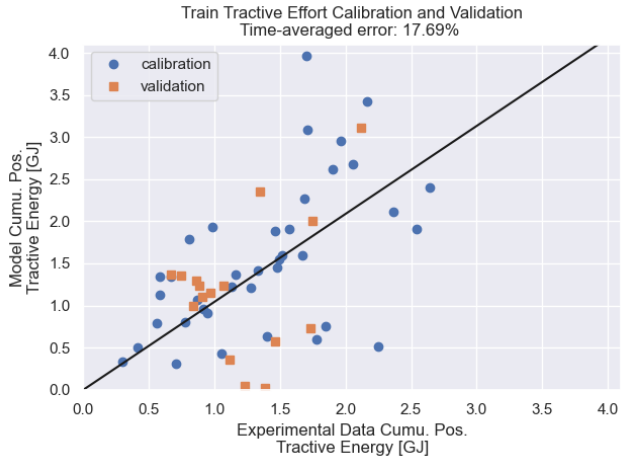

Figure 29. Scatter plot comparing experimental and modeled fuel energy usage for diesel locomotive calibration

ALTRIOS Application Example: Taconite Case Study

A case study was conducted on two routes within the BNSF network to demonstrate the current capabilities of the ALTRIOS framework. The two routes were chosen to demonstrate the dependance of BEL performance on route geography and freight flows.

The first route, shown in Figure 30, was between the Allouez ore docks in Superior, Wisconsin, and the ore mines in Hibbing, Minnesota. The trains on this route haul taconite iron ore from the Mesabi Iron Range to the port in Superior. The trains return empty when headed north to the Mesabi Range. This means that the loaded train heads downhill on the way to port, while the empty train must work against the grade to return to the mines. Hypothetically, in an ideal application, the dynamic braking energy recovered by the BEL when controlling the speed of the heavy loaded train on the descending grade to the port will exceed the traction energy required to move the much lighter empty train back uphill with no need for any terminal charging between runs. Internationally, several iron ore operators have proposed implementing BELs in this manner, dubbing the concept “Infinity Train,” as no diesel or electricity is required, and the train is effectively powered by the gravitational potential energy of the loaded railcars. Although the specific topography of the BNSF Taconite case study may not achieve this same level of performance, it is anticipated that a BEL will demonstrate substantial fuel savings on this route.

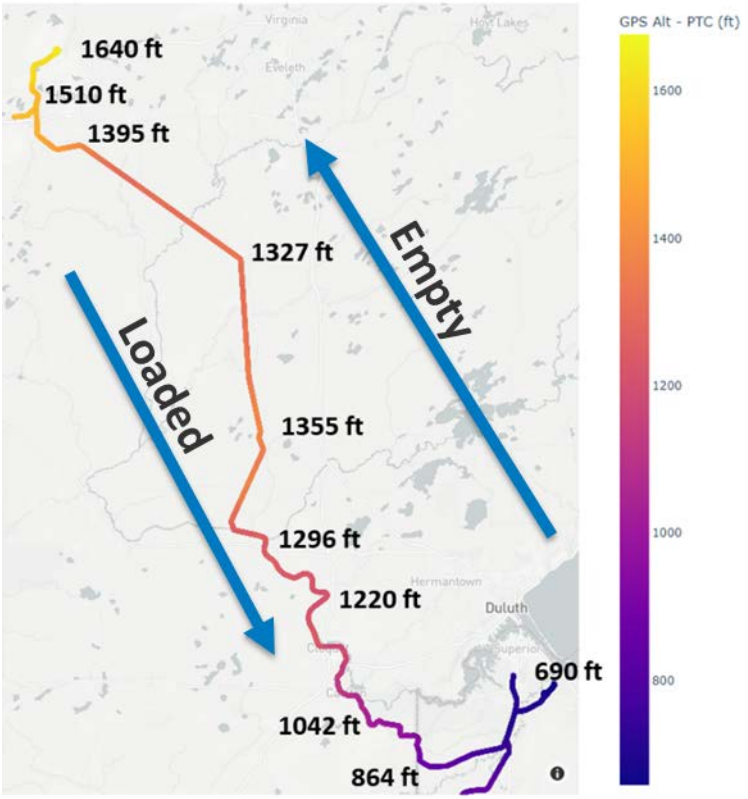

Figure 30. Map of BNSF Taconite route between the Mesabi Iron Range and Superior, Wisconsin

The second route also terminates in Superior, Wisconsin, at its northern end (Figure 31). The southern end of this route is the Northtown Yard on the north side of Minneapolis, Minnesota. The trains on this route are mixed-freight trains that haul general types of freight in both directions. The geography on this route is quite flat. It is anticipated that the BEL performance will not be as significant on this route because of fewer opportunities to capture dynamic braking energy and the balanced train weights in both directions.

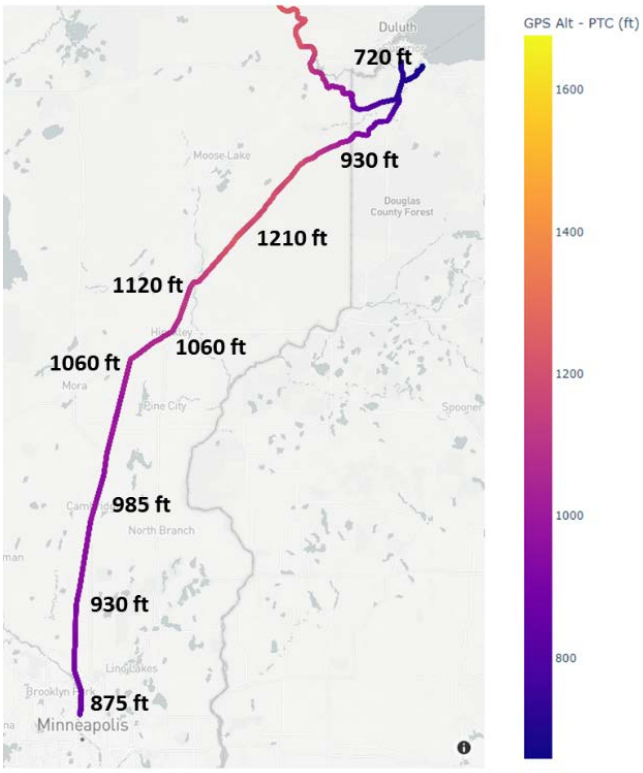

Figure 31. Route between Minneapolis and Superior, Wisconsin

Model Development & Calibration

The development of the model for this case study involved two key tasks. The first was the development and validation of the network. The second was calibration of the freight demand and the train planner to match train length, number of locomotives, and train weight. The development of the network is detailed in the "Network and Topology" section of this report.

A network simulation was conducted using conventional locomotives to fine-tune the train planner and freight demand. The exercise consisted of simulating conventional locomotives through each route while varying target train length, freight demand, car masses, target horsepower per ton, and car length. The results were then compared to event recorder data to verify that they fell within similar ranges.

Event recorder data and train information were collected from eight trains on each route. This is the same dataset that was used to calibrate the elevation model for the network. The values derived from these data are shown in Table 13.

Table 13. Values Derived From Actual Information Supplied by BNSF Used To Calibrate the Model

Parameter	Taconite North	Taconite South	Minneapolis North	Minneapolis South
Average train length (ft)	6,300	6,300	5,100	6,200
Average number of loads	0	180	31	57
Average number of empties	180	0	56	44
Average car length (ft)	35	35	59	62
Average car weight (tons)	29	129	66	87
Average gross weight (tons)	5,250	23,200	5,700	8,600
Average locomotive count	3	3	3	3
Average estimated Horsepower Per Ton	2.6	0.6	1.7	1.1
Number of stops	2.8	3.5	6.2	7.9
Average speed (m/s)	11.7	9.5	13.9	9.6
Average distance (km)	164	164	222	217

The model was calibrated to match the number of locomotives per train, train length, number of cars, distance traveled, and gross weight. Not all performance metrics were matched exactly, due to differences in how ALTRIOS functions compared to operating decisions made by BNSF within their larger network context. Examples of ALTRIOS outputs that were verified to be reasonable but were not calibrated to match perfectly are average speed and number of stops. Differences in speed were attributed to differences in train scheduling and routing. The differences in the number of stops were attributed to the lack of other types of train traffic on each route interacting with the modeled iron ore and manifest trains. The other sources of error were starting and stopping within a rail yard at the beginning or end of a trip. Summary outputs for the modeled trains are presented in Table 14.

Table 14. Values From Simulated Train Operation

Parameter	Taconite North	Taconite South	Minneapolis North	Minneapolis South
Average train length (ft)	6,320	6,320	4,600	3,600
Average number of loads	0	180	44	59
Average number of empties	180	0	37	28
Car length (ft)	35.1	35.1	59	59
Empty car weight (tons)	29.2	29.2	29.2	29.2
Loaded car weight (tons)	129	129	143	143
Average gross weight (tons)	5,900	23,800	7,800	8,300
Average locomotive count	3	3	2	1.5
Number of stops	2	1	5.5	3
Average speed (m/s)	5.0	8.8	13.1	8.5
Average distance (km)	99	99	118	117

Table 15. Table of Model Parameters Used To Achieve Model Calibration

Parameter	Value
Unit train Horsepower Per Ton	0.7
Unit train empty Horsepower Per Ton	2.0
Manifest Horsepower Per Ton	1.5
Manifest empty Horsepower Per Ton	1.5
Unit car loaded weight (kg)	117,000
Unit car empty weight (kg)	26,500
Manifest car loaded weight (kg)	28,500
Manifest car empty weight (kg)	130,000
Manifest train target length (cars)	94
Unit train target length (cars)	180

Rollout Study

A rollout study was conducted in which BELs were adopted over a 30-year period for each route. Each route was simulated using the maximum BEL adoption possible within the constraints of the simulation. This was limited for both routes by the train planner constraint that required at least one conventional diesel locomotive per consist.

Each route was simulated with three levels of freight transportation demand. These demand levels were set to generate one, two, or three trains per day in each direction. Each line color in the following plots represents one of these demand levels. The line style represents the various parameters being plotted.

The BEL for this baseline study has a battery capacity of 2.4 MWh. This capacity was selected to match the prototype Wabtec BEL that was used for the ZANZEFF demonstration. This is viewed as a minimum battery capacity that will be available in future BELs.

The percentage reduction in diesel fuel during the final year of each rollout study relative to the initial year (which planned the same number of trains per day using all-diesel consists) was 57% for the Taconite route and 45% for the Minneapolis route. This can be seen in Figure 32 and Figure 33. These results were somewhat expected based on route geography and freight flows and are detailed in the following plots. The impact of freight demand was minimal.

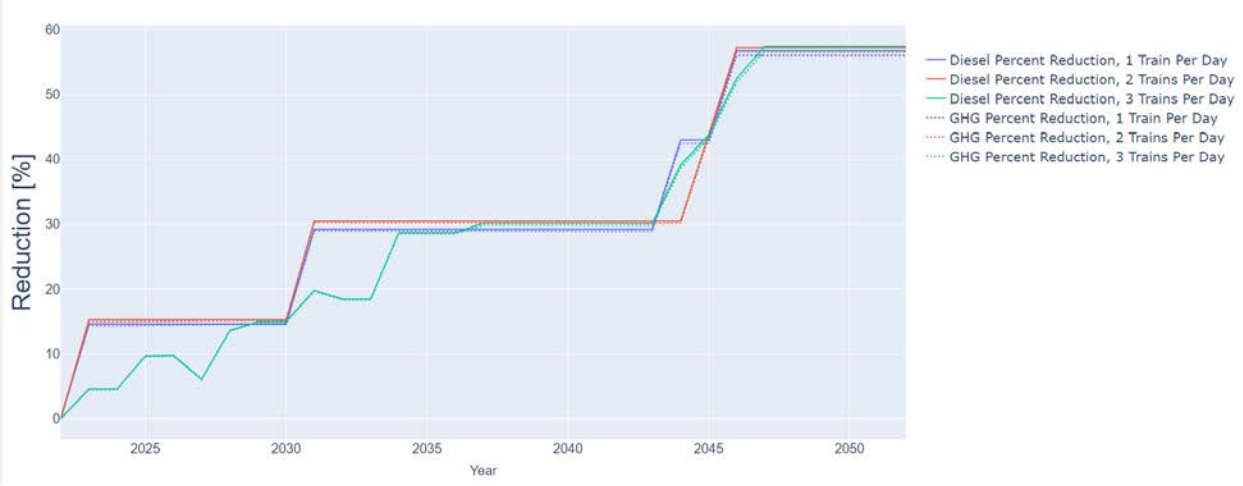

Figure 32. Plot of emissions and diesel fuel percentage reduction for the Taconite route

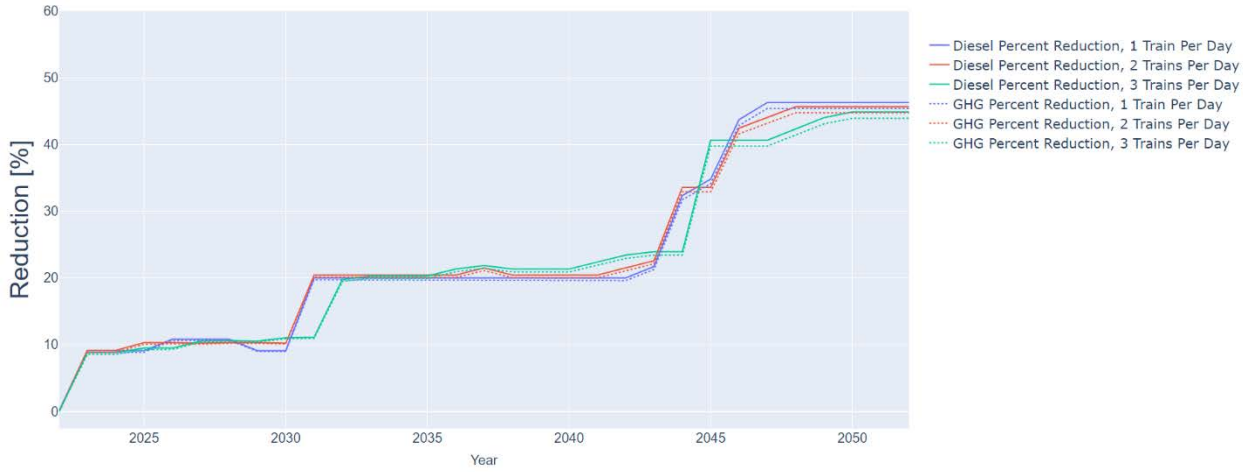

Figure 33. Plot of emissions and diesel fuel percentage reduction for the Minneapolis route

Reduced emissions from the operation of these trains is explained by the reduction in diesel fuel consumption. The data presented in Figure 34 and Figure 35 show how diesel fuel consumption is reduced in gallons as BELs are adopted. The overall reductions in these figures reflect the percentage reductions in Figure 32 and Figure 33. The important thing to note about these two routes is that the initial fuel usage for the Taconite route was much greater than the usage on the Minneapolis route but was almost equal by the end of the BEL rollout. This means that an equivalent percentage reduction on the Taconite route would be more significant than the same reduction on the Minneapolis route.

Figure 34. Plot of annual diesel fuel usage in gallons for the Taconite route

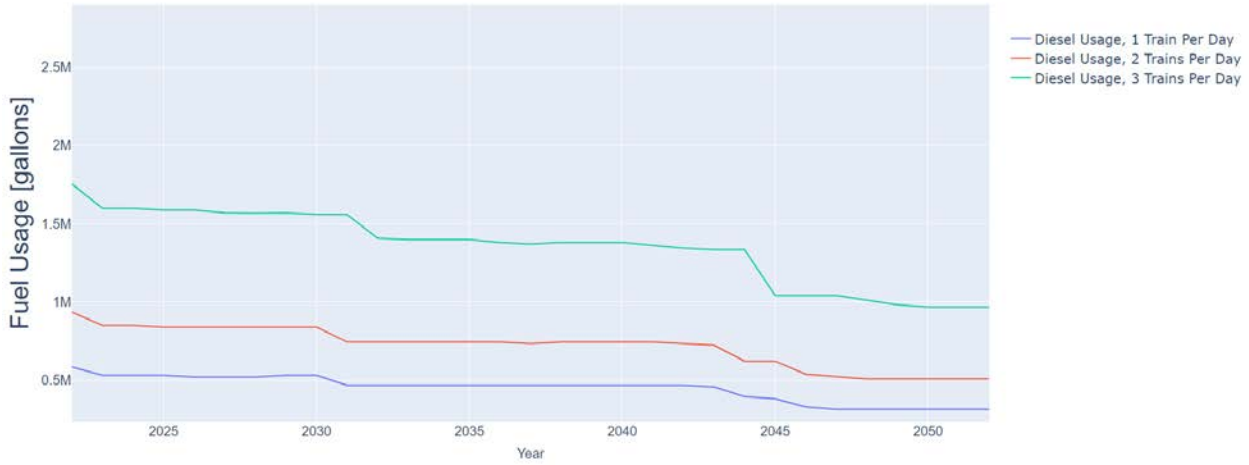

Figure 35. Plot of annual diesel fuel usage in gallons for the Minneapolis route

The reduction in diesel combustion emissions is accompanied by an increase in emissions from electric grid power production. However, the increase in electricity emissions is quite small in magnitude relative to diesel combustion emissions and is expected to be further reduced as grid CI decreases. The grid CI was Cambium CO_2 intensities outlined in the Greenhouse Gas Life Cycle Analysis Input Data section. The relative impacts of these two trends can be seen in Figure 36 and Figure 37.

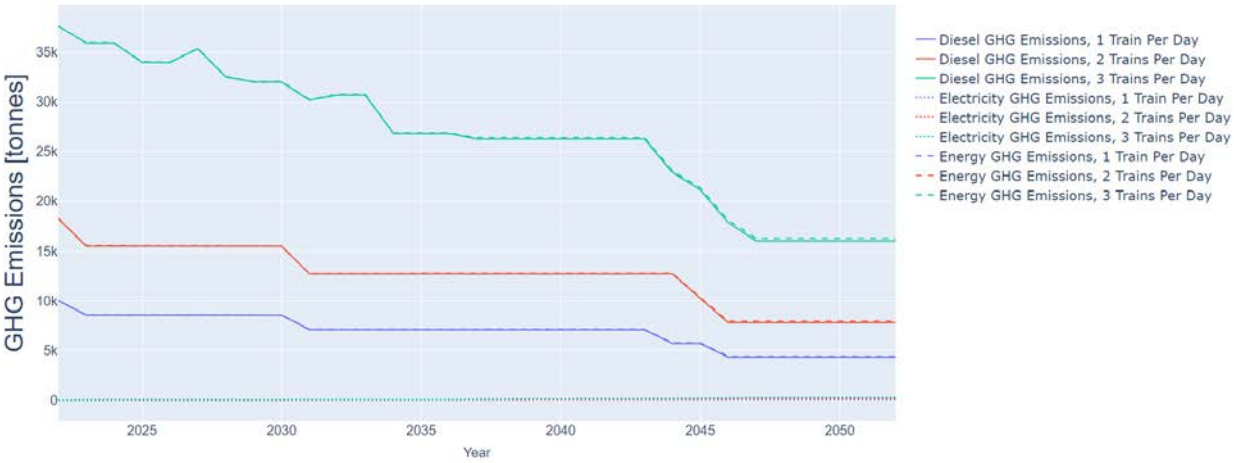

Figure 36. Plot of annual GHG emissions by source for the Taconite route

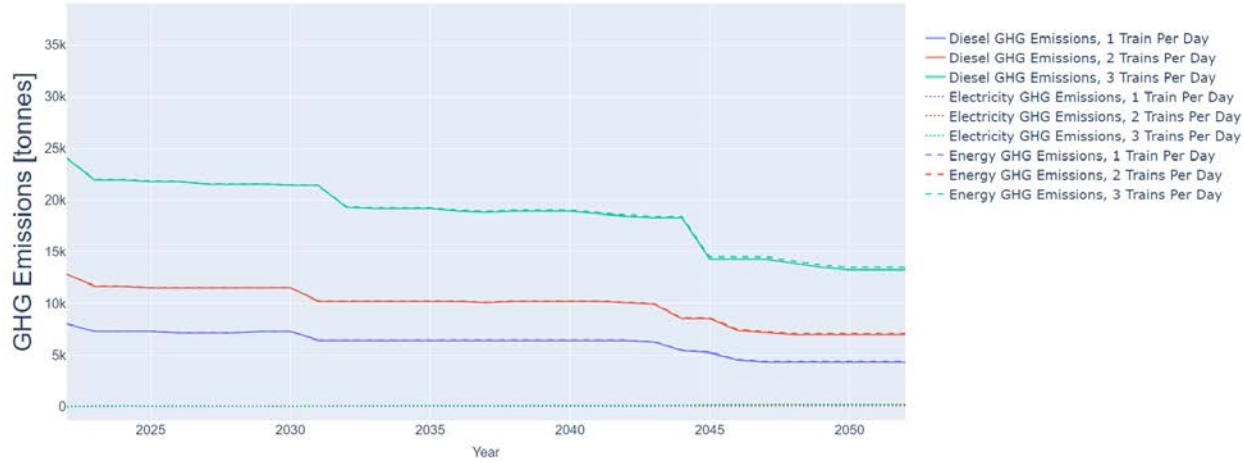

Figure 37. Plot of annual GHG emissions by source for the Minneapolis route

Locomotive investments are needed to enable switching energy sources from diesel to electricity, and those investments impact overall costs. Simulated locomotive counts—total, BEL, and conventional—are shown in Figure 38 and Figure 39. These counts include locomotives already in the locomotive fleet, as well as those purchased each year, whether as investments in electrification or as scheduled replacements of the existing fleet with like locomotives (assuming 5% annual turnover, which may represent an aggressive rate of turnover relative to current industry trends).

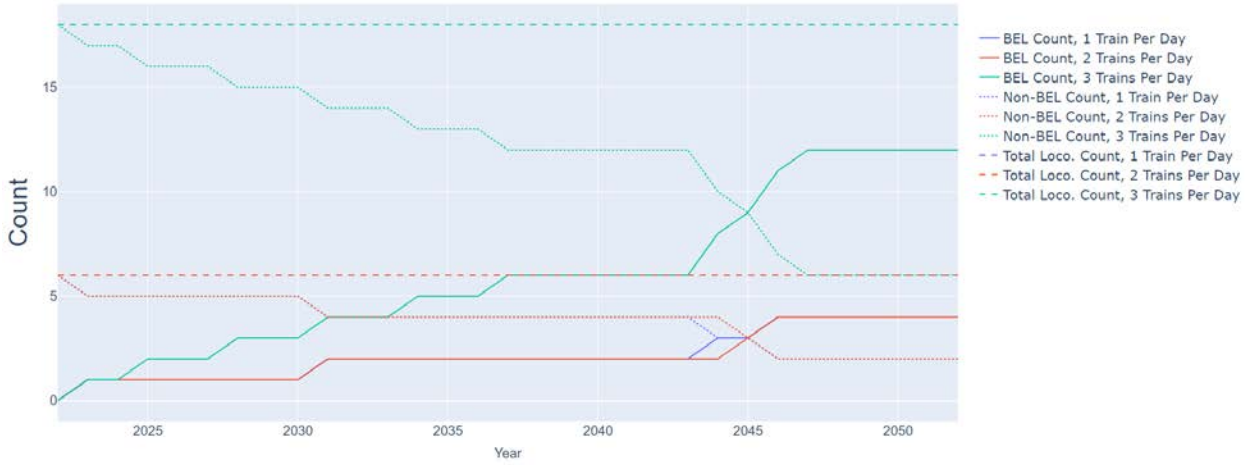

Figure 38. Plot of locomotive counts by year for the Taconite route

Figure 39. Plot of locomotive counts by year for the Minneapolis route

The fraction of BEL locomotives used within each route is shown in Figure 40 and Figure 41. Both rollout strategies peaked at a BEL fraction of about 2/3. BEL implementation is limited by the need to include a diesel-electric locomotive in each consist because an equivalent number of locomotives in an all-BEL consist does not have sufficient battery storage capacity to power the train over either route.

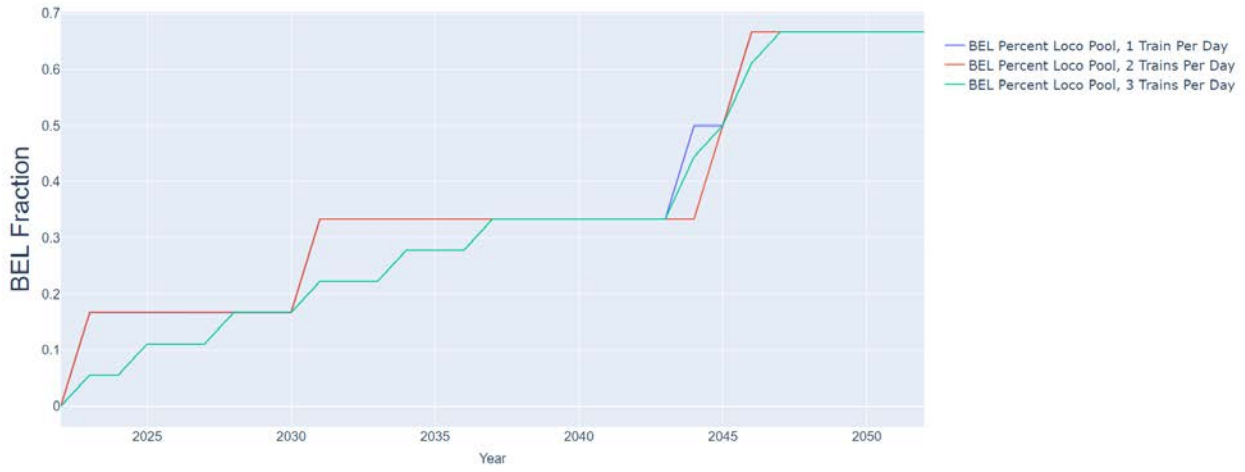

Figure 40. Plot of the fraction of BELs in the locomotive pool by year for the Taconite route

While this mismatch in goals versus operations may not be optimal financially, it does highlight the need for coordination between groups operating the railroad and planning the locomotive fleet. If more locomotives are purchased than can be used, the actual usage in the fleet will still be capped at the percentage that can reliably haul freight.

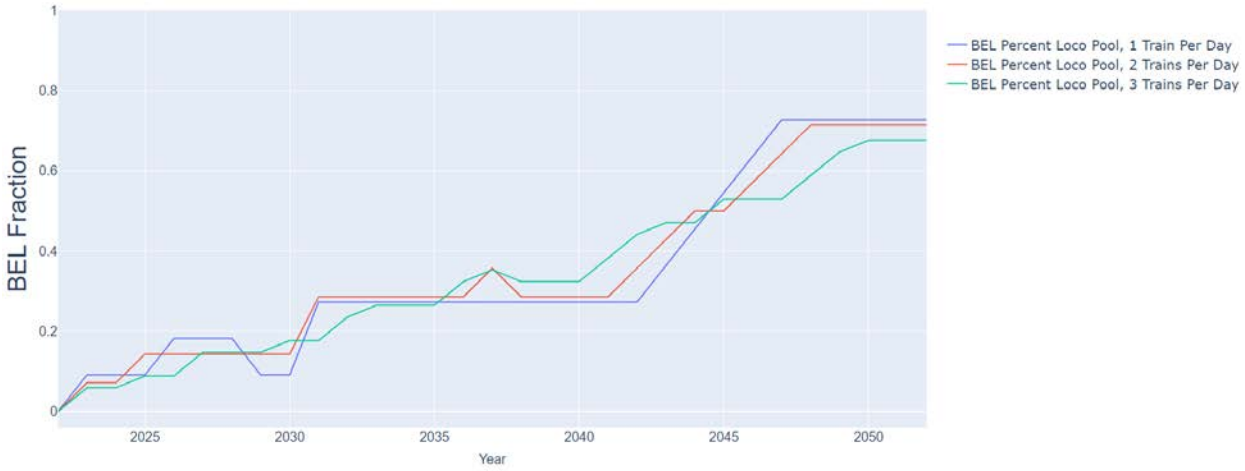

Figure 41. Plot of the faction of BELs in the locomotive pool by year for the Minneapolis route

The normalized costs per megatonne-kilometer are presented in Figure 42 and Figure 43. These costs associated with each route are similar, but there are some differences that can be observed. The two largest drivers of these differences are locomotive purchases and energy costs, which are discussed in subsequent figures. Recharging infrastructure investment and installation costs also affect these differences, but they represent a smaller share of total costs due to the relatively low number of chargers needed in this scenario and their being less costly per unit than locomotives.

Figure 42. Plot of levelized cost per megatonne-kilometer and ton-mile for the Taconite route

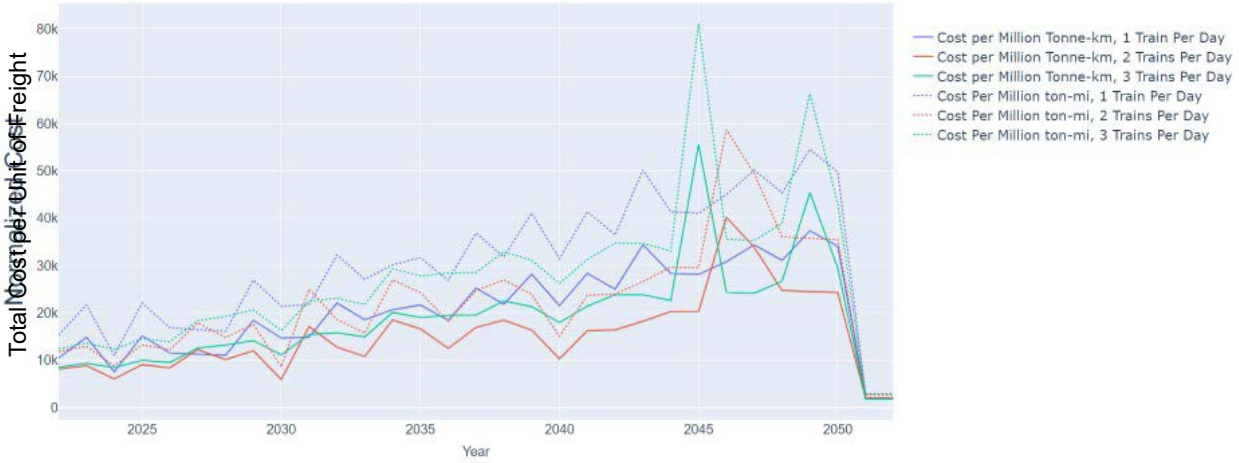

Figure 43. Plot of levelized cost per megatonne-kilometer and ton-mile for the Minneapolis route

Energy costs are a major contributor to the total cost of operating a railroad. The annual energy costs for this study are presented in Figure 44 and Figure 45. The reduction in diesel cost is much greater than the increase in electricity cost as BEL usage is increased. This is much more significant on the Taconite route because there are many more opportunities to charge BELs through regenerative braking as the loaded train is traveling downhill toward the port. However, the regenerative braking on both routes increases the efficiency of each train, so a reduction in diesel usage is not reflected in an equivalent increase in electricity usage. These estimates assumed a constant price for both electricity and diesel. The prices for diesel and electricity were based on the 2023 U.S. Energy Information Administration Annual Energy Outlook. The average price of diesel over this period was $3.88 per gallon. The average cost of electricity over this period was assumed to be $6.90/MWh, including taxes and transmission and distribution fees. A key source of uncertainty pertains to whether railroads may more closely follow trends for commercial or industrial electricity rates as their energy and power demand increases; for this case study, projected industrial rates were used.

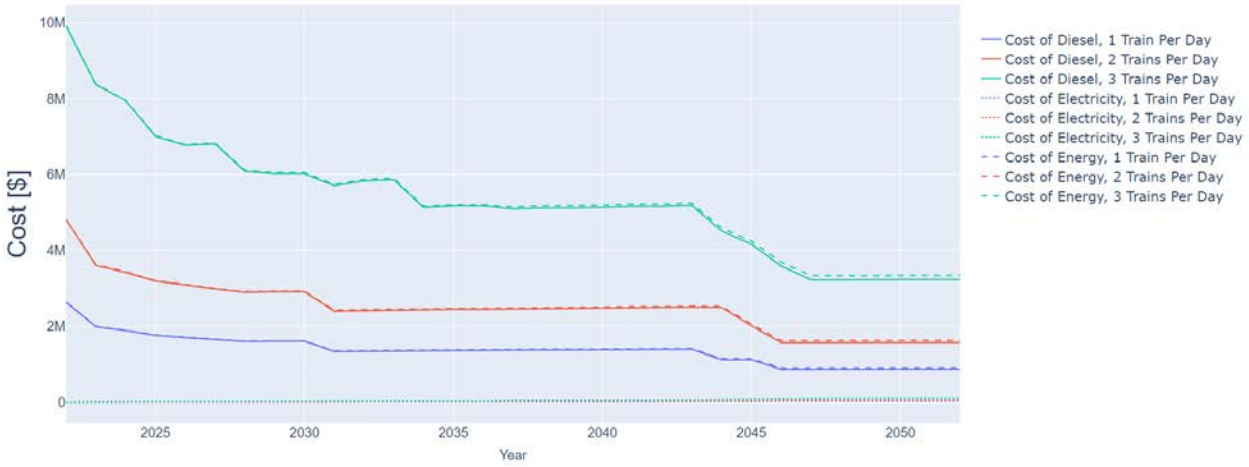

Figure 44. Plot of annual cost of energy by type for the Taconite route

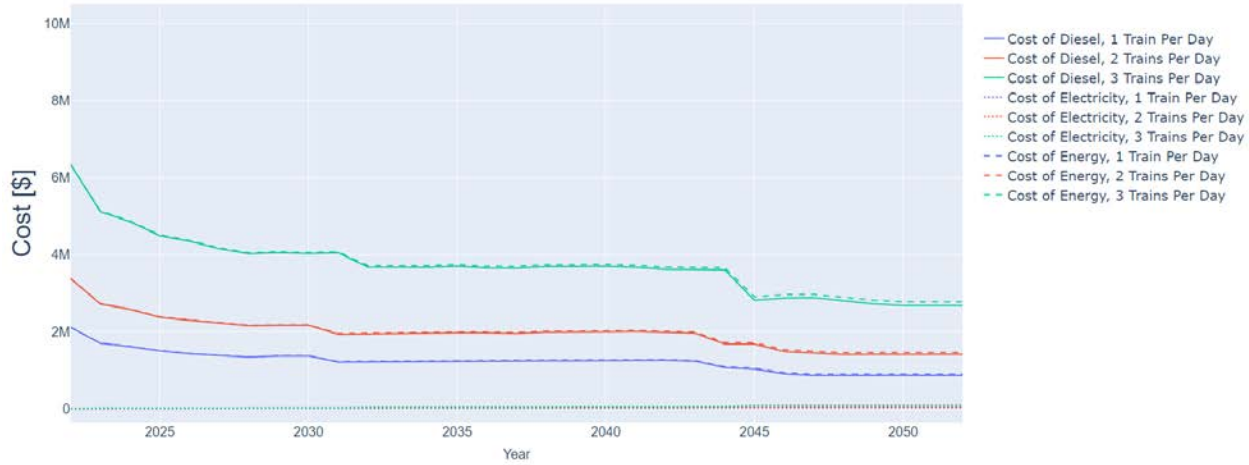

Figure 45. Plot of annual cost of energy by type for the Minneapolis route

The total costs required each year for fuel, infrastructure, and new locomotives are presented in Figure 46 and Figure 47. Charging infrastructure investments were a small share of total costs in this case, so they are included in total costs but not plotted as a separate line. The biggest cost for both routes is energy. A reduction in energy usage will impact overall financial performance. However, there were a few years where large locomotive purchases dominate the annual cost. It is unknown why the train planner chose to make large BEL purchases in these years, but it should be investigated in the future.

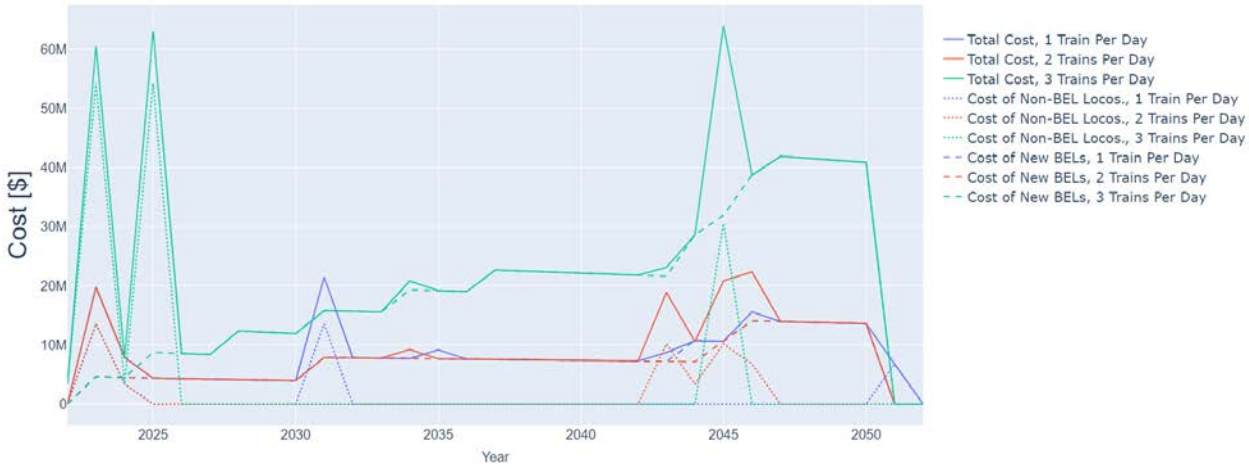

Figure 46. Plot of annual costs and new locomotive costs for the Taconite route

Figure 47. Plot of annual costs and new locomotive costs for the Minneapolis route

Understanding the summary statistics for these simulations is important, but it is also important to understand why these parameters exhibited the trends that they did. Figure 48–Figure 51 show the speed, SOC, and elevation of a single train as it progresses through its route.

The data presented in Figure 48 show a Taconite train traveling from Superior, Wisconsin, to Hibbing, Minnesota. This train is hauling empty cars north to the mine. The grade is uphill most of the trip, which limits the opportunities for the BEL to capture energy through regenerative braking. The trajectory of the SOC reflects this, as it is depleted during the first 45 km of the trip and remains at this level for the duration.

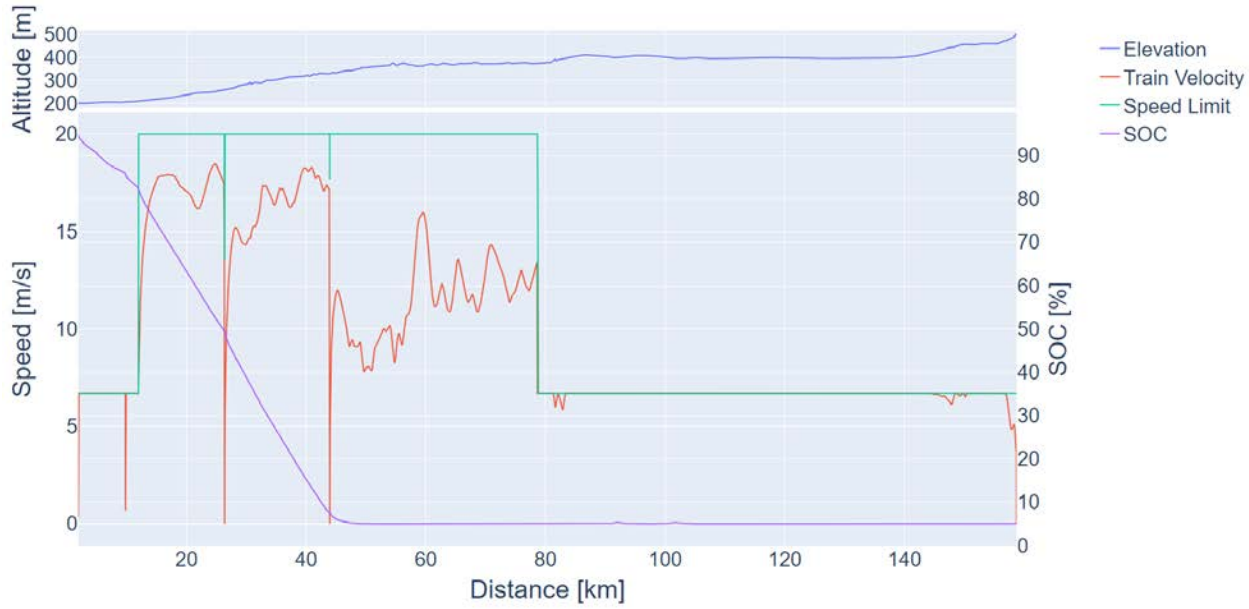

Figure 48. Plot of SOC, speed, speed limit, and elevation for an empty Taconite train traveling from Superior, Wisconsin, to Hibbing, Minnesota

Figure 49 shows data from a loaded Taconite train heading back to the port in Superior, Wisconsin. This trip is downhill most of the way. The SOC does not deplete until 75 km (47 mi) into the trip despite being four times heavier than the northbound train. It can also be seen around 80 km (50 mi) and 135 km (84 mi) that the BEL is able to charge while maintaining speed. This energy would normally be lost as heat through dynamic braking.

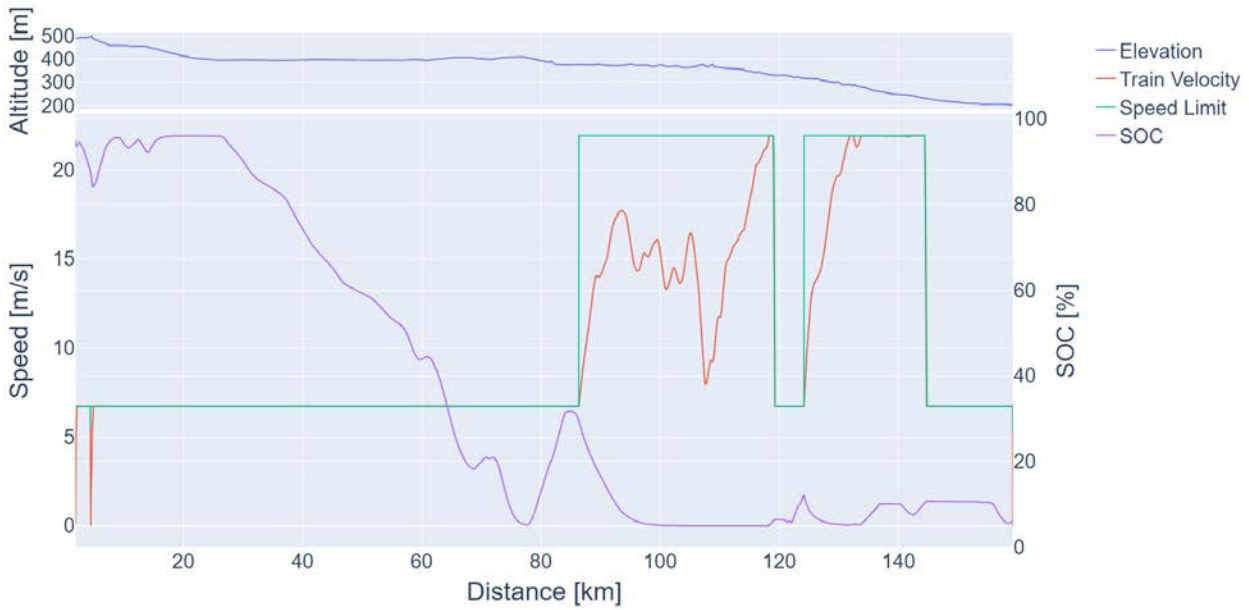

Figure 49. Plot of SOC, speed, speed limit, and elevation for a loaded Taconite train traveling from Hibbing, Minnesota, to Superior, Wisconsin

The trip shown in Figure 49 demonstrates the importance of charging strategy. This train had a fully charged BEL when departing. This resulted in energy being lost as heat through braking.

The simulations were originally conducted in this manner. However, the charging strategy was modified to charge the BEL only to 50% in Hibbing to ensure enough battery capacity for regenerative braking during the initial portion of the trip.

The biased freight flow for this route is what allows the BEL to perform this well. The bias in freight flow allows loaded trains to haul freight in a downhill direction while empty trains return uphill. This difference allows for capturing the potential energy of the freight being transported. The difference in elevation between the start and end of the route is about 300 m. The iron ore accounts for 75% of the train mass. This means only 25% of the loaded train weight must be hauled uphill back to the mines.

The BEL rollout did not yield such significant improvements on the Minneapolis route. The geography of this route has fewer areas with a steep grade. The profile elevation of this route can be seen in Figure 50. This results in the BEL being depleted early in the trip and never recovering. It only takes about 35 km for this to occur for this train with a single BEL containing a 2.4-MWh battery.

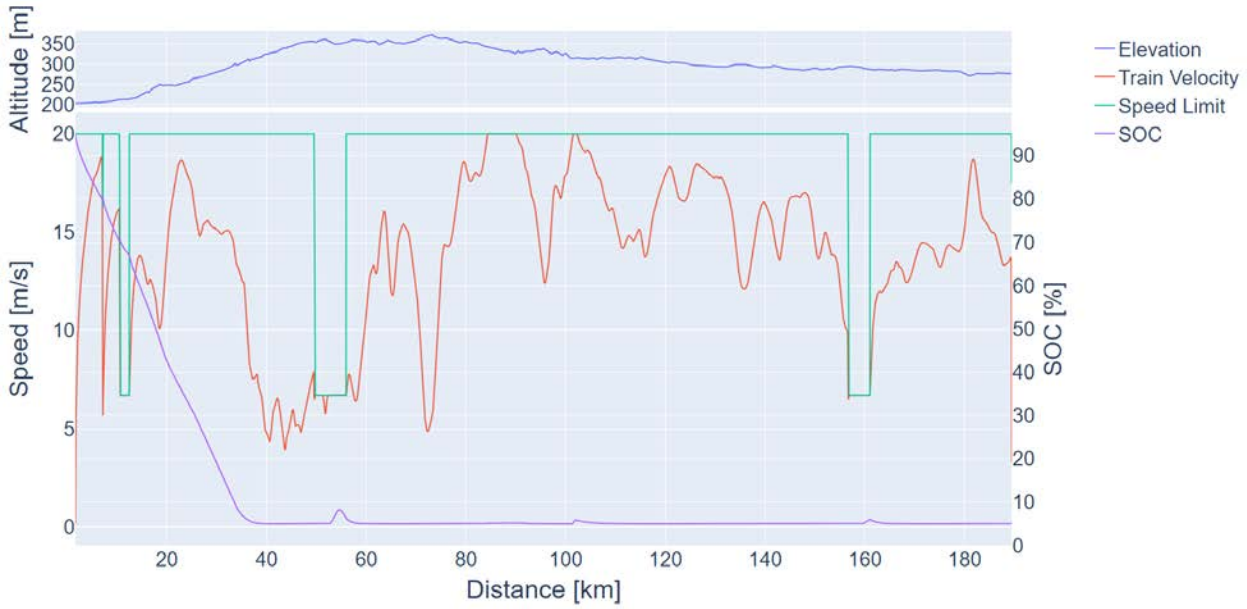

Figure 50. Plot of SOC, speed, speed limit, and elevation for a manifest train traveling from Superior, Wisconsin, to Minneapolis, Minnesota

The freight flows for this route are also more balanced. The masses of the trains traveling in each direction are similar. This means the freight is pulled over the hill rather than down the hill like the Taconite route. The BEL performance during the initial portion of this trip leaving Minneapolis, Minnesota, is very similar to the train leaving Superior, Wisconsin, as shown in Figure 51.

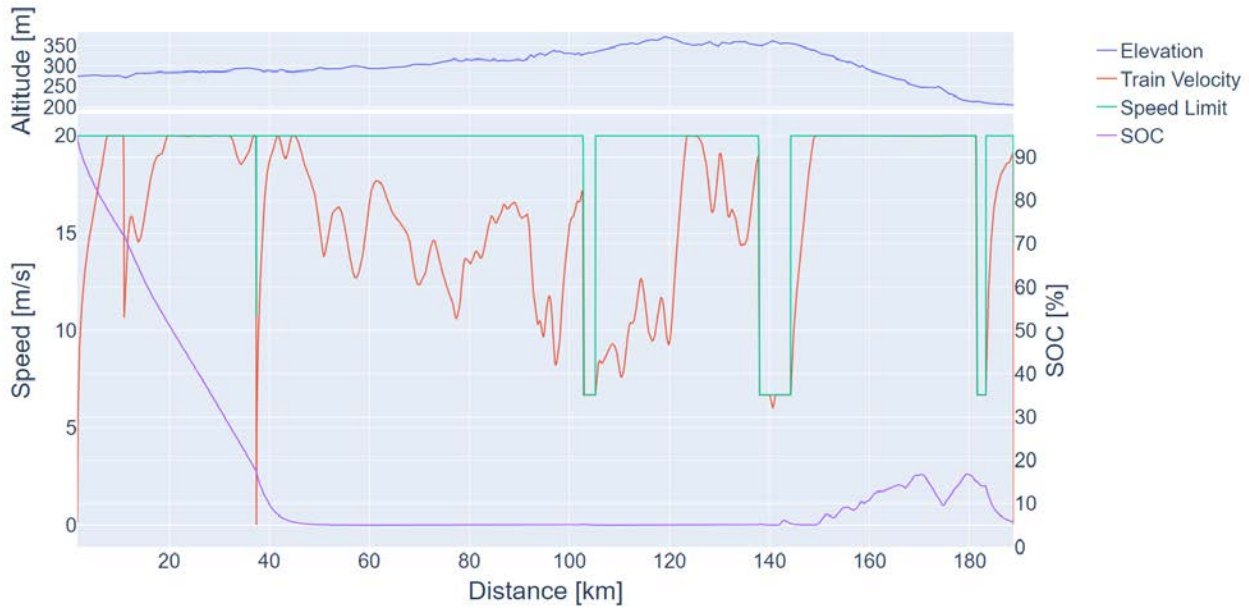

Figure 51. Plot of SOC, speed, speed limit, and elevation for a manifest train traveling from Minneapolis, Minnesota, to Superior, Wisconsin

When traveling from Minneapolis to Superior, the 2.4-MWh BEL is able to contribute to the train for about 45 km. This is due to the flatter grade near Minneapolis. However, the BEL is able to recover some energy as it descends the grade into Superior.

BEL Battery Capacity Study

A second study was conducted to determine the impact of BEL battery capacity and charging strategy. This study used 2.4-, 6-, 8-, and 14-MWh battery capacities. The charging strategy for the Taconite route varied the departing SOC in Hibbing from 5% to 95%. The Minneapolis route varied the departing SOC from both locations from 5% to 95%. (Real-world applications may not allow SOC to drop as low as 5% or to charge as high as 95% depending on battery manufacturer constraints or recommendations, but these values allowed for testing a wider range of charge strategies.) The freight demand was kept constant at two trains per day. Therefore, the 2.4-MWh cases for this study will match the results from the final year of the rollout study.

The reduction in diesel usage and emissions is presented in Figure 52–Figure 55. The BEL performance trends were consistent between the two routes. Larger BEL battery capacity yields a greater reduction in CO_2 and diesel consumption. Increased departing SOC yielded a greater reduction in CO_2 and diesel consumption. However, there are some subtle behaviors at work within these trends.

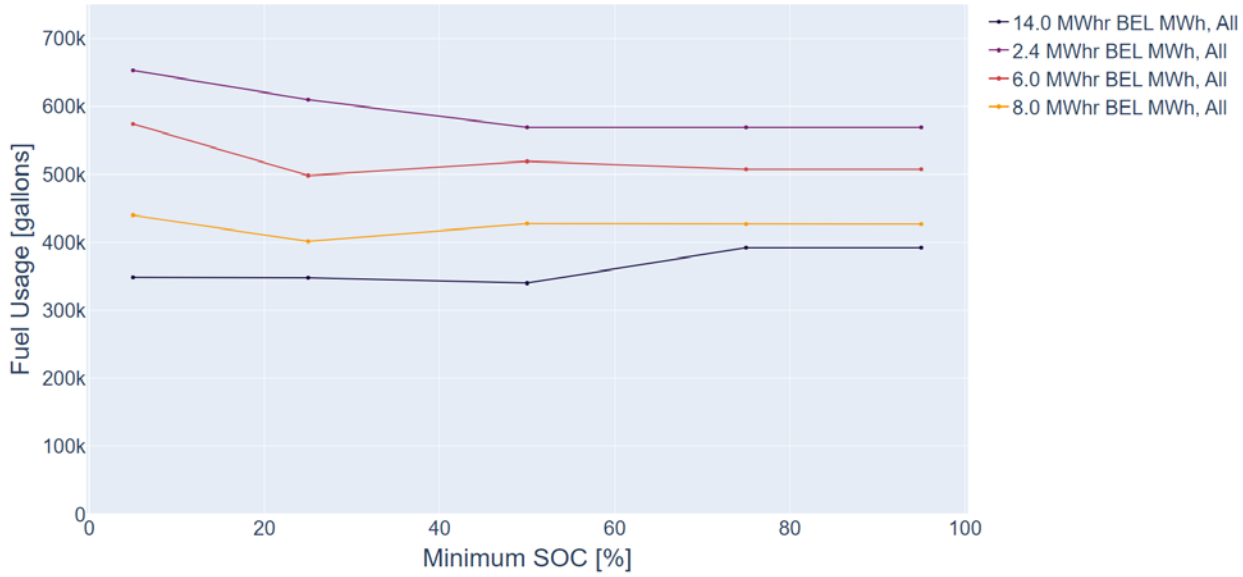

Figure 52. Plots of projected diesel usage as BEL charging strategy and battery capacity are swept for the Taconite route

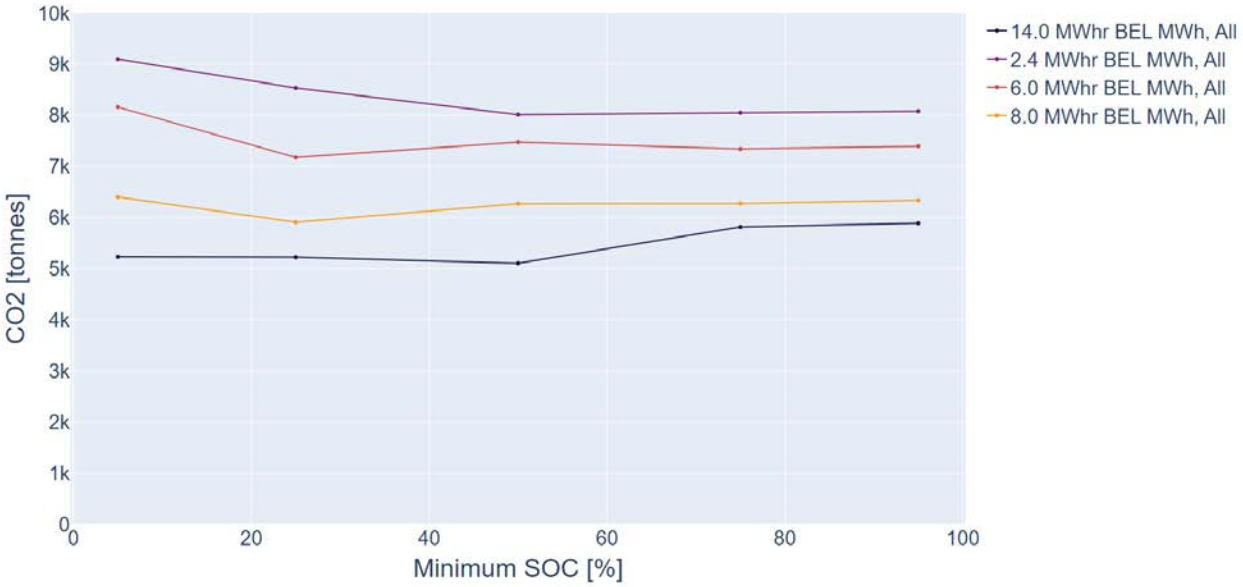

Figure 53. Plots of projected GHG emissions as BEL charging strategy and battery capacity are swept for the Taconite route

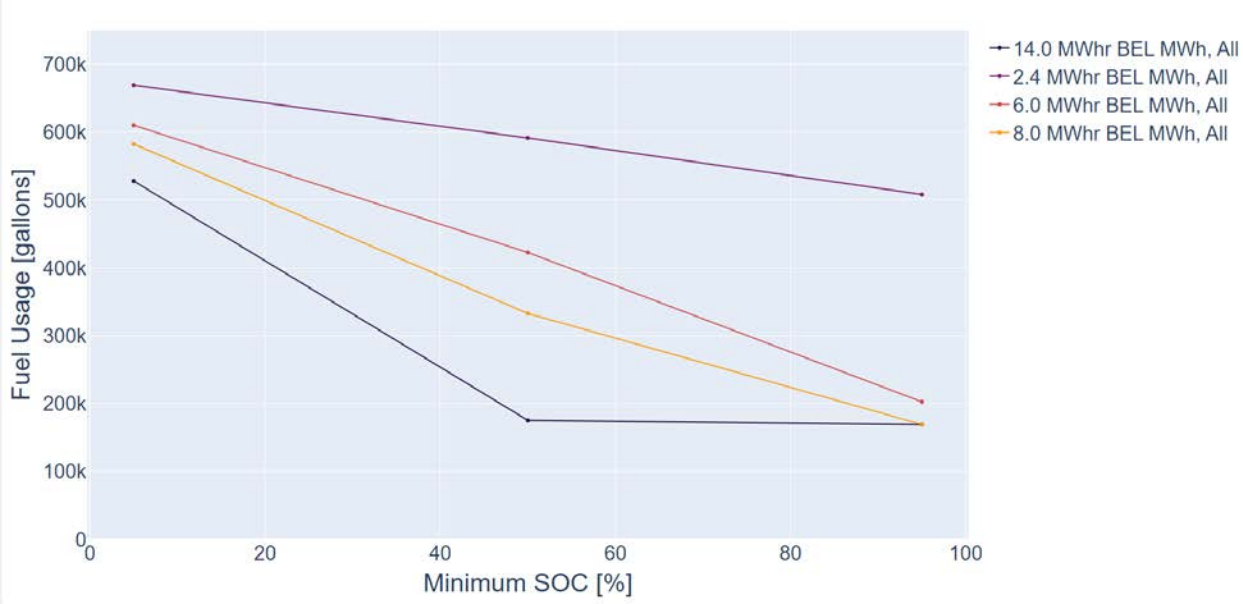

Figure 54. Plots of projected diesel usage as BEL charging strategy and battery capacity are swept for the Minneapolis route

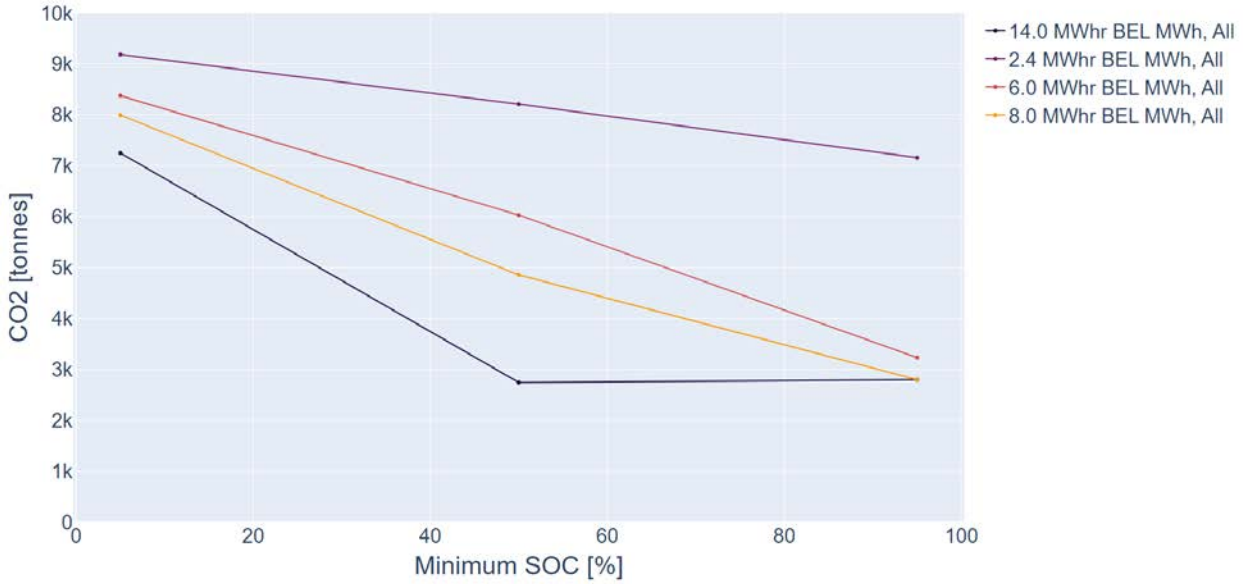

Figure 55. Plots of projected GHG emissions as BEL charging strategy and battery capacity are swept for the Minneapolis route

The 14-MWh and 8-MWh BELs yielded identical savings on the Minneapolis route in the final year, while there was a small difference on the small route between the two battery capacities. The 6-MWh BEL performance on the Minneapolis route was also near the performance of the 14- and 8-MWh BELs. This diminishing return for increasing battery sizes may indicate a "rightsizing" opportunity for these routes.

The time-series data of specific trains give some insight as to why these performance levels were achieved. The data presented in Figure 56–Figure 59 show the SOC trajectory for both routes by direction. The color of each line in the lower plot of these figures represents a discrete BEL battery capacity.

The other trend seen in the Taconite route is that the reduction in CO_2 is not entirely consistent between the different battery capacities. The 14-MWh BEL has increased emissions if it is fully charged in Hibbing. However, the 6-MWh and 8-MWh BELs had their minimum emission levels when charged to 25% SOC in Hibbing. The reasons for these trends can be seen when studying the SOC trajectory throughout a round trip.

Figure 56 shows the SOC trajectories for trains that were fully charged in Hibbing and Allouez. This shows how an increase in battery capacity allows for BEL operation for most, if not all, of the trip. The 14-MWh BEL was never depleted during the round trip. The 6-MWh and 8-MWh BELs were able to provide power during the southbound segment of the trip. This explains why they exhibited similar reductions in fuel usage and emissions.

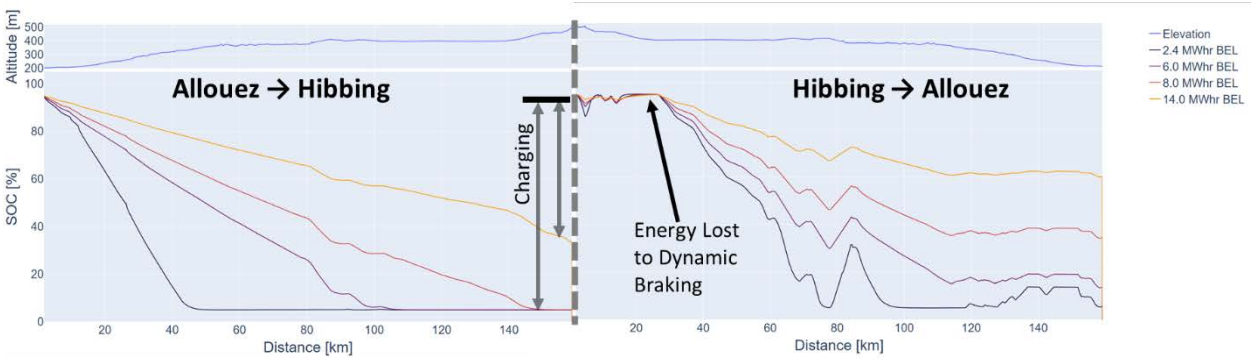

Figure 56. Plot of SOC and elevation for trains containing BELs with battery capacities from 2.4 MWh to 14 MWh making a round trip from Superior, Wisconsin, to Hibbing, Minnesota, that were fully charged in Hibbing

Figure 56 also shows why charging strategy is important. A significant amount of energy is lost through braking during departure from Hibbing. Figure 57 shows SOC trajectories for the trains that were only charged to 50% in Hibbing. The first half of the trip is identical, but the second half differs because there is sufficient room in the BEL to capture energy when departing Hibbing. A departing SOC of 50% was almost optimal for the 2.4-MWh BEL. The locomotive battery became fully charged, and some energy was not recovered by braking.

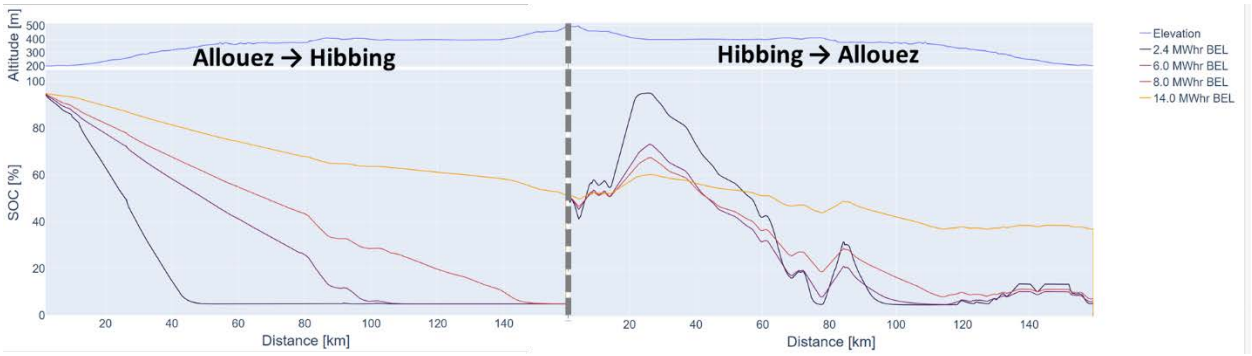

Figure 57. Plot of SOC and elevation for trains containing BELs with battery capacities from 2.4 MWh to 14 MWh making a round trip from Superior, Wisconsin, to Hibbing, Minnesota, that were charged to 50% SOC in Hibbing

The 6-MWh and 8-MWh BELs did not exhibit optimal performance with a departing SOC of 50%. The reason for this can be seen when comparing Figure 56 and Figure 57. These BELs are depleted between 100 km and 120 km in the southbound segment of the trip. When fully

charged in Hibbing they were never depleted. The 75% departing SOC allowed these BELs to capture the potential energy when departing Hibbing but not become depleted prior to arriving in Allouez.

The data presented in Figure 58 show the trains that were not charged in Hibbing. The 14-MWh BEL performed similar to the other strategies. These data show that the 14-MWh BEL has significant margin for this application. This might be required for running accessory loads or moving cars while in Hibbing. The other BEL capacities were depleted most of the trip, which explains why these cases used the most fuel.

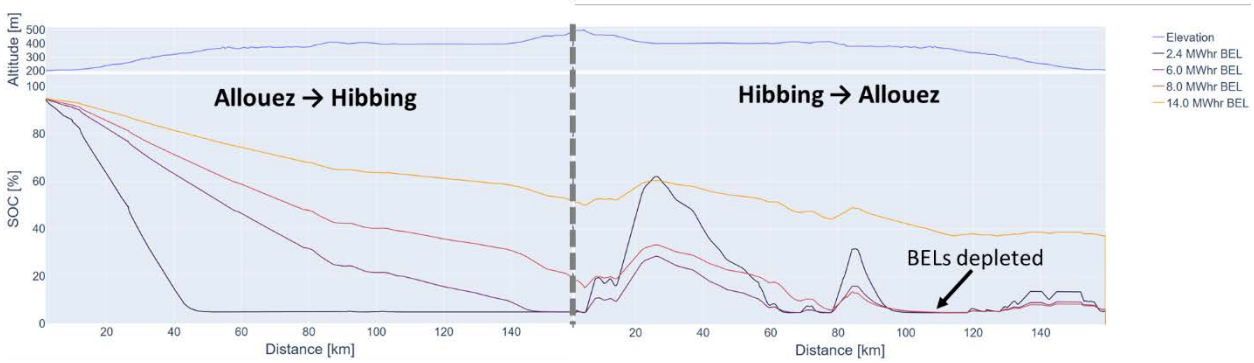

Figure 58. Plot of SOC and elevation for trains containing BELs with battery capacities from 2.4 MWh to 14 MWh making a round trip from Superior, Wisconsin, to Hibbing, Minnesota, that were not charged in Hibbing

Figure 58 shows data from a loaded Taconite train that is heading toward the port in Superior, Wisconsin. The 6-, 8-, and 14-MWh BELs were never depleted during this trip and were able to contribute to train operation the entire time. The savings on these trips would have been identical.

The BELs on the Minneapolis route were not able to recover as much energy as the trains on the Taconite route. The data presented in Figure 59 show how the SOC decreases as the train travels in each direction. The SOC behavior is varied between each of the battery capacities. The 14-MWh and 8-MWh BELs never depleted, while the others did. The distance traveled before being depleted increased with each increase in battery capacity. The only place where significant regenerative braking occurred was descending the hill into Superior.

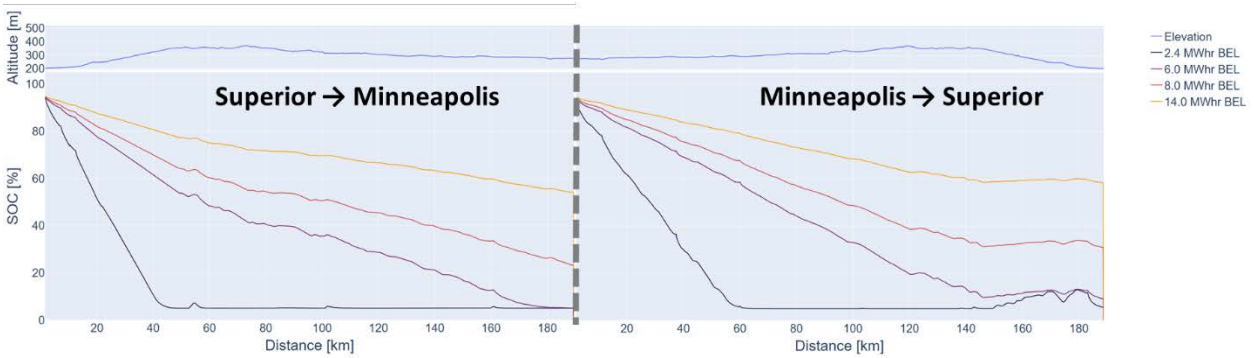

Figure 59. Plot of SOC and elevation for trains containing BELs with battery capacities from 2.4 MWh to 14 MWh traveling from Hibbing, Minnesota, to Superior, Wisconsin

The mostly linear decrease in SOC during each segment of the trip and the only significant energy recovery at the end of a trip segment yielded very uninteresting trends in fuel consumption. Increased battery capacity and increased charging reduced fuel consumption up until the battery was big enough to remain above the minimum SOC for the duration of the trip.

Conclusions

The two studies carried out on these two routes give some insight into optimal BEL adoption. This is related to where they are used and what specifications are required.

The Taconite route highlights the significance of geography and the flow of freight. The asymmetric flow of freight downhill on the Taconite route is a perfect opportunity to capture energy. Routes like this will offer the greatest opportunity to reduce diesel fuel usage and harmful emissions, while also having more favorable economics relative to other routes.

Both routes demonstrate the importance of BEL specifications. Emissions and diesel fuel reduction were impacted by battery size, charging strategy, and, to a lesser degree, the assumption that SOC could range from 5% to 95%. However, there was a point on both routes where the increase in battery size had a diminishing return on fuel and emissions reductions. Rightsizing the BEL for each application will be important for optimizing the cost for each ton of GHG emissions. “Rightsizing” these batteries will also help to optimize the complete life cycle CO_2 emissions for these locomotives, because battery manufacturing contributes significantly to life cycle CO_2 emissions.

These findings also show areas for future improvements in the tool. First is the incorporation of battery size for estimated BEL cost. Battery costs for the BEL battery sweep were intentionally avoided because the financial analysis in the version of the tool used for this case study assumed all BELs had the same cost, which was intended to be a placeholder assumption. A new feature has been implemented that estimates BEL cost and weight based on battery capacity. This new feature will be incorporated into analyses soon.

The second improvement would be to modify the train planner to not require at least one conventional locomotive per consist. This requirement was created to ensure trains could complete each trip even if all BELs were depleted. However, the simulations for the 14-MWh BEL indicate that BEL-only consists could be acceptable on some routes. Complete removal of this requirement would probably not work, but it may be beneficial to include BEL capacity in consist development.

Project Activities

NREL, the University of Illinois Urbana-Champaign, Southwest Research Institute, and BNSF Railway successfully developed and released ALTRIOS, www.nrel.gov/transportation/altrios. ALTRIOS is a unique, fully integrated, open-source software tool used to evaluate strategies for cost-effectively deploying advanced locomotive technologies and associated infrastructure. ALTRIOS simulates energy conversion and storage dynamics, locomotive and train dynamics, meet-pass planning (detailed train timetabling), and freight-demand-driven train scheduling. It

was validated using conventional locomotives and BELs, showing substantial agreement for both locomotives and trains. Over the trips suitable for use, the conventional locomotives showed a time-averaged trip error of 4.2%. The team chose not to reverse-engineer the BEL controls, but despite this, the model shows good trendwise agreement with the BEL test data. The train data have substantially more uncertainty due to a variety of unknown environmental and train configuration factors resulting in a time-averaged error of 17.7%. Given the uncertainties in locomotive and train performance and operational data, this agreement was determined to be acceptable and possibly within the uncertainty. ALTRIOS was then applied to a 30-year rollout case study electrifying two BNSF routes: taconite mines near Hibbing, Minnesota, to Superior, Wisconsin, and manifest trains running from Minneapolis, Minnesota, to Superior, Wisconsin. By dispatching an increasing share of 2.4-MWh BELs over 30 years, achieving a two-thirds fraction of locomotives, annual diesel fuel usage was reduced by 55% for the Taconite route and 23% for the Minneapolis route, yielding substantial energy efficiencies. For both routes, results indicate that an optimal battery size exists for energy recovery. Additional analysis is needed to quantify the optimal based on economics assumptions.

Due to contracting delays and the impacts of the COVID-19 pandemic, the project period of performance was extended to June 30, 2023, with no increase in cost. The ALTRIOS team successfully met all project objectives and milestones and is actively pursuing follow-on opportunities to apply and expand ALTRIOS to help inform and accelerate advanced rail technology deployments.

Project Outputs

A. Journal Articles

The team is drafting a journal submission.

B. Papers

Anderson, G.A., et al. 2023. "ALTRIOS - Advanced Locomotive Technology and Rail Infrastructure Optimization System, Exploring Pathways to Freight Rail Decarbonization." *Proceedings of the Locomotive Maintenance Officers Association (LMOA) 85th Annual Meeting*, 3–4 Oct. 2023, Indianapolis, IN.

Dick, C.T., G.S. Roscoe, S. Shi, S. Fritz, G. Anderson, J. Lustbader, and C. Baker. 2023. "Evaluating rollout strategies for alternative locomotive propulsion technology on North America freight rail corridors using simulation." *Proceedings of the 12th International Heavy Haul Association Conference,* August 2023, Rio de Janeiro, Brazil.

C. Status Reports

The ALTRIOS team provided quarterly status reports to the U.S. Department of Energy from FY 2022 Q1 through FY 2023 Q3.

D. Media Mentions

- Press Releases

    - "New Software Puts Rail Freight on Express Track to Net-Zero Emissions." NREL, Oct. 13, 2021. www.nrel.gov/news/program/2021/new-software-puts-rail-freight-on-express-track-to-net-zero-emissions.
    - "All Aboard! NREL Releases First Comprehensive, Open-Source Software for Freight Rail Decarbonization." NREL, Aug. 2, 2023. www.nrel.gov/news/program/2023/nrel-altrios-release.
    - "SwRI helps create open-source software to assist rail industry decarbonization efforts." Southwest Research Institute, Aug. 7, 2023. www.swri.org/press-release/swri-helps-create-open-source-software-assist-rail-industry-decarbonization-efforts.
- Magazine Articles
    - "US team delivers open-source rail freight decarbonisation tool." *The Engineer*, Aug. 8, 2023. www.theengineer.co.uk/content/news/us-team-delivers-open-source-rail-freight-decarbonisation-tool.
    - "Parallel Systems Wins $4.4MM DOE Grant." *Railway Age*, Feb. 15, 2022. www.railwayage.com/mechanical/freight-cars/parallel-systems-wins-4-4mm-doe-grant.
    - "NREL Releases Open-Source ALTRIOS Decarbonization Modeling Software." *Railway Age*, Aug. 9, 2023. www.railwayage.com/mechanical/locomotives/nrel-releases-open-source-altrios-decarbonization-modeling-software.
    - "World first open source software developed for freight rail decarbonization." *Rail Technology Magazine*, Aug. 10, 2023. www.railtechnologymagazine.com/articles/world-first-open-source-software-developed-freight-rail-decarbonisation.
- News Articles
    - "New Software Puts Rail Freight on Express Track to Net-Zero Emissions." *CleanTechnica*, Oct. 19, 2021. cleantechnica.com/2021/10/18/new-software-puts-rail-freight-on-express-track-to-net-zero-emissions.
    - "SwRI debuts world-first rail decarbonization platform." *RailTech*, Aug. 11, 2023. www.railtech.com/innovation/2023/08/11/swri-debuts-world-first-rail-decarbonization-platform.
    - "World's first open-source software for exploring rail decarbonization is launched." *Electric and Hybrid Rail Technology*, Aug. 9, 2023. www.electricandhybridrail.com/content/news/world-s-first-open-source-software-for-exploring-rail-decarbonization-is-launched.
    - "US team delivers open-source rail freight decarbonisation tool." *World News*, Aug. 8, 2023. article.wn.com/view/2023/08/08/US_team_delivers_opensource_rail_freight_decarbonisation_too.
    - "Open-Source Platform Simulates Energy Transition Strategies for Rail Infrastructure." *EEPower*, Aug. 21, 2023. eepower.com/news/open-source-platform-simulates-energy-transition-strategies-for-rail-infrastructure.
    - "Open-source software aims to get freight decarbonisation on track." *Institution of Mechanical Engineers*, Aug. 10, 2023. www.imeche.org/news/news-article/open-source-software-aims-to-get-freight-decarbonisation-on-track.

    - "Open-source software available for rail decarbonization." *Diesel & Gas Turbine Worldwide*, Aug. 22, 2023. www.dieselgasturbine.com/news/open-source-software-available-for-rail-decarbonization/8030789.article.
- Podcasts and Multimedia
    - "A Clean Locomotive Revolution, Renewable Deployment Setback Ordinances, and Using Water to Cool Supercomputers." *Transforming Energy: The NREL Podcast*, Aug. 23, 2023. transformingenergy.buzzsprout.com/2202535/13443820-a-clean-locomotive-revolution-renewable-deployment-setback-ordinances-and-using-water-to-cool-supercomputers.

E. Invention Disclosures

N/A

F. Patent Applications

N/A

G. Licensed Technologies

N/A

H. Networks/Collaborations Fostered

- NREL, the University of Illinois Urbana-Champaign, Southwest Research Institute, and BNSF Railway have developed a strong team and fostered collaboration between our organizations. The transition of the University of Illinois co-PI to the University of Texas at Austin late in the project further expands opportunities for collaboration between the original project partners and this rapidly emerging railway academic research program. NREL, Southwest Research Institute, and the University of Texas at Austin have submitted collaborative research proposals in response to subsequent funding opportunities.
- Discussion with the Federal Railroad Administration were productive. NREL was able to support a Federal Railroad Administration workshop by providing a tour of NREL. This was very successful and helped support the broader mission of advanced rail technology deployment.
- The team presented to the Locomotive Maintenance Officers Association Mechanical Committee meeting in February 2023 at the Southwest Research Institute in San Antonio, expanding awareness of ALTRIOS.
- The ALTRIOS team organized a LOCOMOTIVES session at the Railroad Environmental Conference. This was a great networking event.

I. Websites Featuring Project Work Results

ALTRIOS website: www.nrel.gov/transportation/altrios
ALTRIOS public GitHub: github.com/NREL/altrios
ALTRIOS PyPI installation: pypi.org/project/altrios

J. Other Products (e.g., Databases, Physical Collections, Audio/Video, Software, Models, Educational Aids or Curricula, Equipment or Instruments)

NREL for the U.S. Department of Energy under Contract No. DE-AC36-08GO28308, the Board of Trustees of the University of Illinois, and Southwest Research Institute. 2023. "Advanced Locomotive Technology and Rail Infrastructure Optimization System (ALTRIOS)." Computer software.

K. Awards, Prizes, and Recognition

N/A

Follow-On Funding

This will be updated for the final closeout report before submitting.

Table 16. Follow-On Funding Received

Source	Funds Committed or Received
• ARPA-E Open Award, Subcontractor to Parallel Systems: NREL	$475,000
• ARPA-E Open Award, Subcontractor to Parallel Systems: University of Texas at Austin	$245,000
• ARPA-E INTERMODAL, Intermodal Freight Optimization for a Resilient Mobility Energy System (INFORMES): NREL (lead) with multiple partners	$2,200,000

References

[1] G.S. Roscoe, "Dispatching Logic, Corridor Simulation, and Train Following Algorithms to Quantify the Benefits of Virtual and Moving Block Control Systems on North American Freight Railroad Mainlines. Master's Thesis.," Urbana, IL: University of Illinois at Urbana-Champaign, Department of Civil and Environmental Engineering., 2021.

[2] G.S. Roscoe and T. Dick, "Incremental Free Path Heuristic Algorithm for Deadlock-Free Train Dispatching on Long Complex North American Rail Corridors.," in *Proceedings of the 5th International Seminar on Railway Operations Modelling and Analysis (RailBeijing).*, Beijing, China., 2021.

[3] W.F Dirsh and S.P. Singh, *Train Energy Model Validation Using Revenue Service Unit Coal Train Data*. Chicago, IL: Association of American Railroads, 1991.

[4] Garrett Anderson, Steve Fritz, and Christopher Hennessy, "BNSF ZERO-AND NEAR ZERO-EMISSION FREIGHT FACILITIES PROJECT (ZANZEFF) DATA ACQUISITION SUPPORT." May 2021. [Online]. Available: https://ww2.arb.ca.gov/sites/default/files/2022-11/zanzeff-bnsf-belreport.pdf

[5] B. Borlaug, M. Muratori, M. Gerdes, and S. Salisbury, "Levelized Cost of Charging Electric Vehicles." National Renewable Energy Laboratory - Data (NREL-DATA), Golden, CO (United States); National Renewable Energy Laboratory (NREL), Golden, CO (United States), p. 2 files, 2020. doi: 10.7799/1661199.

[6] "Estimating electric vehicle charging infrastructure costs across major U.S. metropolitan areas," International Council on Clean Transportation. Accessed: Apr. 27, 2023. [Online]. Available: https://theicct.org/publication/estimating-electric-vehicle-charging-infrastructure-costs-across-major-u-s-metropolitan-areas/

[7] F. Zenith, R. Isaac, A. Hoffrichter, M. S. Thomassen, and S. Møller-Holst, "Techno-economic analysis of freight railway electrification by overhead line, hydrogen and batteries: Case studies in Norway and USA," *Proceedings of the Institution of Mechanical Engineers, Part F: Journal of Rail and Rapid Transit*, vol. 234, no. 7, pp. 791–802, Aug. 2020, doi: 10.1177/0954409719867495.

[8] "2022 Annual Technology Baseline," National Renewable Energy Laboratory. Accessed: Apr. 27, 2023. [Online]. Available: https://atb.nrel.gov/electricity/2022/about

[9] "Benefit Cost Analysis Guidance for Rail Projects," U.S. Federal Railroad Administration, 2016.

[10] "Annual Energy Outlook 2023 - U.S. Energy Information Administration (EIA)." Accessed: Apr. 27, 2023. [Online]. Available: https://www.eia.gov/outlooks/aeo/index.php

[11] "LCFS Life Cycle Analysis Models and Documentation | California Air Resources Board." Accessed: Oct. 25, 2022. [Online]. Available: https://ww2.arb.ca.gov/resources/documents/lcfs-life-cycle-analysis-models-and-documentation

[12] O. US EPA, "Diesel Fuel Standards and Rulemakings." Accessed: Oct. 25, 2022. [Online]. Available: https://www.epa.gov/diesel-fuel-standards/diesel-fuel-standards-and-rulemakings

[13] G. Cooney, M. Jamieson, J. Marriott, J. Bergerson, A. Brandt, and T. J. Skone, "Updating the U.S. Life Cycle GHG Petroleum Baseline to 2014 with Projections to 2040 Using Open-Source Engineering-Based Models," *Environ. Sci. Technol.*, vol. 51, no. 2, pp. 977–987, Jan. 2017, doi: 10.1021/acs.est.6b02819.

[14] H. Xu, L. Ou, Y. Li, T. R. Hawkins, and M. Wang, "Life Cycle Greenhouse Gas Emissions of Biodiesel and Renewable Diesel Production in the United States," *Environ. Sci. Technol.*, vol. 56, no. 12, pp. 7512–7521, Jun. 2022, doi: 10.1021/acs.est.2c00289.
[15] J. Littlefield, D. Augustine, A. Pegallapati, G. G. Zaimes, S. Rai, and G. Cooney, "Life Cycle Analysis of Natural Gas Extraction and Power Generation," National Energy Technology Laboratory (NETL), Pittsburgh, PA, Morgantown, WV, and Albany, OR (United States), DOE/NETL-2019/2039, Apr. 2019. doi: 10.2172/1529553.
[16] "Hydrogen Production Tool - Hydrogen Production Energy Conversion Efficiencies." Accessed: Dec. 07, 2022. [Online]. Available: Hydrogen Production Energy Conversion Efficiencies
[17] "Hydrogen Production Tool - Merchant Hydrogen Plant Capacities in North America." Accessed: Dec. 07, 2022. [Online]. Available: Hydrogen Production Energy Conversion Efficiencies
[18] S. Nicholson and G. Heath, "Life Cycle Greenhouse Gas Emissions from Electricity Generation: Update".
[19] US Environmental Protection Agency, "Emissions & Generation Resource Integrated Database (eGRID)," US EPA. Accessed: Nov. 19, 2020. [Online]. Available: https://www.epa.gov/egrid
[20] "eGRID2020 Technical Guide".
[21] P. Gagnon, B. Cowiestoll, and M. Schwarz, "Cambium 2022 Scenario Descriptions and Documentation," National Renewable Energy Lab. (NREL), Golden, CO (United States), NREL/TP-6A40-84916, Jan. 2023. doi: 10.2172/1915250.
[22] Geofabrik GmbH, "Geofabrik Download Server." Accessed: Dec. 18, 2022. [Online]. Available: https://download.geofabrik.de/
[23] OpenRailwayMap Contributors, "OpenRailwayMap." Accessed: Dec. 18, 2022. [Online]. Available: https://www.openrailwaymap.org/
[24] OpenStreetMap Contributors, "OpenStreetMap database." Accessed: Dec. 18, 2022. [Online]. Available: https://www.openstreetmap.org/copyright/
[25] U.S. Geological Survey, *USGS 3D Elevation Program Digital Elevation Model*. (2019). Accessed: Dec. 18, 2022. [Online]. Available: https://elevation.nationalmap.gov/arcgis/rest/services/3DEPElevation/ImageServer
[26] *SAGA GIS*. (Nov. 27, 2020). Accessed: Dec. 10, 2022. [Online]. Available: https://saga-gis.sourceforge.io/en/index.html
[27] QGIS Development Team (2023), *QGIS Geographic Information System*. (Dec. 19, 2022). Accessed: Feb. 26, 2023. [Online]. Available: https://www.qgis.org/en/site/
[28] "Section508.gov." Accessed: Jan. 28, 2023. [Online]. Available: https://www.section508.gov/